

**The Preparation and Study of Lipophilic S-Nitrosothiols for Improving the  
Biocompatibility of Medical Grade Polymers**

by

Alex R. Ketchum

A dissertation submitted in partial fulfillment  
of the requirements for the degree of  
Doctor of Philosophy  
(Chemistry)  
in The University of Michigan  
2016

**Doctoral Committee:**

Professor Mark E. Meyerhoff, Chair

Professor Kyung Dall Lee

Associate Professor Nicolai Lehnert

Associate Professor John P. Wolfe

*All religions, arts, and sciences are branches of the same tree.*

*-Albert Einstein*

©Alex R. Ketchum

---

2016

## DEDICATION

*I dedicate this to my parents, whose unending love is inspiring and has made all things possible.*

## ACKNOWLEDGEMENTS

First and foremost, I would like to thank you, Dr. Mark Meyerhoff, for without your support I would not be where I am now. Your insight and encouragement have taught me so much during the past 5 years and has shaped who I'll be for the rest of my life. I've gained more than chemistry skills and a degree; because of you I've gained an outlook on life that I will carry with me forever.

Thank you to Dr. Kyung-Dall Lee, Dr. John P. Wolfe, and Dr. Nicolai Lehnert for serving on my committee and providing me with valuable perspectives and suggestions. The biocompatibility experiments would not have been possible without the help of Mr. Michael Kappler and Dr. Jianfeng Wu. Thank you both for lending your skills to my research, and all the patience when telling me whether bacteria were stained red or green.

I've been blessed to be surrounded by so many talented and wonderful people during my time in graduate school. Thank you to Stephen Ferguson, Zheng Zheng, Hang Ren, Yaqi Wo, Yu Chen, Elizabeth Brisbois, Bo Peng, Andrea Bell-Vlaskov, Si Yang, Gary Jensen, Kyoung Ha Cha, Natalie Crist, Ian VonWald, Anant Balijepalli, Alessandro Colletta, Dakota Suchyta, Kebede Gemene, Kun Liu, Dipanker Koley, Michael Kappler, Gergely Lautner, Xuewei Wang, Joshua Doverspike, Joanna Zajda, Colleen Dugan, Casey Dougherty, Laura Pfund, Brian Larsen, Wendi Hale, and many others. A special thanks to Alexander Wolf, whose kindness, wit, and friendship has kept me sane during graduate school. In addition, thank you Amit Pithadia for your support and friendship over the past 6 years; your ambition and perspectives on life are inspiring. By the way, I let you win at racquetball every time.

I am truly privileged to have had wonderful friends throughout every stage of my life. Jeremy, Mike, and Nick, thank you for so much enjoyment and support in life; from tennis to music, and H.C. to hospitals—you've been there for all of it. Sam, Eric, and Andy: thank you for making college some of the best years of my life and helping me to discover who I am. Thank you, Sheri, for the last 5 years; you're truly a beautiful person and I am the luckiest husband in the world.

Lastly, thank you to my family. Mom and Dad, I can't begin to express the gratitude I have for you. You've made everything possible. Thank you for coming to all my tennis matches and trombone solos, for supporting me in everything academic, and encouraging creativity. Thank you for never giving up on me when times were dark, nor losing faith in the face of adversity. Your impeccable sense of morality and compassion is my biggest inspiration in life. Grandpa, thank you for so many fish-less fishing trips, for playing baseball with me, and for expanding my vocabulary during golf outings. Grandma, your unwavering love and support in the face of adversity is second to none. I'll never forget the love you showed me.

## TABLE OF CONTENTS

DEDICATION.....	ii
ACKNOWLEDGEMENTS.....	iii
LIST OF FIGURES.....	viii
LIST OF TABLES.....	xiii
LIST OF REACTIONS.....	xiv
LIST OF ABBREVIATIONS.....	xv
ABSTRACT.....	xvii
<b>CHAPTER 1. Introduction .....</b>	<b>1</b>
1.1. Health Concerns Resulting from Medical Device Incompatibility .....	1
1.2. Recent and Current Efforts to Improve the Biocompatibility of Medical Devices .....	6
1.3. Nitric Oxide .....	8
1.4. S-Nitrosothiols: .....	10
1.5. Summary .....	15
1.6. References.....	17

## **CHAPTER 2. The Synthesis and Study of Lipophilic Alkyl and**

<b>Aryl S-Nitrosothiols .....</b>	<b>21</b>
2.1. Introduction .....	21
2.2. Experimental .....	24
2.3. Results and Discussion .....	29
2.4. Conclusions .....	62
2.5. References .....	66

## **CHAPTER 3. The Preparation and Characterization of Nitric Oxide Releasing Silicone Rubber Materials Impregnated with S-Nitroso-*tert*-dodecyl**

<b>Mercaptan.....</b>	<b>68</b>
3.1. Introduction.....	68
3.2. Experimental.....	72
3.3. Results and Discussion .....	77
3.4. Conclusions .....	90
3.5. References .....	91

## **CHAPTER 4. Photoactivated Nitric Oxide Release From Lipophilic**

<b>S-Nitrosothiols Within Biomedical Grade Polymers.....</b>	<b>95</b>
1.1. Introduction .....	95
1.2. Experimental.....	96
1.3. Results and Discussion .....	98
1.4. Conclusions.....	108



1.5. References .....	109
<b>CHAPTER 5. Conclusions and Future Directions.....</b>	<b>111</b>
5.1 Conclusions.....	111
5.2. Future Directions.....	113
5.3. References.....	119
<b>APPENDIX A. Synthesis, Spectroscopy, and Stability of the Nitric Oxide Donor S-Nitroso-N-acetylpenicillamine: An Undergraduate Laboratory Experiment.....</b>	<b>121</b>

## LIST OF FIGURES

Figure 1.1:	Thrombus formation on the polymeric surface of a biomedical device.	4
Figure 1.2:	Biofilm formation on the polymeric surface of a biomedical device.	5
Figure 1.3:	Sources of NO for potential use in medical applications.	10
Figure 1.4:	Two endogenous small molecule RSNOs: <i>S</i> -nitrosocysteine and <i>S</i> -nitrosoglutathione, and the exogenous species, <i>S</i> -nitroso- <i>N</i> -acetylpenicillamine.	11
Figure 1.5:	<i>S</i> -Nitrosothiols' general structure and stabilizing effects of alkyl substitution.	13
Figure 2.1:	The model NO-release system utilizes polymers incorporated with RSNOs.	24
Figure 2.2:	Structures of six RSNOs prepared in this work.	31
Figure 2.3:	SNHT's nitrosation at different temperatures depicts the relative effects on the nitrosation and decomposition rate.	33
Figure 2.4:	Nitrosating agents of varying alkyl substitution.	34
Figure 2.5:	Nitrosation progress as indicated by the RSNO concentration.	35
Figure 2.6:	Additional lipophilic RSNOs.	36
Figure 2.7:	The increased equivalents of <i>t</i> -BuNO <sub>2</sub> enhances the reaction rate of the nitrosation of SNCT and overall yield of the reaction.	36

Figure 2.8: RSNOs with considerable instability as indicated by rapid decomposition (color loss) under ambient conditions.	38
Figure 2.9: SNDDT, SNUDT, and SNTDM share similar molecular masses, and minimal functional groups, thus facilitating a direct comparison of the effects of their alkyl substitution.	39
Figure 2.10: SNTDM's, SNUDT's, and SNDDT's response to stimulation by heat and light as indicated by the remaining % of initial RSNO.	39
Figure 2.11: NO release flux from SR incorporated with SNTDM, SNUDT, and SNDDT over 3 d.	40
Figure 2.12: The relationship between temperature and NO release from both the solid and liquid phases of SNHDT.	42
Figure 2.13: Testing for correlation between the alkyl RSNOs' mass and stability.	43
Figure 2.14: <sup>1</sup> HNMR spectra for the synthesis and decomposition of lipoic acid's dinitroso analog.	44
Figure 2.15: <sup>1</sup> HNMR spectra for the synthesis of S-nitrosocholesterolthiol and disulfide formation upon decomposition.	46
Figure 2.16: Structure of SNAP-NHC <sub>6</sub> H <sub>13</sub> , a target SNAP derivative.	47
Figure 2.17: <sup>1</sup> HNMR of the thiol precursor, NAP-NHC <sub>6</sub> H <sub>13</sub> , and the novel RSNO product, SNAP-NHC <sub>6</sub> H <sub>13</sub> , following synthesis.	48
Figure 2.18: NO release from SR films prepared with 5 wt% SNTDM, SNTPMT, SNTBT, and SNDDT stored in (a) freezer, (b) cupboard, and (c) shelf.	50
Figure 2.19: 5 wt% SNTDM and SNAP incorporated into SR, CS and E2As and stored at -20C° for 1 month.	51
Figure 2.20: 5 wt% SNTPMT and SNAP incorporated into SR, CS and E2As and stored at -20C° for 1 month.	52

Figure 2.21: The % of leached RSNO from (a) SR, (b) CS, and (c) E2As films doped with 5 wt% SNTDM, SNTPMT, SNDDT, SNTBT, and SNAP.	54
Figure 2.22: Relationship between SNDDT's leached RSNO concentration and low stability.	55
Figure 2.23: Long-term NO release from SR, CS, and E2AS films doped with 10 wt% SNTDM, SNTPMT, and SNAP stored at 37 C in the dark over time.	57
Figure 2.24: Adhered platelets when lysed with a surfactant release LDH that in turn reduces NAD <sup>+</sup> to NADH, the molecule tested.	59
Figure 2.25: Control polymers' inherent platelet adherence.	59
Figure 2.26: SNTDM's, SNTPMT's, and SNAP's effects on platelet reduction in SR.	60
Figure 2.27: SNTDM's, SNTPMT's, and SNAP's effects on platelet reduction in E2As.	61
Figure 2.28: SNTDM's, SNTPMT's, and SNAP's effects on platelet reduction in CS.	61
Figure 3.1: The synthesis of <i>S</i> -nitroso- <i>tert</i> -dodecylmercaptan and NO release.	73
Figure 3.2: UV-Vis spectra displaying the inverse relationship between SNTDM and DTDD's absorbances during decomposition.	74
Figure 3.3: SR tubing segments swelled with SNTDM/solvent solution.	75
Figure 3.4: Small segments and cross sections of silicone rubber catheters impregnated with (a) 6.8, (b) 4.0, (c) 1.3, and (d) 0% wt% SNTDM.	78
Figure 3.5: The relationship between the soaking solution concentration, impregnation, and leaching.	80
Figure 3.6: Initial NO release for SR tubing impregnated with various wt% RSNO.	81
Figure 3.7: Long-term NO release for 6.8 wt% SNTDM/SR stored under physiological conditions.	82
Figure 3.8: The effects of light sources and phase dependence on SNTDM's NO release.	84

Figure 3.9:	SNTDM/SR catheter storage in dark environments.	84
Figure 3.10:	Freezer storage for SNTDM in various phases.	85
Figure 3.11:	EtO sterilization's effect on SNTDM/SR catheters.	86
Figure 3.12:	Antimicrobial activity of SR catheters impregnated with SNTDM.	87
Figure 3.13:	SNTDM/SR catheters' biofilm and <i>S. aureus</i> levels during a 21 d incubation study.	89
Figure 3.14:	NO flux during antimicrobial experiment compared with oven storage.	90
Figure 4.1:	Equal amounts of SNTDM, SNTPMT, and SNAP's (0.5 $\mu\text{mol}$ ) steady NO flux.	99
Figure 4.2:	SR rubber films doped with 5 wt% of the following RSNOs (a) SNTDM, (b) SNTPMT, and (c) SNAP, and their NO release upon exposure to ambient and broad spectrum light compared to that from the neat phase (n=3).	101
Figure 4.3:	SNTDM/SR shows NO release profiles that are unique to specific polymers.	102
Figure 4.4:	SNTPMT reaches maximum flux rapidly in CS, but takes longer in TF.	103
Figure 4.5:	5 wt% SNTDM, SNTPMT, and SNAP were incorporated into SR, CS, E2As, and TF and their NO flux determined in the dark, with ambient light, and exposed to a halogen bulb.	104
Figure 4.6	SNTDM/SR's proximity to a light source affects its rate of NO release.	105
Figure 4.7	Schematic for SNTDM/SR films with graphite topcoat to control photosensitivity.	106
Figure 4.8:	The comparative responses of SNTDM/SR with and without a GP topcoat to no light, ambient light, and ambient light+halogen.	107
Figure 4.9:	The SNTDM/SR system's stability with and without GP topcoats when exposed to sunlight and ambient light.	108

Figure 5.1:	Proposed synthesis of <i>S</i> -nitroso-2-methyl-2-undecanethiol.	119
Figure 5.2:	Comparative UV-Vis Absorption spectra of 0.7 nM SNTDM and SNDDT.	120
Figure 5.3:	Three commonly proposed reaction mechanisms for NO release from RSNOs.	121
Figure 5.4:	The structure of <i>S</i> -nitroso-tris(2,2'',6,6''-tetramethyl- <i>m</i> -terphenyl-5'-yl)methylthiol.	122
Figure 5.5:	Exposing SNTDM to a green or blue LED, or halogen bulb results in three drastically difference NO release profiles.	123
Figure A.1:	Synthesis of SNAP via the nitrosation of NAP using acidified nitrite.	127
Figure A.2:	SNAP decomposes to from the corresponding disulfide (RSSR) and NO. SNAP's NO release corresponds with the indicated protons shifts.	129
Figure A.3:	<sup>1</sup> HNMR spectra corresponding to (a) SNAP, (b) partially decomposed SNAP, and (c) pure RSSR following the decomposition.	134
Figure A.4:	The zoomed downfield region of Figure A.3's spectra provides facile observation and quantification of nitrosation and decomposition.	135
Figure A.5:	Expanded region showing SNAP and the disulfide's (a) carboxylic acid and (b) methyl protons.	136
Figure A.6:	The UV-Vis spectrum of SNAP at 3 different concentrations and the Corresponding calibration curve used to determine the molar absorptivity.	136
Figure A.7:	0.8 mM SNAP solutions exposed to varying degree of light while stored in 3 different locations.	137
Figure A.8:	SNAP solutions exposed to varying degrees of heat while stored in 4 different locations.	138

## LIST OF TABLES

Table 1.1:	Implantable biomedical devices, biomaterials, and associated health concerns.	2
Table 1.2:	Many factors affect an RSNO's stability.	14
Table 2.1:	RSNOs prepared in this chapter, the % yield obtained following synthesis, and their corresponding CLogP values.	22
Table 2.2:	Solvent effects on nitrosations as indicated by the highest % RSNO observed.	32
Table 2.3:	Nitrosation time until maximum absorption using different nitrosating agents.	34
Table 2.4:	Determining RSNO/polymer ratios to improve consistency in wt% loading.	49
Table 2.5:	Comparison of SNTDM, SNTPMT, and SNAP's best results for leaching, stability, long-term NO release, and antiplatelet experiments.	65
Table 4.1:	Normalized flux values for SNTDM's, SNDDT's, SNAP's, and SNTPMT's responses to ambient and broad light.	102
Table A.1:	Proton shifts, splitting, and coupling constants for SNAP and RSSR.	135

## LIST OF REACTIONS

Rxn. 1.1:	Nitric oxide's oxidation to nitrogen dioxide.	9
Rxn. 1.2:	Nitric oxide's reaction with oxyhemoglobin to form methemoglobin.	9
Rxn. 1.3:	General nitrosation reaction.	11
Rxn. 1.4:	General transnitrosation reaction.	11
Rxn. 1.5:	NO release catalyzed by heat, light, or metal ions.	11
Rxn. 2.1:	Synthesis of thioketal intermediate via ketone.	25
Rxn. 2.2:	Synthesis of thiol from thioketal intermediate.	25
Rxn. 2.3:	Synthesis of penicillamine thiolactone.	26
Rxn. 2.4:	Alkyl amidation reaction starting from thiolactone.	26
Rxn. 3.1:	SNTDM synthesis.	26
Rxn. 3.2:	SNTDM decomposition (NO release).	73
Rxn. 5.1:	Methyl Grignard addition to 2-undecanone.	119
Rxn. 5.2:	Bromide substitution using PBr <sub>3</sub> .	119
Rxn. 5.3:	Thiol substitution reaction.	119
Rxn. 5.4:	S-nitrosation of 2-methyl-2-undecanone.	119
Rxn. 5.5:	Thiyl formation from a thiol.	121
Rxn. 5.6:	Thiyl addition to a nitrosothiol.	121
Rxn. 5.7:	Nitrosothiol dimerization.	121
Rxn. A.1:	NAP's nitrosation to form SNAP.	127
Rxn. A.2:	RSNO decomposition (NO release).	128
Rxn. A.3:	SNAP's decomposition to yield NO and disulfide.	129



## LIST OF ABBREVIATIONS

Alb-SNO: *S*-Nitrosoalbumin

CDCl<sub>3</sub>: Deuterated chloroform

CHCl<sub>3</sub>: Chloroform

<sup>13</sup>CNMR: <sup>13</sup>Carbon NMR

Cys-SNO: *S*-Nitrosocysteine

d6-DMSO: Deuterated dimethyl sulfoxide

d8-THF: Deuterated tetrahydrofuran

DCC: Dicyclohexylcarbodiimide

DMSO: Dimethyl sulfoxide

DTDD: Di-*tert*-dodecyl disulfide

EDC: Ethylene dicarbodiimide

EDTA: Ethylenediaminetetraacetic acid

Et<sub>2</sub>O: Diethyl ether

GSNO: *S*-Nitrosoglutathione

Hb: Hemoglobin

<sup>1</sup>HNMR: Proton NMR

LED: Light emitting diode

MeOH: Methanol

NHS: *N*-hydroxysuccinimide

NMR: Nuclear magnetic resonance

N<sub>2</sub>: Diatomic nitrogen gas.

NO: Nitric oxide

NO<sub>2</sub>: Nitrogen dioxide

NO<sub>2</sub>\*: Excited state nitrogen dioxide  
NOA: Nitric oxide analyzer  
NOS: Nitric oxide synthase  
PBS: Phosphate buffered saline  
PDT: Photodynamic therapy  
PU: Polyurethane  
RSSR: Disulfide  
RT: Room temperature  
SNAP: *S*-Nitroso-*N*-aethylpenicillamine  
SNTDM: *S*-nitroso-tert-dodecylmercaptant  
SR: Silicone rubber  
THF: Tetrahydrofuran  
vWF: von Willebrand's Factor  
1,2-EtDT: 1,2-Ethanedithiol

## **ABSTRACT**

### **THE PREPARATION AND STUDY OF LIPOPHILIC S-NITROSOTHIOLS FOR IMPROVING THE BIOCOMPATIBILITY OF MEDICAL GRADE POLYMERS**

by

Alex R. Ketchum

**Chair:** Mark E. Meyerhoff

Advances in biomaterials, polymer science, and biotechnology have resulted in the development and implementation of a wide array of implantable biomedical devices and drug/device combination products such as catheters, drug-eluting stents, and artificial organs. Unfortunately, inserting a foreign material into the body can cause undesirable effects, the nature of which depends upon the device's biocompatibility with blood or tissue. Common complications resulting from the use of implantable biomedical devices include cellular proliferation, thrombosis, and the increased risk of infection. The work described in this thesis aims to develop novel lipophilic S-nitrosothiols (RSNOs) that, when incorporated into polymers, provide nitric oxide (NO) release capable of greatly improving the material's biocompatibility.

Initial studies focused on developing methodologies to synthesize fourteen lipophilic RSNOs with LogP values ranging from 1.7 to 10.8. Of these, *S*-nitroso-*tert*-dodecylmercaptan (SNTDM) and *S*-nitrosotriphenylmethanethiol (SNTPMT) exhibited the most promising stability for potential practical use in polymeric materials. Silicone rubber (SR), Elasteon-E2As (E2As), and CarboSil (CS) films containing 10 wt% SNTDM released NO at physiological levels for approximately one month. SR and CS films containing 10 wt% SNTPMT released NO at physiological levels for 41 d, while SNTPMT in E2As lasted 33 d. SNTDM and SNTPMT leached minimally from SR ( $2.4 \pm 0.4\%$ ,  $2.0 \pm 0.2\%$ ), CS ( $3.1 \pm 0.5\%$ ,  $1.8 \pm 0.3\%$ ), and E2As ( $2.3 \pm 0.4\%$ ,  $1.5 \pm 0.3\%$ ). An LDH assay was used to measure the relative amounts of platelets adhered to polymers doped with the different RSNOs. SNTDM and SNTPMT demonstrated excellent antiplatelet activity by reducing levels on SR ( $3.0 \pm 0.3\%$ ,  $8.6 \pm 0.1\%$ ), CS ( $12.3 \pm 2.0\%$ ,  $22.1 \pm 5.9\%$ ) and E2As ( $14.0 \pm 3.4\%$ ,  $23.8 \pm 6.2\%$ ) relative to the controls. A solvent swelling method was developed to impregnate SNTDM in SR catheters which released NO at or above physiological levels for ~26 d. The catheters were incubated in a CDC bioreactor containing *S. aureus* for 21 d and killed or inhibited growth of 99.9% of the bacteria. Polymer films containing SNTDM demonstrated substantial photoinduced NO release, more than an order of magnitude greater than any RSNO previously tested in the literature.

## CHAPTER 1.

### INTRODUCTION

#### 1.1 Health Concerns Associated with the Use of Implantable Medical Devices

Current health care employs a vast array of biomedical devices that are used for a range of state-of-the-art medical procedures. Despite their widespread use, current-generation implantable devices without special mitigation strategies are extremely susceptible to thrombosis and infection, decreasing their functional lifetimes and increasing risk associated with their use.<sup>1-3</sup> Catheters, one of the most fundamental biomedical devices, have gastrointestinal, neurovascular, cardiovascular, and urological applications, to name only a few.<sup>4</sup> For example, during hemodialysis (HD), a common treatment for those suffering from kidney failure, intravascular (IV) catheters carry blood to and from the patient via an extracorporeal circuit/filtration unit with a selective membrane to remove waste species (e.g., urea), restore the proper balance of electrolytes, and eliminate extra fluid from the blood, all tasks normally performed by healthy functioning kidneys.<sup>5,6</sup> Bladder catheterization, another ubiquitous application, also involves implantable catheters to drain the bladder into recipient bags, although the procedure is not intravascular.<sup>7</sup> Despite the high frequency in performance of these procedures, serious health complications are very common in both IV and urinary catheters due to the risks associated with introducing foreign bacteria into the body,<sup>3</sup> and in the case of IV catheters, also enhancing the risk of blood clot formation.<sup>2,8</sup>

Catheters are fabricated from polymeric materials; therefore, it is the nature of these polymers, especially at the catheter surfaces, that directly influence the devices' biocompatibilities.<sup>4,9,10</sup> The term "biocompatibility" has a broad definition, but in this instance,

it usually refers to a biomaterial’s ability to perform its intended function without eliciting undesirable effects in a patient.<sup>11,12</sup> In the case of IV catheters, this can be due to a host response (discussed below),<sup>1</sup> or as is the case with urinary and IV catheters, the increased risk of microbial infection.<sup>9</sup> Table 1.1 (below) lists common biomedical devices and polymeric materials, as well as the health concerns resulting from their use.

Implantable medical devices such as venous access ports can provide many benefits for patients undergoing frequent blood-sampling, blood transfusion, or IV drug delivery such as in chemotherapy and hemodialysis, respectively.<sup>13-15</sup> However, placement of these intravenous ports induces a “foreign body response,” increasing risks to patients.<sup>9</sup> A common host response to a blood-contacting polymer is as follows: during the early process of intravenous device implantation, blood/material interactions cause proteins such as von Willebrand Factor (vWF) and fibrinogen to adsorb to the polymer’s surface and a blood-based transient matrix forms on the device.<sup>9,16-19</sup> If there is tissue trauma during device implantation, a complex wound healing cascade will also ensue. Acute inflammation occurs during initial implantation and can last on the order of a few days, during which increased blood flow cleans the area and initiates clot formation through activation of the coagulation cascade pathways. Cytokines and growth factors are released, and leukocytes adhere to the blood vessel’s endothelium at the site of trauma. Longer-term implantation can lead to chronic inflammation increasing macrophage, lymphocyte,

**Table 1.1** Implantable biomedical devices, common biomaterials they are composed of or coated with, as well as health concerns associated with their use.

<b>Biomedical Devices</b>	<b>Common Biomaterials</b>	<b>Biocompatibility Concerns</b>
Catheters	Silicone rubber	Thrombosis
Stents	Polyurethanes	Infection
Pacemakers	Polycarbonates	Cellular proliferation
Intravascular sensors	Poly (vinyl chlorides)	Device malfunction
Shunts	Polyethylene glycol	Toxicity
Orthopedic implants	Polytetrafluoroethylene	Endothelial damage
Breast implants	Polypropylene	
Drug delivery devices	Chitosan	
surgical sutures	Polystyrene	
Heart valves	Polyesters	

and leukocyte levels.<sup>19</sup> Blood vessels proliferate and connective tissue begins to restructure the area. During this restructuring phase, granulation tissues are formed from the acute inflammatory phase's blood clot. Growth factors aid in the generation of fibrous tissue and blood vessels. After blood/material interactions, activated platelets and the cells that are within the clot release chemoattractants that recruit and direct macrophages to the site of injury. Macrophages adhered to the biomaterial surface and fuse to form foreign body giant cells.<sup>9</sup> This provides a microenvironment which is especially conducive to device degradation. For example, when used in artificial joints, polyethylene's surface is oxidized from extended contact with the radical oxygen species produced in the foreign body giant cells' microenvironment.<sup>9,20</sup> Additionally, similar oxidative processes cause damage to pacemaker leads, rendering them brittle and susceptible to cracking and device failure over time.<sup>9</sup>

The inflammatory response resulting from endothelial trauma with device implantation is also associated with the migration of vascular smooth muscle cells. This can thicken arterial walls and result in neointimal hyperplasia. This is observed with polytetrafluoroethylene (PTFE) coated wire conduits during hemodialysis.<sup>6,9,16,20</sup>

Thrombosis is a serious concern with any blood contacting device such as stents, catheters, extracorporeal circuits, etc. Thrombosis can occur due to a damaged endothelium, which often happens during implantation of coronary stents; this results in the exposure of subendothelial matrix. Most applicable to this dissertation, clot formation on the polymer surface of IV catheters can occlude blood or fluid flow through the lumen(s). Following device implantation, a complex cascade of events takes place (see Fig. 1.1). Plasma proteins, such as von Willebrand Factor (vWF) and fibronectin/fibrinogen, are adsorbed on the polymer within minutes of blood contact, and are immediately available to activate circulating platelets and recruit them to the polymer surface. This causes a conformational change, exposing a fibrinogen binding-receptor (a glycoprotein) that is later enzymatically converted to fibrin via thrombin. Platelet aggregation ensues as fibrin forms a cross-linked insoluble network or blood clot. Clots can further impede device function as well as detach and cause an embolism.<sup>2,8,9,16,19,21</sup>

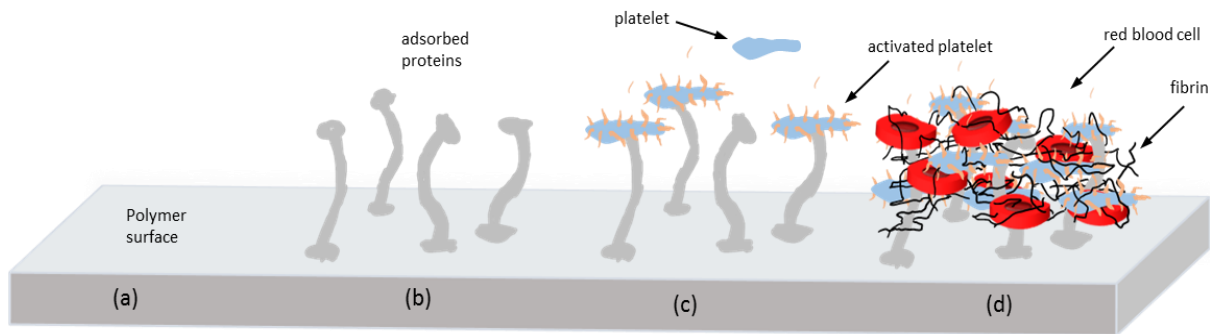


**Figure 1.1** Thrombus formation on the polymeric surface of a biomedical device, *e.g.* intravenous catheter. (a) A newly implanted biomaterial’s surface is rapidly covered with (b) adsorbed proteins, such as vWF, which then (c) activate circulating platelets, causing them to attach and expose fibrin binding sites. (d) Platelet aggregation proceeds as fibrin forms a cross-linked network.

Another health concern with implanted biomedical devices is the increased risk of patient infection. Although, several different sterilization techniques are commonly used, foreign devices can still carry pathogens, which are inevitably present (including on the skin of patients), particularly in high-exposure environments such as hospitals. Further bacteria can enter the body by moving along the surface of the device (*e.g.*, IV catheter).<sup>22,23</sup> Bacteria, which may start as free-floating planktonic cells, excrete extracellular polymeric substances (EPS) which form environmentally-resistant biofilms on foreign surfaces, such as catheters. Bacteria present within a biofilm exhibit antibiotic resistance due to adaptive stress responses and poor antibiotic penetration, as well as protection from the host’s immune system (see Fig. 1.2). In fact, biofilms older than 7 d, require 1000-5000 times the concentration of antibiotics required to kill the same species of planktonic cells.<sup>22,24–26</sup>

In addition to the resistance to the host immune response and antibiotic drug treatment, biofilms also often impact a device’s intended function. Consequently, devices require frequent replacement. This increases medical costs to hospitals and insurance companies, and triggers the harmful effects associated with frequent implantation (*e.g.*, endothelial damage). Although progress has been made in preventing catheter-related bloodstream infections (CRBIs), complications remain prevalent and are estimated to cost between \$670 million and \$2.68 billion USD annually just in the United States alone. More importantly, CRBIs cause >25,000 deaths each



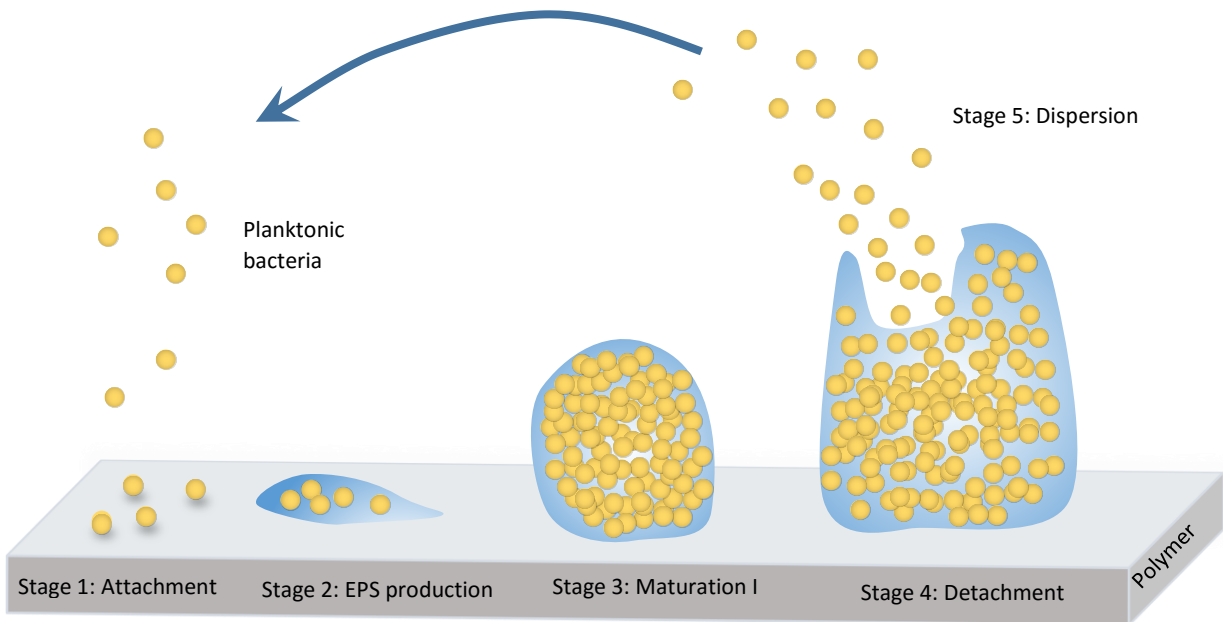


**Figure 1.2.** Biofilm formation on the polymeric surface of a biomedical device. 1) Planktonic bacteria attach to the foreign surface as mediated by cell surface adhesins and (2) release EPS to form a base film. (3) A microcolony develops, and the biofilms mature as mediated by cell-signaling molecules. (4) Finally, bacteria are released to further colonize surfaces and spread systemically.

year in U.S. Hospitals. Further, urinary tract infections (UTIs) are also very commonly associated with use of urinary catheters, accounting for a 75% infection rate for catheters placed chronically.<sup>24,27</sup>

Many types of biomaterials are used for fabricating biomedical devices, several of which are listed earlier in Table 1.1. Rarely do biomaterials alone address all areas that cause biocompatibility issues.<sup>4,11,12,19,28</sup> Polyesters, the most common biodegradable polymer, are commonly used for drug-delivery systems and orthopedic devices (e.g., pins and rods); however, studies have shown their decomposition results in the accumulation of acidic degradation byproducts, triggering local inflammation or systemic reactions.<sup>4,12,28,29</sup> In addition to preventing the direct biocompatible health concerns discussed above, biomaterials must possess appropriate physical characteristics and exhibit minimal toxicity from chemical leaching or degradation. For example, although poly(vinyl chloride), or PVC, is one of the most common biomaterials, it requires the addition of phthalate plasticizers to impart soft and flexible physical properties.<sup>4</sup> This compound was discovered to induce acute inflammation in patients and as well

as liver toxicity in animals. Following a Public Health Notification by the US FDA in 2002, this polymer system is being replaced with other polymeric biomaterials.<sup>4</sup>

Polyurethane derivatives (PU) and silicone rubbers (SR) are the primary focus of this dissertation as they are two of the most common clinically-used polymers for preparing typical biomedical devices and possess hydrophobic character (i.e., lower water uptake).<sup>4,30</sup> Despite their frequency of use, PU and SR remain plagued by thrombosis and biofilm formation issues.<sup>9,11,16</sup> The target bioactive species for incorporation into such devices, lipophilic S-nitrosothiols (RSNOs) (discussed in detail within Section 1.3), are hypothesized to display increased retention (minimal leaching) within certain PU and SR materials given their common non-polar environments,<sup>31</sup> imparting additional biocompatibility to the materials in which they are loaded. Devices made with PU and SR are discussed in more detail within Chapters 2 and 4.

## **1.2 Recent and Current Efforts to Improve the Biocompatibility of Medical Devices**

Considerable research has attempted to increase the biocompatibility of biomedical devices. Although progress has been made on several strategic fronts, the use of implantable devices remains associated with higher risk of the aforementioned health-concerns. Heparin, an anticoagulant medication, is frequently injected into patients to prevent thrombosis during hemodialysis and unwanted clotting during open-heart surgery. Unfortunately, the heparin treatments can induce thrombocytopenia, or a decreased number of platelets, and thus carry an increased risk of hemorrhage.<sup>32-34</sup> Drugs administered to prevent bacterial infection and biofilm formation during procedures such as urinary catheterization exhibit significantly decreased potency given the biofilm's protective effects.<sup>24,26</sup> The use of antibiotics can result in undesirable side-effects and facilitate the growth of drug-resistant bacteria.<sup>35</sup>

Certain biomaterials/polymers exhibit some degree of biocompatibility; however, it is often insufficient to adequately prevent the common health concerns. Each polymer possesses unique properties causing certain polymers to have increased biocompatibility for specific applications, but often insufficient or reduced biocompatibility for others.<sup>10,4,6,11</sup> Researchers have reported trends showing that polymers mimicking the endothelium are less prone to the foreign body response.<sup>9,36,37</sup> By covalently modifying the surface, or through the use of passive

and active coatings, scientists have been able to increase device biocompatibility. For example, wire coatings made from PTFE exhibit reduced transient electron distributions due to the polymer's carbon-fluorine bonds. This results in less Van der Waals interactions with proteins, and decreased thrombogenicity; however, its low coefficient of friction correlates with wire slippage and arterial perforation.<sup>38,39</sup> Biomedical devices have exhibited reduced biofilm formation and infection resulting from protein and microorganisms via use of repellent coatings. Polymeric brush coatings, such as polyethylene glycol (PEG), have also been shown to reduce biofilm and bacterial adhesion. Water molecules hydrate the surface due to PEG's hydrophilic character and form a steric barrier.<sup>40-43</sup> Unfortunately, this brush coating is chemically unstable and there is little control over the quality of the monolayer.<sup>9,16,44</sup>

In addition to surface modification, drug-eluting biomedical devices are a growing and promising area of research; however, each has their own advantages and disadvantages. Drug-releasing biomaterials aim to enhance the polymer's healing or antimicrobial properties through the controlled release of active pharmaceutical ingredients to the surrounding tissue or blood stream.<sup>45-48</sup> A number of wound dressings featuring this methodology have been commercialized.<sup>46</sup> One of the most promising was developed by Suzuki et al. The reported wound dressing releases gentamycin from a poly(vinyl alcohol) derivative when the peptide linker is cleaved by a proteinase near *P. aeruginosa* infections.<sup>49</sup> Unfortunately, these temporary dressings require frequent changing, which is uncomfortable for the patient and can increase the risk of secondary infections.<sup>46,47</sup> In another attempt to enhance the biocompatibility of commercial medical devices through controlled drug release, Foley urinary catheters have been coated with silver salts intended to prevent infections. Such devices have been commercialized. Unfortunately, Ag<sup>+</sup> eluting urinary catheters have not solved the problem of infection given that The Healthcare Infection Control Practices Advisory Committee (HICPAC) states that silver-alloy coated catheters lead to similar infection rates compared to the conventional silicone ones. Silver salt coated Foley catheters also significantly increase the cost of this product over typical catheters, leaving the door open for the development of less-expensive and longer-lasting antimicrobial devices.<sup>7,50</sup>

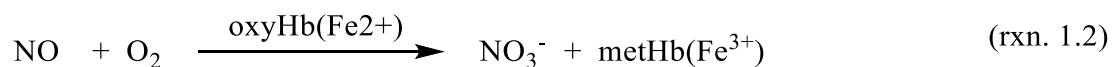
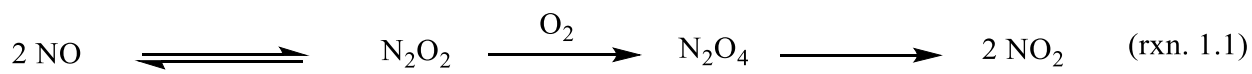
### 1.3 Nitric Oxide

A growing method currently under academic study for improving medical devices' biocompatibility involves the use of nitric oxide (NO). Since the discovery that NO is produced within our body by several enzymes, scientists have learned that NO exhibits a diverse range of benefits including potent antimicrobial and antithrombotic properties.<sup>51,52,53</sup> Consequently, many of NO's effects on cells and tissues can be used to improve the biocompatibility of medical devices.<sup>36</sup> In our bodies, NO is catalytically produced from arginine in a wide variety of cells by three isoforms of the enzyme nitric oxide synthase (NOS): endothelial (eNOS), neuronal (nNOS), and inducible nitric oxide synthase (iNOS). nNOS and iNOS are soluble and present in the cytosol, having roles involved with neuro-signalling and immune defense against pathogens, respectively. eNOS is associated with membranes and regulates vascular function and clot formation.<sup>52,53,54</sup> Endothelial cells release NO and prostacyclin to regulate thrombosis by prevention of platelet activation and adhesion to the endothelium. Activated platelets, in turn, release NO to inhibit further thrombosis propagation via a negative feedback mechanism. Following damage to the endothelium, prothrombin is converted to thrombin, which increases intracellular  $Ca^{2+}$  levels. Within platelets, the increased  $Ca^{2+}$  associates with calmodulin and initiates NO production via eNOS. The produced NO stimulates soluble guanylyl cyclase to produce cyclic GMP, which in turn stimulates a cGMP dependent protein kinase that finally reduces fibrinogen binding.<sup>17,19,52,53</sup> Given NO's ability to prevent platelet adhesion and aggregation, NO-releasing biomedical devices have been shown to consistently reduce thrombus formation and minimized risks, such as the potential for pulmonary embolism.<sup>37,55</sup>

Additionally, NO-releasing biomaterials have repeatedly demonstrated reduced bacteria adhesion and biofilm formation compared to controls; consequently, this opens the opportunity to utilize such materials to prevent infections associated with implantable devices such as catheters. There are several possible routes and explanations for NO's antimicrobial activity, depending on various factors including, but not limited to, the specific microbe. DNA is a target for reactive nitrogen species. NO can deaminate DNA, as well as damage it oxidatively by the formation of other antimicrobial species such as peroxyxynitrite. The additional antimicrobial species are formed due to increased levels of superoxide produced during inflammation. NO has

also been observed to inactivate various enzymes containing Fe-S clusters, thus inhibiting their metabolic activity and causing cytotoxicity.<sup>36,51,52,56,57,58</sup>

In the presence of oxygen, NO rapidly oxidizes to form NO<sub>2</sub> via the reaction shown below (Reaction 1.1). NO<sub>2</sub> is a toxic species and its generation must be avoided or controlled when dealing with biomedical applications. Within the bloodstream, NO is converted to nitrate by reaction with oxyhemoglobin within a few seconds (Reaction 1.2), preventing the accumulation of high NO concentrations. One of the main applications, NO inhalation therapy (INO), has been used for many years to provide vasodilation of arteries during respiratory failure without causing a systemic effect; however, NO's short half-life limits its use for any other applications.<sup>36,51,52,59</sup>



Although gaseous NO's direct medical applications are limited, NO donors have increased stability, and thus can act as controlled, localized sources of NO. Nitroglycerin (NG) has been used for over 130 years to treat heart conditions through the vasodilatory action of NO (see Figure 3a). Although NG is not a NO-donor by the strictest definition, since it requires an aldehyde dehydrogenase for the *in vivo* conversion to NO, it still serves as a stable and controllable source of NO. Physiologically, the body stores its own reservoir of NO as nitrosonium groups (N≡O<sup>+</sup>) bound to the sulfurs in S-nitrosothiols (RSNOs), the class of NO-donors studied in this dissertation work (see Figure 1.3c). Such species have greatly increased stability relative to NO itself.<sup>36,51,52,59</sup> RSNOs will be discussed further in Section 1.4.

Various classes of exogenous NO-donors have also been studied as potential NO sources for biomedical applications including diazeniumdiolates (NONOates), nitrogen oxides (NO<sub>x</sub>), and metal-nitrosyl compounds (see Figure 1.3a-d). NONOates have progressed furthest toward clinical use, with a NO releasing anti-acne product currently in phase 3 clinical trials.<sup>31,36,45,59,60,61,62</sup>

One of the most promising applications, and the focus of this dissertation, involves the incorporation of NO-donors into polymers, producing NO-releasing biomedical devices. These

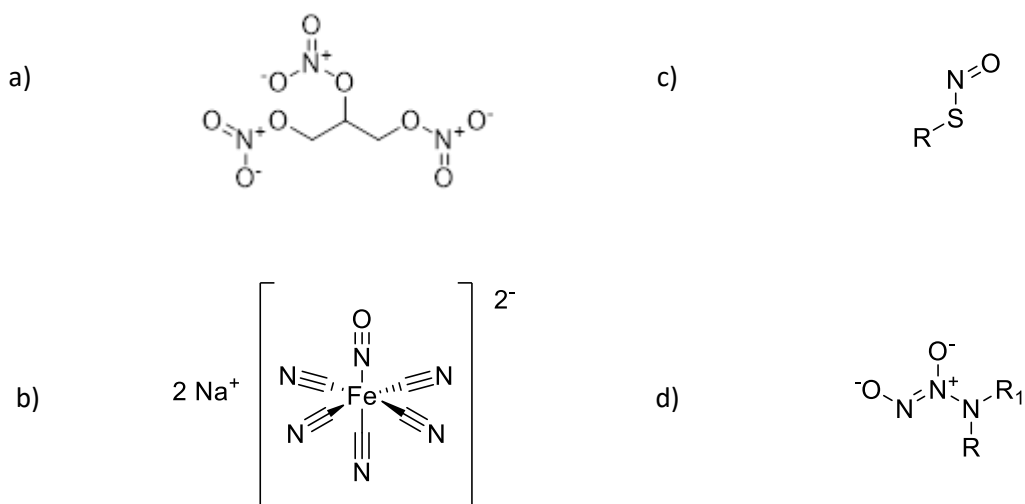


**Figure 1.3.** Sources of NO for use or potential use in medical applications. (a) Trinitrolycerin and (b) sodium nitroprusside are currently used clinically. (c) Endogenous S-nitrosothiols serve as NO donors and reservoirs, while exogenous species are still in clinical trials. (d) Ointments with diazeniumdiolate based ingredients/species are currently in phase III clinical trials.

biomaterials commonly exhibit superior biocompatibility given NO's salubrious antithrombotic and antimicrobial effects. Such NO-releasing devices can provide treatment at localized sites, thus minimizing side effects and complications accompanying the use of systemic or local antibiotics (e.g., drug interactions), especially given the ever-growing rise of antibiotic resistant bacteria. Due to NO's propensity to oxidize, the biomaterials should release NO in controlled amounts, for specific durations, and at discrete locations.<sup>2,7,30,63</sup> One target NO-release system with incorporated RSNOs is specifically depicted and described in Chapter 2.

#### 1.4 S-Nitrosothiols

S-Nitrosothiols, or RSNOs, are a class of molecules defined by a nitroso group bound to the sulfur of a thiol (see Figure 1.4). Although the NO synthesized by endothelial cells can diffuse randomly to the surrounding environment, RSNOs serve as a physiological NO-donor by providing a more stable reservoir of NO, which can be released as needed at discrete locations upon exposure to various stimuli. Endogenous RSNOs include the small molecules S-nitrosocysteine (CysNO) and S-nitrosogluthathione (GSNO) (see Figure 1.4), as well as the protein, S-nitrosoalbumin.<sup>52,53,59</sup>

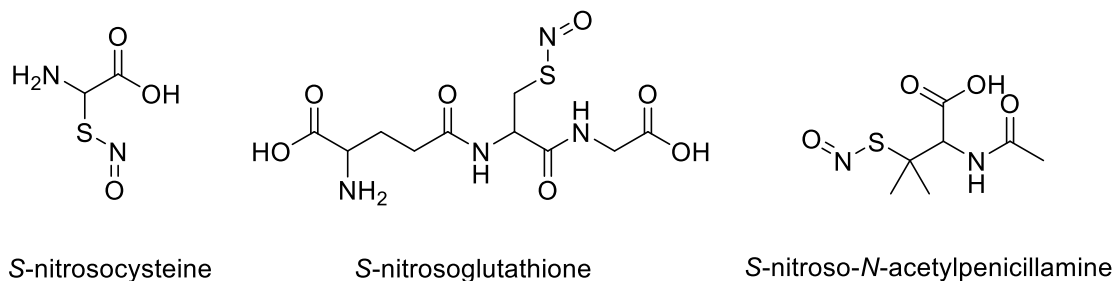
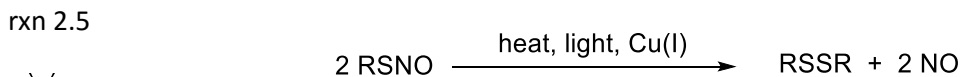
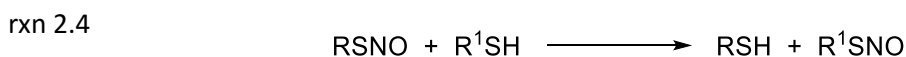


**Figure 1.4.** Two endogenous small molecule RSNOs: *S*-nitrosocysteine and *S*-nitrosoglutathione, and the exogenous species, *S*-nitroso-*N*-acetylpenicillamine, have each been extensively studied for use as NO donors in biomedical applications.

Many potential explanations for RSNOs' biological synthesis have been proposed and it's almost certain that multiple pathways exist. The dominant pathway involves NO's reaction with oxygen followed by an additional NO molecule to form  $N_2O_3$ , which in turn creates  $NO_2$  and  $NO^+$ , the nitrosating agent added to proximal thiols. Other pathways are circumstantially dependent, such as the reaction between peroxynitrite and a thiol, which could occur at locations of inflammation given the increased concurrent generation of NO and superoxide. Synthetically, RSNOs can be prepared via the nitrosation of thiols using alkyl or acidified nitrites (see Reaction 1.3) or via a transnitrosation reaction with a different RSNO (Reaction 1.4). Finally, RSNOs release NO via thermal or photolytic decomposition, or upon exposure to certain metal ions such as Cu(I) (see Reaction 1.5).<sup>2,59,64</sup>



Given the endogenous RSNOs' inherent biocompatibility, they have been thoroughly studied as a means to create controllable NO delivery from biomaterials and consequently increase biocompatibility; however, they have limitations including low stability in the presence of certain environmental factors and susceptibility towards thermal and photolytic decomposition.<sup>30,59,64</sup> These traits make device preparation and storage of RSNOs difficult.<sup>36,59</sup>

Further, the endogenous RSNOs are highly water soluble, resulting in extraction out of the polymeric materials when in contact with blood or urine. Therefore, various exogenous NO donors have been incorporated into biomedical polymers in attempt to utilize NO's effects, one of the most promising being *S*-nitroso-*N*-acetylpenicillamine (SNAP) (Figure 1.4).<sup>19-21,30,65</sup> Indeed, members/collaborators in the Meyerhoff lab recently demonstrated SNAP's ability to release NO over long durations (> 3 weeks) and decrease thrombus formation at localized treatment sites when it is doped within biomedical polymers.<sup>30</sup> Additionally, Colletta *et al.* recently reported that silicone rubber Foley catheters impregnated with SNAP were able to greatly decrease *Staphylococcus epidermidis* and *Proteus mirabilis* levels on the surface of the catheters for 2 weeks relative to controls (in an *in vitro* bioreactor model).<sup>7</sup> One limitation, however, is that an appreciable amount of SNAP, and likely the NAP disulfide dimer, leach from the polymers. Leaching decreases NO's efficacy and longevity at the localized polymer site and can cause NO's effects at unintended locations within the body.<sup>65</sup>

RSNOs have been covalently bound to the polymer backbone of biomaterials, as well as non-covalently dispersed.<sup>30,66</sup> Given RSNOs' inherent instability, device preparation steps requiring extended time allocation can cause premature NO release. While it would be desirable to incorporate RSNOs into the polymeric catheters via an extrusion process, RSNOs cannot withstand the elevated temperatures required for catheter extrusion.<sup>7</sup> Covalently-bound RSNOs do not suffer from leaching, but they often require significant preparation time. In comparison, non-covalently dispersed RSNOs can be loaded into a polymer much quicker, although they may be more prone to leaching.<sup>67,68</sup> RSNOs dissolved in polymer solutions can be cast without the need for elevated temperatures. Additionally, polymers can be solvent swelled in RSNO solutions. After the solvent has evaporated, the catheters are left impregnated with the RSNO species.<sup>65</sup> This technique allows loading of specific amounts of RSNO (given the soaking solution's original concentration), and was extensively studied in this thesis work with silicone rubber (see Chapter 3).

SNAP has been reported to have log P value (octanol-water partition coefficient) of 0.96, meaning that when exposed to comparable volumes of a nonpolar environment (i.e., hydrophobic polymer) and a polar environment such as blood or urine, ~10% of the loaded RSNO



is leached into the surrounding solution.<sup>30</sup> Given that the volume of blood in the body is considerably greater than that of the biomaterials used during applications, leaching can become a significant problem. For example, although Seabra *et al.* improved GSNO's lifetime by dispersing it throughout poly(vinyl alcohol) films. It was found that 90% of the GSNO was released during the first 24 h when the material was exposed to physiological conditions.<sup>69,70</sup> This dissertation aims to address the phenomenon leaching by incorporating lipophilic RSNOs into hydrophobic polymers. Given their shared non-polar character (and minimal aqueous solubility) it was hypothesized that lipophilic RSNOs will be better retained in hydrophobic polymers (see above and experimental sections of chapters in this thesis for further discussion of the strategy).

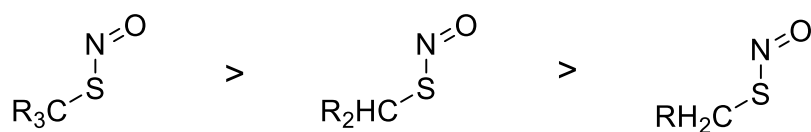


**Figure 1.5.** S-Nitrosothiols' general structure and substitution. Alkyl substitution is one of the factors effecting RSNOs' stability in terms of NO release. If other factors remain consistent, tertiary RSNOs are more stable than secondary, which in turn are more stable than primary RSNOs.

In addition to leaching, one of the important factors to consider when designing and studying RSNOs is their relative NO release stability. This directly affects the duration of potential treatments as well as the practicality of device storage. One of the defining characteristics of an RSNO that affects its stability is the alkyl substitution at the site of the S-nitroso functionality. It has been repeatedly observed that increased alkyl substitution correlates with greater stability (see Figure 1.5).<sup>59,64</sup> Although this is true, there are many other factors which are not well understood that also affect the stability of given RSNO species. The effects of alkyl substitution are noticed with RSNOs bearing similar structures; however, as will be demonstrated throughout this dissertation, variations of other functional groups can play a significant role in stability of the S-NO bond. A direct example of this relates to the two physiological small molecule RSNOs. Although GSNO and CysNO are both primary RSNOs, GSNO is widely accepted to be much more stable than CysNO under most conditions.<sup>67,71,72</sup> GSNO contains an additional carboxylic acid and multiple amide functionalities. This also increases the size and molecular weight of the RSNO.

While the effects of functional groups between CysNO and GSNO have a larger impact than the substitution (both are primary), this trend does not extend to SNAP, which does not have the added extensive functionality of GSNO, yet is almost always drastically more stable than the other RSNOs under all conditions.

Other factors affecting the stability of RSNOs include state of matter, molecular weight, polarity, steric bulk, and the solvent/polymeric environment.<sup>30,36,59,64</sup> Indeed, as will be demonstrated throughout this dissertation, different RSNOs are stabilized by certain polymers, while others are unaffected or even exhibit decreased stability.<sup>30</sup> There are a few explanations for this wide range of RSNO behavior. One hypothesis was proposed recently in which SNAP is stabilized in certain polymers such as Elasteon E2As, a polyurethane via formation of microcrystals depending on its concentration.<sup>7</sup> Data from this dissertation has supported this

**Table 1.2.** Many factors affect an RSNOs' stability including environmental factors and traits that are specific to the RSNO

Stimuli/Environmental Factors	RSNO Traits
Light	Sterics
Heat	Substitution
Cu(I)	Intramolecular SNO proximity
Solvent	Polarity (intemolecular dipole-dipole)
Polymer	Chelating functional groups
Concentration	Electron withdrawing and donating groups

hypothesis in several situations. For example, if SNAP derivatives with minor modifications affect the RSNOs' ability to crystallize, such derivatives are considerably less stable. Additionally, SNAP dissolved in solution (even containing phosphate buffered saline (PBS) and ethylene diamine tetra-acetic acid (EDTA)) is very unstable, while in the solid form it can last indefinitely under certain conditions.<sup>30,73</sup> While some RSNOs are labeled as possessing superior stability, researchers often fail to recognize that the stability depends on the stimulus that causes decomposition.<sup>73</sup> Consequently, this dissertation research aims to understand the newly prepared RSNOs' behavior in a variety of environments and conditions.

While RSNOs' stability is often a concern, and stimuli need to be avoided, applications which desire a sudden off/on NO release can benefit from photolytic cleavage of RSNOs. Exposing RSNOs to controlled light sources and specific wavelengths can provide a way to release NO at a desired flux and duration.<sup>74</sup> Throughout this dissertation, the photoactivity of many of the new RSNOs prepared was evaluated for potential use in related applications. Incorporating a catalyst into or onto biomaterials has been explored as a method to facilitate NO release. Previous work from the Meyerhoff group demonstrated that poly(vinyl chloride) containing a copper(II) cyclen analog was able to catalytically increase the natural NO release from the endogenous RSNOs.<sup>75</sup>

## **1.5 Summary**

Despite the widespread use of polymeric devices for modern medical procedures, serious health complications commonly occur as a result of the inherent limitations of the materials used. Enhancement of biomedical device surfaces or compositional materials with NO's dual antiplatelet and antimicrobial properties offers the potential to address many of these concerns, extending the lifetime of functionality of the devices. Progress has been made towards developing NO-releasing biomedical devices via the incorporation of NO-donors; however, several factors have hindered greater progress. Factors include small molecule leaching, stability, and control over the NO release levels and duration.

## **Research Statement**

The aim of the research reported in this dissertation is to study novel RSNOs, in and out of polymers, to determine their behavior with regard to potentially improving the biocompatibility of biomedical devices. The results from this work contributes to the ever-growing body of scientific knowledge regarding NO donors and their behavior in various environments. Specific goals throughout the thesis are to: 1) understand the behavior and performance of a wide range of RSNOs—including novel species; 2) develop RSNO/polymer systems that utilize NO's antiplatelet and antimicrobial properties to decrease platelet adhesion

and/or prevent the risk of infection; and 3) create such RSNO doped polymers systems that exhibit, long-term NO-release, minimal leaching, and substantial stability.

In Chapter 2, a wide range of lipophilic RSNOs—the majority of which are novel—are prepared and studied. The RSNOs were screened for the effects of various stimuli such as light and heat on their NO release while in the neat state, in solution, and within polymeric phases. These RSNO species were kept in environments with varying temperatures and light exposures to determine their storage stability. The RSNO/polymer systems exhibiting superior stability were then tested for leaching and their long-term NO release under physiological conditions. Finally, the stable RSNOs with optimized polymeric retention systems were tested for their ability to prevent platelet adhesion.

Chapter 3 focuses specifically on *S*-nitroso-*t*-dodecylmercaptan (SNTDM), one of the most promising RSNOs examined in Chapter 2. The behavior of SNTDM was studied in great detail under a wide array of conditions in response to several stimuli. Its leaching from several polymers when incorporated at varying concentrations was examined. Further, a swelling impregnation method was developed to incorporate SNTDM into PDMS catheters at various concentrations. SNTDM's photo-induced NO release in SR was studied as well, and is shown to be promising for potential photodynamic therapy. Lastly, the antimicrobial activity of NO releasing SR catheters containing SNTDM were tested against *S. aureus* by observing the bacterial killing effects and inhibition of biofilm formation. Much of this work was published in the *Journal of Material's Chemistry B* (2016,4, 422-430).

In Chapter 4, the most stable RSNOs, and polymers in which they were best retained, were further studied with respect to their photo-induced NO release. Research was aimed at developing a source of NO that possesses adequate photosensitivity for a controllable photoactivated NO release, but does not lose NO at undesirable times. While SNAP and SNTPMT are both fairly stable in response to light, SNTDM exhibited an unprecedented photosensitivity, with dramatic differences between the NO release in the dark, with ambient light, and upon exposure to a halogen bulb.

Chapter 5 summarizes the conclusions drawn from the research reported in this dissertation as well as provides future directions for further developing and understanding the

RSNO/polymer systems that were studied. Potential applications of the new molecules reported are proposed, and based upon the findings from this work, additional potentially useful RSNOs are suggested for future preparation and study. Appendix A contains a devised undergraduate organic laboratory experiment, written with my esteemed colleague, Dr. Alexander Wolf, and includes results that are similar to what students should obtain.

### 1.5 References

- 1 B. D. Ratner, *Biomaterials*, 2007, **28**, 5144–7.
- 2 E. J. Brisbois, R. P. Davis, A. M. Jones, T. C. Major, R. H. Bartlett, M. E. Meyerhoff and H. Handa, *J. Mater. Chem. B*, 2015, **3**, 1639–1645.
- 3 J. P. Guggenbichler, O. Assadian, M. Boeswald and A. Kramer, *GMS Krankenhaushygiene Interdiszip.*, 2011, **6**, Doc18.
- 4 J. Curtis and P. Klykken, *Dowcorningcom*, 2008, 1–8.
- 5 K. A. Marr, *Ann. Intern. Med.*, 1997, **127**, 275.
- 6 H. Handa, T. C. Major, E. J. Brisbois, K. A. Amoako, M. E. Meyerhoff and R. H. Bartlett, *J. Mater. Chem. B. Mater. Biol. Med.*, 2014, **2**, 1059–1067.
- 7 A. Colletta, J. Wu, Y. Wo, M. Kappler, H. Chen, C. Xi and M. E. Meyerhoff, *ACS Biomater. Sci. Eng.*, 2015, **1**, 416–424.
- 8 I. H. Jaffer, J. C. Fredenburgh, J. Hirsh and J. I. Weitz, *J. Thromb. Haemost.*, 2015, **13 Suppl 1**, S72–81.
- 9 J. M. Anderson, A. Rodriguez and D. T. Chang, *Semin. Immunol.*, 2008, **20**, 86–100.
- 10 S. B. H. S. P. G. F. F. M. M. Touraj Shirzadian, *J. Inj. Violence Res.*, 2012, 4.
- 11 D. F. Williams, *Biomaterials*, 2008, **29**, 2941–53.
- 12 *Biomedical Polymers*, Elsevier, 2007.
- 13 Y.-H. Joung, *Int. Neurorol. J.*, 2013, **17**, 98–106.
- 14 R. L. Poorter, F. N. Lauw, W. A. Bemelman, P. J. M. Bakker, C. W. Taat and C. H. N. Veenhof, *Eur. J. Cancer*, 1996, **32**, 2262–2266.
- 15 *Vascular Access: Principles and Practice*, Lippincott Williams & Wilkins, 2010.
- 16 Y. Onuki, U. Bhardwaj, F. Papadimitrakopoulos and D. J. Burgess, *J. diabetes Sci. Technol.*, 2008, **2**, 1003–1015.

- 17 S. Schopka, T. Schmid, C. Schmid and K. Lehle, *Materials (Basel)*, 2010, **3**, 638–655.
- 18 T. A. Horbett, *Cardiovasc. Pathol.*, 1993, **2**, 137–148.
- 19 M. B. Gorbet and M. V Sefton, *Biomaterials*, 2004, **25**, 5681–703.
- 20 A. W. Bridges and A. J. García, *J. Diabetes Sci. Technol.*, 2008, **2**, 984–94.
- 21 B. Hiebl, C. Hopperdietzel, H. Hünigen, K. Dietze, F. Jung and S. M. Niehues, *Clin. Hemorheol. Microcirc.*, 2014, **58**, 107–13.
- 22 A. Vertes, V. Hitchins and K. S. Phillips, *Anal. Chem.*, 2012, **84**, 3858–66.
- 23 A. L. Casey and T. S. J. Elliott, *Br. J. Nurs.*, **19**, 78, 80, 82 passim.
- 24 U. Römling and C. Balsalobre, *J. Intern. Med.*, 2012, **272**, 541–61.
- 25 D. Pavithra and M. Doble, *Biomed. Mater.*, 2008, **3**, 034003.
- 26 P. S. Stewart, *Int. J. Med. Microbiol.*, 2002, **292**, 107–13.
- 27 H. Shah, W. Bosch, K. M. Thompson and W. C. Hellinger, *The Neurohospitalist*, 2013, **3**, 144–51.
- 28 W. M. Saltzman, *Drug Delivery: Engineering Principles for Drug Therapy*, Oxford University Press, 2001.
- 29 M. Tanaka, K. Sato, E. Kitakami, S. Kobayashi, T. Hoshiba and K. Fukushima, *Polym. J.*, 2014, **47**, 114–121.
- 30 E. J. Brisbois, H. Handa, T. C. Major, R. H. Bartlett and M. E. Meyerhoff, *Biomaterials*, 2013, **34**, 6957–66.
- 31 M. M. Batchelor, S. L. Reoma, P. S. Fleser, V. K. Nuthakki, R. E. Callahan, C. J. Shanley, J. K. Politis, J. Elmore, S. I. Merz and M. E. Meyerhoff, *J. Med. Chem.*, 2003, **46**, 5153–61.
- 32 S. E. Sakiyama-Elbert, *Acta Biomater.*, 2014, **10**, 1581–7.
- 33 A. G. Kidane, H. Salacinski, A. Tiwari, K. R. Bruckdorfer and A. M. Seifalian, *Biomacromolecules*, **5**, 798–813.
- 34 D. L. Rabenstein, *Nat. Prod. Rep.*, 2002, **19**, 312–331.
- 35 J. Marcinkiewicz, M. Strus and E. Pasich, *Pol. Arch. Med. Wewnętrznej*, 2013, **123**, 309–13.
- 36 M. R. Miller and I. L. Megson, *Br J Pharmacol*, 2007, **151**, 305–321.
- 37 Y. Wu, Z. Zhou and M. E. Meyerhoff, *J. Biomed. Mater. Res. A*, 2007, **81**, 956–63.
- 38 M. Al-Mukhaini, P. Panduranga, K. Sulaiman, A. A. Riyami, M. Deeb and M. B. Riyami, *Heart Views*, 2011, **12**, 63–70.
- 39 J. Schröder, *Cardiovasc. Intervent. Radiol.*, 1993, **16**, 93–97.

- 40 H. Chen, Z. Zhang, Y. Chen, M. A. Brook and H. Sheardown, *Biomaterials*, 2005, **26**, 2391–9.
- 41 M. Shen, L. Martinson, M. S. Wagner, D. G. Castner, B. D. Ratner and T. A. Horbett, *J. Biomater. Sci. Polym. Ed.*, 2002, **13**, 367–90.
- 42 M. B. Gorbet and M. V Sefton, *J. Lab. Clin. Med.*, 2001, **137**, 345–55.
- 43 M. J. Wright, G. Woodrow, S. Umpleby, S. Hull, A. M. Brownjohn and J. H. Turney, *Am. J. Kidney Dis.*, 1999, **34**, 36–42.
- 44 M. Salwiczek, Y. Qu, J. Gardiner, R. A. Strugnell, T. Lithgow, K. M. McLean and H. Thissen, *Trends Biotechnol.*, 2014, **32**, 82–90.
- 45 W. B. Liechty, D. R. Kryscio, B. V. Slaughter and N. A. Peppas, *Annu. Rev. Chem. Biomol. Eng.*, 2010, **1**, 149–173.
- 46 J. S. Boateng, K. H. Matthews, H. N. E. Stevens and G. M. Eccleston, *J. Pharm. Sci.*, 2008, **97**, 2892–923.
- 47 S. Guo and L. A. Dipietro, *J. Dent. Res.*, 2010, **89**, 219–29.
- 48 M. Zilberman, A. Kraitzer, O. Grinberg and J. J. Elsner, *Handb. Exp. Pharmacol.*, 2010, 299–341.
- 49 Y. Suzuki, M. Tanihara, Y. Nishimura, K. Suzuki, Y. Kakimaru and Y. Shimizu, *ASAIO J.*, 1997, **43**, M858.
- 50 M. L. W. Knetsch and L. H. Koole, *Polymers (Basel)*, 2011, **3**, 340–366.
- 51 S. Habib and A. Ali, *Indian J. Clin. Biochem.*, 2011, **26**, 3–17.
- 52 A. R. Butler and D. L. H. Williams, *Chem. Soc. Rev.*, 1993, **22**, 233.
- 53 S. Hayat, S. A. Hasan, M. Mori, Q. Fariduddin and A. Ahmad, *Nitric Oxide Plant Physiol.*, 2009, 1–16.
- 54 W. K. Alderton, C. E. Cooper and R. G. Knowles, *Biochem. J.*, 2001, **357**, 593–615.
- 55 C. Tziros and J. E. Freedman, *Curr. Drug Targets*, 2006, **7**, 1243–51.
- 56 F. C. Fang, *Nitric Oxide*, 2012, **27**, S10.
- 57 P. Valliance and I. Charles, *Gut*, 1998, **42**, 313–314.
- 58 F. C. Fang, *J. Clin. Invest.*, 1997, **99**, 2818–25.
- 59 H. Al-Sa'doni and A. Ferro, *Clin. Sci. (Lond)*, 2000, **98**, 507–20.
- 60 L. K. Keefer, *ACS Chem. Biol.*, 2011, **6**, 1147–55.
- 61 W. L. Storm, M. H. Schoenfisch, *ACS Appl. Mater. Interfaces*, **2013**, 5 (11), pp 4904–4912
- 62 H. Ren, J. Wu, C. Xi, N. Lehnert, T. Major, R. H. Bartlett and M. E. Meyerhoff, *ACS Appl.*

- Mater. Interfaces*, 2014, **6**, 3779–83.
- 63 E. J. Brisbois, R. P. Davis, A. M. Jones, T. C. Major, R. H. Bartlett, M. E. Meyerhoff and H. Handa, *J. Mater. Chem. B. Mater. Biol. Med.*, 2015, **3**, 1639–1645.
- 64 K. A. Broniowska and N. Hogg, *Antioxid. Redox Signal.*, 2012, **17**, 969–80.
- 65 A. R. Ketchum, M. P. Kappler, J. Wu, C. Xi and M. E. Meyerhoff, *J. Mater. Chem. B*, 2016.
- 66 Y. Lu, A. Shah, R. A. Hunter, R. J. Soto and M. H. Schoenfisch, *Acta Biomater.*, 2015, **12**, 62–9.
- 67 J. M. Joslin, S. M. Lantvit and M. M. Reynolds, *ACS Appl. Mater. Interfaces*, 2013, **5**, 9285–94.
- 68 A. M. A. de Menezes, G. F. P. de Souza, A. S. Gomes, R. F. de Carvalho Leitão, R. de A. Ribeiro, M. G. de Oliveira and G. A. de Castro Brito, *J. Periodontol.*, 2012, **83**, 514–21.
- 69 A. B. Seabra and M. G. De Oliveira, *Biomaterials*, 2004, **25**, 3773–82.
- 70 A. B. Seabra, L. L. da Rocha, M. N. Eberlin and M. G. de Oliveira, *J. Pharm. Sci.*, 2005, **94**, 994–1003.
- 71 D. L. H. Williams, in *Nitrosation Reactions and the Chemistry of Nitric Oxide*, 2004, pp. 137–160.
- 72 M. R. Miller and I. L. Megson, *Br. J. Pharmacol.*, 2007, **151**, 305–21.
- 73 B. Roy, A. du Moulinet d’Hardemare and M. Fontecave, *J. Org. Chem.*, 1994, **59**, 7019–7026.
- 74 D. A. Riccio, K. P. Dobmeier, E. M. Hetrick, B. J. Privett, H. S. Paul and M. H. Schoenfisch, *Biomaterials*, 2009, **30**, 4494–502.
- 75 K. Liu and M. E. Meyerhoff, *J. Mater. Chem.*, 2012, **22**, 18784–18787.



## CHAPTER 2.

### THE SYNTHESIS AND STUDY OF LIPOPHILIC ALKYL AND ARYL S-NITROSOTHIOLS

#### 2.1 Introduction

As discussed in Chapter 1, considerable research has focused on improving the biocompatibility of medical devices by preventing thrombosis and reducing the risk of infection. Nitric oxide donors such as *S*-nitrosothiols have demonstrated the potential to do so.<sup>1,2</sup> The most commonly studied small molecule RSNOs are the synthetic species *S*-nitroso-*N*-acetylpencillamine (SNAP) and the physiological species, *S*-nitrosocysteine (CysNO) and *S*-nitrosoglutathione (GSNO). These three RSNOs are inherently biocompatible, but their applications have been limited in several ways.<sup>3</sup> CysNO and GSNO are both primary RSNOs, which limits their stability since alkyl substitution has repeatedly been demonstrated as a major factor affecting the rate of NO-release.<sup>4</sup> SNAP, a tertiary RSNO, is considerably more stable and consequently better suited for biomedical device preparation and storage. SNAP, CysNO, and GSNO are all hydrophilic, which is partially responsible for their decreased retention within polymers when exposed to aqueous solutions (leaching).<sup>5,6</sup> Given the unique NO release profiles of different RSNOs (as well as other NO-donors), considerable research has focused on adding to the library of NO releasing compounds for understanding their behavior and potential medical applications.

The Meyerhoff research group has determined that SNAP's stability can be increased by incorporating it into different biomedical grade polymers such as Elasteon-E2As (E2As), CarboSil (CS), and silicone rubber (SR).<sup>7</sup> SNAP is retained in these hydrophobic polymers more so than in

hydrophilic ones such as Tecoflex SG-80A (TF), likely due to their reduced water uptake.<sup>7</sup> However, leaching of these NO donors is still a significant concern and this reduces the duration of device use. Also these devices can excrete the disulfide of SNAP, the byproduct of NO release, into the body.

Given the relationship between a molecule's polarity and preference to retain in an environment of similar polarity, research in this chapter is focused on preparing and studying a variety of lipophilic RSNOs without other functional groups. Throughout this chapter a range of lipophilic RSNOs will be discussed with regard to their performance in environments relevant to biomedical applications. The RSNOs pertinent to this chapter are listed in Table 2.1 with their corresponding LogP values (log octanol/water partition coefficient). Their Lewis structures are depicted in each corresponding section. Leaching values are compared with SNAP's in certain polymers as well. The effects of SNAP's LogP on leaching is discussed in further detail below.

**Table 2.1** RSNOs prepared in this chapter, the percentage yields obtained following synthesis, and their corresponding LogP values. n=3 for RSNOs with a standard deviations indicated.

Alkyl RSNO	% RSNO	LogP	RSNO w/Additional Funct. Groups	% RSNO	LogP
S-nitroso-t-butylthiol (SNTBT)	90.4 ± 7.1	1.7	S-nitrosoglutathione (GSNO)	100	-3.2
S-nitrosohexanethiol (SNHT)	82.3 ± 0.9	3.1	S-nitroso-N-acetylpenicillamine (SNAP)	100	0
S-nitroso-2-ethylhexanethiol (SNEHT)	72	4.1	S-nitrosocholesterolthiol (SNCT)	8.1 ± 6.4	10.8
S-nitrosooctanethiol (SNOT)	79.2 ± 3.3	4.2	S-nitroso-triphenylmethanethiol (SNTPMT)	99.0 ± 3.8	5
S-nitrosodecanethiol (SNDT)	90.1 ± 4.2	5.3	S-nitrosobenzenethiol (SNBzT)	?	1.9
S-nitroso-t-dodecanemercaptan (SNTDM)	98.4 ± 2.9	6	S,S-dinitrosolipoic acid (SSDNLA)	?	2.4
S-nitrosododecanethiol (SNDT)	96 ± 7.0	6.3			
S-nitrosohexadecanethiol (SNHDT)	8.0 ± 5.1	8.4			
S-nitrosooctadecanethiol (SNODT)	5.3	10			

Reducing leaching is important since NO's inherent instability limits its utility to localized treatments. NO is oxidized in the presence of oxygen to form nitrogen dioxide (NO<sub>2</sub>), which is toxic. Additionally, as occurs in the blood, NO is rapidly consumed by oxyhemoglobin, forming methemoglobin—thus deactivating it for any beneficial reactions.<sup>8</sup> Due to its reactivity, NO should be released from biomedical devices in controlled amounts, for specific durations, and at discrete locations. RSNOs are considerably more stable than NO itself; however, they decompose

to release NO under thermal and photolytic conditions. Consequently, minimizing leaching can greatly increase a device's efficacy.

Most of the lipophilic alkyl RSNOs studied in this dissertation have seen little to no use for biomedical applications. RSNOs' stability regarding NO release is not fully understood in many instances and as a result, is attributable to factors beyond those commonly considered. The RSNOs examined here are relatively simple, with minimal additional functional groups. Initially, this was hypothesized to form a direct trend: the higher the alkyl substitution, the longer the duration of NO release. Different biomedical applications can benefit from unique durations of NO release, and the goal here was to correlate NO release duration with structure, to provide a continuum of NO release times. For example, long-term NO-releasing catheters would be applicable for indwelling urinary catheterization since they are often required for several weeks or longer.<sup>3</sup> Procedures such as angioplasty could benefit from NO-releasing balloons designed to release NO on the timescale of only a few hours. The inherent stability of an RSNO manifests in several ways including the duration of NO release and response to the three principle stimuli for decomposition (heat, light, and Cu(I)). Also, because the kinetics of NO release are dependent on so many variables the rate order is often inconsistent. RSNOs' response to environmental stimuli is important for the practicality of device storage as well as potentially offering a means to control NO release during medical applications.<sup>9-12</sup>

During research for this chapter, the following properties are evaluated for the most promising RSNOs:

- Storage stability (varying temperature and light exposure)
- Effect of phase on NO release (neat, solution, polymer)
- Duration and flux of NO release (polymer specific)
- RSNO Leaching (polymer specific)
- Activity toward reducing platelet adhesion

These factors serve as ideal goals for designing novel RSNOs and developing a NO releasing biomaterial with improved biocompatibility.<sup>1,3,13</sup> The model RSNO incorporated polymer system is depicted in Figure 2.1. After determining the lipophilic RSNOs with superior

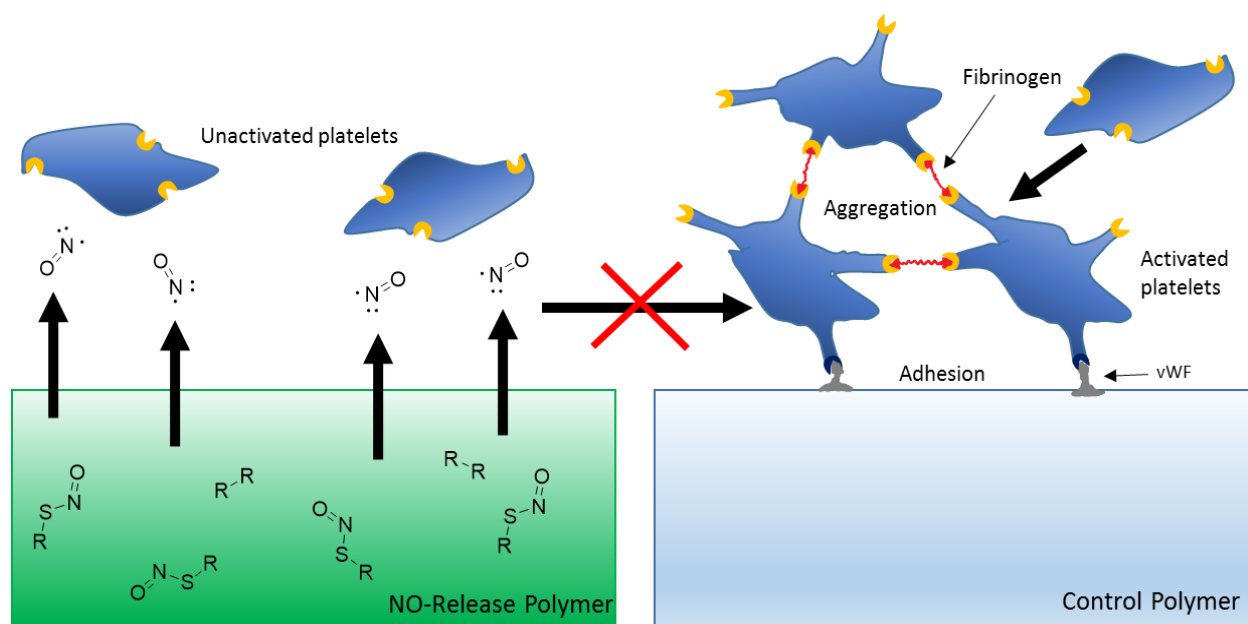


**Figure 2.1.** The model NO-release system utilizes polymers incorporated with RSNOs. As NO is released it has the ability to prevent platelet activation, and thus inhibit thrombus formation. This contrasts with the control polymer, where clot formation can occur following the unimpeded platelet adhesion.

performance based on the above criteria, and optimizing behavior in the most promising polymers, they were tested for their ability to decrease platelet adhesion. NO has previously and consistently demonstrated the ability to reduce platelet adhesion and consequently inhibit thrombus formation.<sup>14</sup> Demonstrating that the target RSNO/polymer systems can do this suggests they possess the potential for improving the biocompatibility of the biomaterial with regard to thrombus formation.

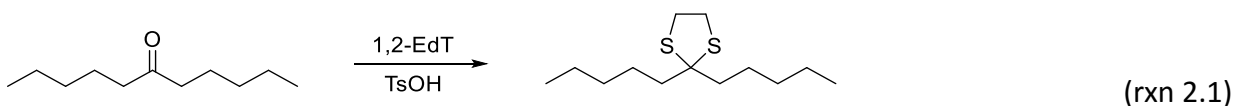
## 2.2 Experimental

### 2.2.1 Materials

N-Acetyl-DL-penicillamine (NAP), penicillamine, acetic anhydride, pyridine, glutathione, sodium chloride, magnesium sulfate, sodium phosphate dibasic, potassium phosphate monobasic, ethylenediaminetetraacetic acid (EDTA), tetrahydrofuran (THF), sulfuric acid, diethyl ether (Et<sub>2</sub>O), N,N-dimethylacetamide (DMAc), hexane, chloroform (CHCl<sub>3</sub>), silica gel, molecular sieves, methanol (MeOH), sodium nitrite (NaNO<sub>2</sub>), *t*-butylnitrite (*t*-BuNO<sub>2</sub>), *n*-butylnitrite (BuNO<sub>2</sub>), methylnitrite, ethylnitrite, 2-butyl nitrite (*sec*-BuNO<sub>2</sub>), dodecanethiol (DDT), 6-undecanone (UDT), *tert*-dodecylmercaptan (TDM), *tert*-butanethiol (TBT), *n*-butyl lithium (*n*-BuLi), *d*<sub>6</sub>-chloroform (CDCl<sub>3</sub>), dimethylsulfoxide (DMSO),

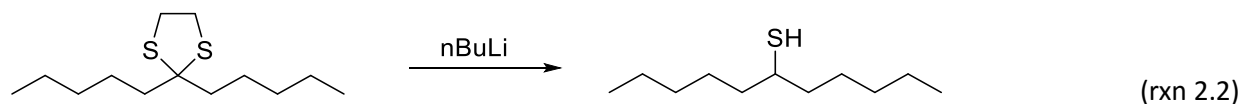
triphenylmethanethiol (TPMT), 1S-hexanethiol, 1S-octanethiol, 1S-decanethiol, 1S-hexadecanethiol (HDT), 1S-octadecanethiol (ODT), cholesterolthiol (ChoT), hexylamine were purchased from Sigma-Aldrich (St. Louis, MO). Hydrochloric acid and sulfuric acid were purchased from Fisher Scientific (Pittsburgh, PA). Tecophilic SP-60D- 60 and Tecoflex SG-80A were obtained from Lubrizol Advanced Materials Inc. (Cleveland, OH). Dow Corning RTV 3140 Silicone Rubber (SR) was purchased from Ellsworth Adhesives (Germantown, WI). CarboSil 20 90A was obtained from the Polymer Technology Group (Berkeley, CA). Elast-eon TM E2As was purchased from AorTech International, plc (Scoresby, Victoria, Australia). Fresh platelet rich plasma from a pig was obtained from Dr. Robert H. Bartlett's laboratory in the Department of Surgery, University of Michigan Medical School. All aqueous solutions were prepared with 18.2 MΩ deionized water using a Milli-Q filter (Millipore Corp., Billerica, MA). Phosphate buffered saline (PBS), pH 7.4, containing 138 mM NaCl, 2.7 mM KCl, 10 mM sodium phosphate, 100 μM EDTA was used for all *in vitro* experiments.

### 2.2.2 2,2-Dipentyl-[1,3]dithiolane Synthesis



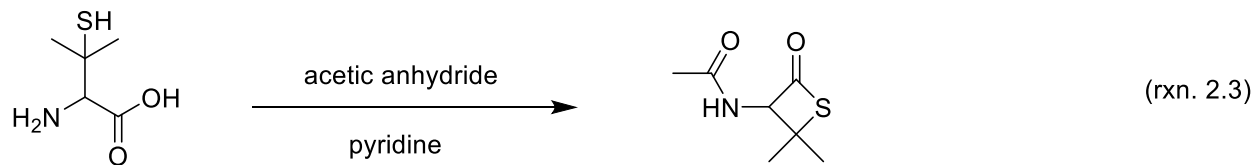
The thioketal was prepared using a previously reported method.<sup>15</sup> Briefly, 6-undecanone, 1,2-ethanedithiol, TsOH, and benzene were added to a round bottom flask and azeotropically distilled. The reaction mixture was washed with water, and the organic layer dried with MgSO<sub>4</sub> before removing the benzene via rotary evaporation.

### 2.2.3 6-Undecanethiol Synthesis



This thiol was synthesized as reported previously.<sup>15</sup> Briefly, 2,2-dipentyl-[1,3]dithiolane was added to 0 °C Et<sub>2</sub>O under N<sub>2</sub>. Excess n-BuLi was added dropwise via a syringe and allowed to warm to RT overnight. After quenching the solution with water, the organics were separated, dried with MgSO<sub>4</sub>, and the Et<sub>2</sub>O removed via a stream of N<sub>2</sub> to give a red/brown liquid.

### 2.2.4 N-(2,2-Dimethyl-4-oxothietan-3-yl) acetamide Synthesis

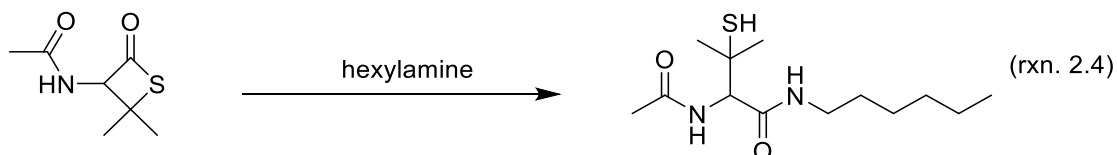


Penicillamine

*N*-(2,2-dimethyl-4-oxothietan-3-yl)acetamide

The thiolactone was prepared using an established method.<sup>16</sup> Briefly, penicillamine was dissolved in pyridine and chilled to 0 °C. Two and two tenths (2.2) equiv. of acetic anhydride were added dropwise and the solution warmed to room temperature for ~20 h. Dilute HCl was added and the thiolactone extracted into CHCl<sub>3</sub>. The orange residue was dissolved in EtOH and precipitated from -78 C pentane.

### 2.2.5 2-Acetamido-*N*-hexyl-3-mercapto-3-methylbutanamide (SNHC<sub>6</sub>H<sub>13</sub>)



*N*-(2,2-dimethyl-4-oxothietan-3-yl)acetamide

2-acetamido-*N*-hexyl-3-mercapto-3-methylbutanamide

The NAP amide derivative was synthesized using a variation of a previously reported method.<sup>16</sup> The thiolactone above was reacted in chloroform with hexylamine for 24 h, washed with dilute HCl, and dried with MgSO<sub>4</sub>.

### 2.2.4 General Nitrosation



Nitrosations of a wide variety of thiols are well documented and straightforward.<sup>17</sup> Lipophilic thiols are typically nitrosated in THF or Et<sub>2</sub>O using *t*-BuNO<sub>2</sub> at room temperature (RT).<sup>17,18</sup> All nitrosations were performed in vessels wrapped in aluminum foil so as to exclude light. Nitrosations are not particularly sensitive to equivalents used, most often only requiring a slight excess of nitrosating agents (1.1-2.0 eq.).<sup>18</sup> The majority of nitrosation reactions for the RSNOs prepared herein were completed in less than 45 min, commonly with quantitative yields. Purifications typically required only rotary evaporation so as to remove excess nitrosating agent

and the *t*-BuOH byproduct. The percentage of RSNO obtained following synthesis can readily be determined by stimulating NO release with heat/light/Cu(I) while the sample is attached to a chemiluminescence nitric oxide analyzer (NOA). The direct 1:1 ratio between NO/RSNO allows NO integration to correlate with the amount of RSNO tested. For tests to determine the extent of nitrosation, product solutions were exposed to heat/light to convert all RSNO to disulfide (RSSR).<sup>19</sup> Variations on specific RSNOs' nitrosation procedures are mentioned in their respective sections, below.

### **2.2.5 Preparation of RSNO-Doped Films**

A known mass of RSNO was dissolved in a THF/polymer solution. The solution was stirred for a few minutes to ensure homogeneity of the film casting solution composition. The solutions were then cast into Teflon rings on a Teflon plate and dried overnight under a low stream of N<sub>2</sub>. Following solvent evaporation, discs were punched out of the films using a d=0.7 cm hole punch, weighed, and if desired for the experiment, dip-coated in a pure 200 mg polymer/4 mL THF solution before being dried under vacuum.<sup>7</sup>

### **2.2.6 NO Release Measurements**

Nitric oxide was measured using a Sievers chemiluminescence Nitric Oxide Analyzer (NOA) 280 (Boulder, CO). Samples were placed in the sample vessel either neat, dissolved in DMSO, or when in films, immersed in PBS (pH 7.4) containing 100 μM EDTA. Nitrogen was bubbled into the solution. Nitric oxide was then purged and swept from the headspace using the N<sub>2</sub> gas stream into the chemiluminescence detection chamber of the NOA. The sample vessels varied depending on the experiment—either clear or amber cells were used to provide control over light exposure. The RSNOs or RSNOs within polymer films were exposed to a light source (100 W halogen floodlight (GE model 17986)) at variable distances for photolysis experiments, as well as heated in a water bath. If applicable, a DMSO/CuSO<sub>4</sub>/cysteine solution could be injected to catalyze NO release. To ensure film samples remain submerged in the chamber buffer during experiments, they were impaled on needles and suspended in solution to measure NO release rates with the NOA.<sup>19</sup>

### **2.2.7 Determining the RSNO Levels in Polymer Films**

For initial experiments, the amount of RSNO was determined by stimulating NO release from a piece of polymer with a known mass using heat, light, and a Cu(II)/cysteine solution, and integrating the NO release curve. After obtaining the molar absorptivity of compounds, the amount of RSNO in a polymer could also be determined by extracting the RSNO content into solution (usually CHCl<sub>3</sub>), or as with the case of soluble polymers, dissolving a known mass (usually in THF or DMAc).<sup>19</sup>

### **2.2.8 Determining the RSNOs' Molar Absorptivity Coefficients**

Given the fact that an unknown amount of RSNO could have decomposed during sample preparation, it was necessary to determine the percent of RSNO which was attributable to the mass being tested. Consequently, solutions of the various RSNOs were simultaneously injected into the NOA sample cell and also tested on the UV-Vis Spectrophotometer. The ratio of RSNO:mass could then be used to back calculate the amount tested on the UV-Vis spectrophotometer, so as to obtain an accurate molar absorptivity of the given RSNO at the  $\lambda_{\max}$  around 340 nm.<sup>19</sup>

### **2.2.9 Storage Stability Studies**

The new RSNOs were tested for stability in neat as well as in solution and polymeric phases under various conditions including -20 °C freezer, 4 °C refrigerator, RT cupboard, north or west facing windowsills, shelves exposed to ambient room conditions and some sun exposure, or a dark PT oven. Concentrations of RSNOs in the stored samples were tested at various time points as described above. Samples were stored in vials for the duration of storage stability studies, with the films impaled on needles above desiccant.<sup>19</sup>

### **2.2.10 Long Term NO-Release Measurements**

Stored films/needles were removed from vials and rinsed to physically remove any residual surface RSNOs, before testing their NO release as described above—taking care to



ensure measurement conditions were comparable to those during incubation (pH=7.4 PBS/EDTA, 37 °C, dark). The soaking buffer solutions were kept to test for leached species, if appropriate.<sup>7</sup>

#### **2.2.11 Leaching Measurements**

The soaking solutions from the suspended films were shaken with immiscible solvent to extract/wash any leached species. The solution was injected into the NOA or tested via the RSNO's ultraviolet absorbance at ~340 nm to quantify the amount of leached (and non-decomposed) RSNO.<sup>19</sup>

#### **2.2.12 Preparation of NO Releasing Polymer Coated Plates**

Polymer/THF solutions were prepared with varying amounts of RSNOs dissolved in different samples. After the solutions were homogenized, 0.25 mL aliquots were pipetted into the wells of a polypropylene 96-well plate. The plates were dried for ~18 h under dark ambient conditions and ~6 h under vacuum.<sup>14</sup>

#### **2.2.13 *In Vitro* Platelet Adhesion Studies**

Porcine blood was drawn into a citrate anticoagulant in a 9:1 volumetric ratio. The blood with anticoagulant was centrifuged at 110 g for 15 min at RT. The resulting platelet-rich plasma was collected and the [Ca<sup>2+</sup>] raised to 2 mM using CaCl<sub>2</sub>. The polymers within the microtiter plate wells were prehydrated with 200 μL PBS at 37 C for 1 h. After decanting the PBS, 100 μL of the recalcified platelet-rich plasma was added to each polymer-coated well. The trays were incubated for 1 h at 37 C. The PBS was decanted, and the wells washed with 200 uL of PBS.<sup>14</sup>

#### **2.2.14 LDH Assay**

The lysing buffer was added to each well and incubated for 1 h at 37 C. The tray was gently agitated. One hundred μL of each lysate solution was then pipetted into a different 96-well microtiter plate containing 100 μL LDH assay reagent. After 1 h, each well's absorbance at λ=450 was monitored for 1 h.<sup>14</sup>

### **2.3 Results and Discussion**

#### **2.3.1 Nitrosations**

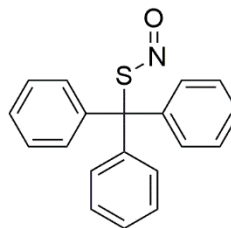
RSNOs are nitrosated from the corresponding thiol via the chemical Reaction 1.3. Nonpolar thiols, particularly those insoluble in aqueous solutions, are commonly nitrosated using *tert*-butyl nitrite (*t*-BuNO<sub>2</sub>), as is the case in this work. Acidified inorganic nitrite is the predominate nitrosating agent for thiols in aqueous solutions, such as SNAP. The reactions are usually quantitative with potential impurities solely limited to unreacted thiol and the disulfide decomposition product.<sup>17,20</sup> Given that RSNOs have intense colors (green for tertiary, red for secondary or primary alkyl substitution), their nitrosation and NO release can be observed visually for the most reactive species. For example, the least stable RSNOs such as SNCT and SNODT exhibit a rapid loss of color within a matter of minutes. Relating an RSNOs' color change and NO release was developed into an undergraduate laboratory experiment (see Appendix A).

Depending on the stability of a given RSNO, some may have decomposed by the time the product is isolated. If the decomposition is significant, the RSNOs are less useful for potential applications as a greater mass of the RSNO preparation would be needed to obtain comparable starting concentrations of RSNOs in the polymers. The resulting higher concentrations of RSNO will increase leaching. Such rapid decomposition also suggests they are unstable and storage would not be feasible for devices made with these RSNOs. The main RSNOs that were prepared for this chapter are listed in Table 1 above, with the amount of RSNO present following nitrosation and separation indicated as well.

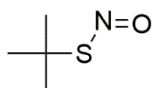
Several variables were examined to rule out the less useful RSNOs and determine optimal conditions including nitrosating agent, solvent, temperature, and the reaction time. Optimal conditions should minimize decomposition during nitrosations. The most promising RSNOs, SNTDM and SNTPMT, as subsequent experiments will indicate, were obtained in pure form, following removal of solvent, excess nitrosating agent, and its byproduct (*t*-BuOH). Their structures are shown below in Figure 2.2 with other RSNOs that are the most pertinent to this chapter's experiments.



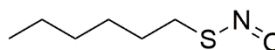
S-nitroso-*tert*-dodecylmercaptan (SNTDM)



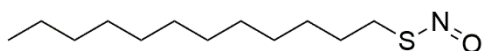
S-nitroso-triphenylmethanethiol (SNTPMT)



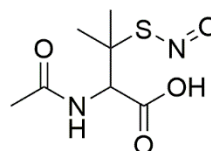
S-nitroso-*tert*-butylthiol (SNTBT)



S-nitrosohexanethiol (SNHT)



S-nitrosododecanethiol (SNDDT)



S-nitroso-*N*-acetylpenicillamine (SNAP)

**Figure 2.2.** Structures of six RSNOs prepared in this work. SNTDM and SNTPMT are the most promising lipophilic hydrocarbon RSNOs to date. The primary RSNOs, SNDDT and SNHT, are less stable; however, they, along with SNTBT provide a useful contrast to explore the effects of the RSNOs' structure on their behavior in response to various reaction and storage conditions. SNAP is a stable and well-studied RSNO that serves as a point of comparison for several different testing methods employed in these studies.

For the tested species, varying solvents had minimal effect on the RSNOs' decomposition during nitrosation. SNTDM, SNDDT, and SNHT were synthesized under comparable conditions in various solvents and their maximum concentrations noted in Table 2.2. The highest concentrations (measured by UV absorbance) indicate the maximum level of RSNO and account for any loss by decomposition as well as incomplete nitrosation. RSNO concentrations in hexane were slightly lower during synthesis than in the other solvents; however, these differences were minimal and would need to be repeated with additional samples and more frequent measurements to draw any clear-cut conclusion regarding the slight variation between levels.

Regardless, most follow-up nitrosations were not performed in hexane. Although hexane is the least polar solvent, a trend regarding polarity was not observed given the fact DMSO is the most polar solvent yet it does not yield the highest levels of any of the RSNOs that were prepared and tested. Other published RSNOs with lower aqueous solubility such as SNTDM have previously been synthesized using toluene, with further purification not performed nor explained.<sup>18,21,22</sup> Before subsequent experiments were conducted, the research groups accounted for the impurities but did not remove them.<sup>21,22</sup> Given the negligible effects of solvent on NO release during preparation, those with low boiling point (BP) such as CHCl<sub>3</sub>, THF, and Et<sub>2</sub>O are most suitable for the research herein given their facile removal (see Table 2.2). The effects of temperature were investigated as well.

Increasing the temperature unfortunately did not prove to be advantageous. Although elevated temperature may increase the reaction rate of nitrosation, it also increases the rate of thermal decomposition. Decreasing the solvent's temperature was somewhat beneficial for the less stable RSNOs. The two effects are demonstrated by the synthesis of *S*-nitrosohexanethiol (SNHT), one of the least stable RSNOs. SNHT was nitrosated at 0 °C, RT, and PT (see Figure 2.3).

**Table 2.2.** Shows the highest % of RSNO observed during a nitrosation in the listed solvents.

	SNTDM	SNDDT	SNHT
Hexane	93	92	93
THF	95	102	97
Et <sub>2</sub> O	94	95	97
CHCl <sub>3</sub>	102	95	97
DMSO	94	101	94

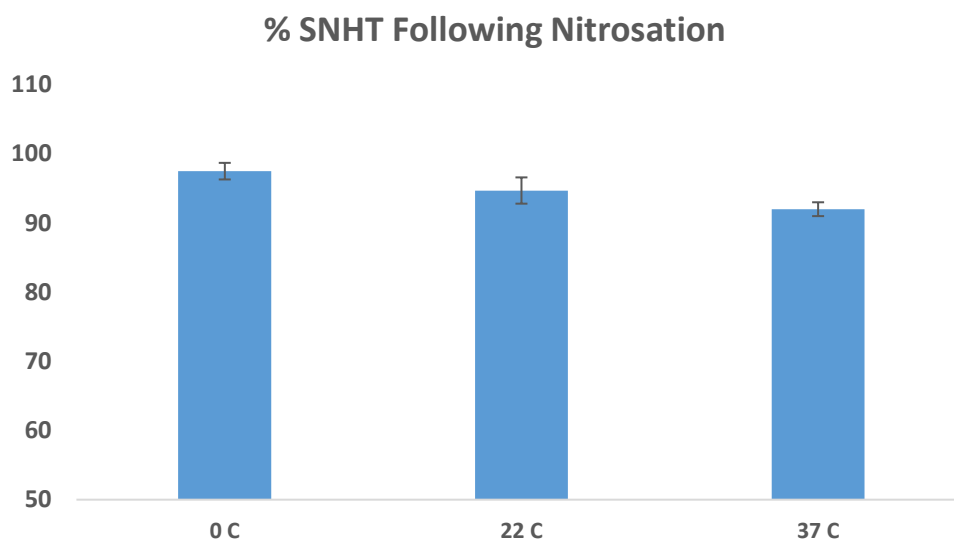


**Figure 2.3.** SNHT's nitrosation at different temperatures depicts the relative effects on the nitrosation and decomposition's rate. n=3

This suggests, at least for the less stable RSNO species (e.g., SNHT, SNCT, SNODT), that reducing the temperature decreases the rate of decomposition more than the rate of nitrosation and is thus advantageous. Measurements were taken directly using aliquots without purification to minimize further NO release. Although nitrosating hexanethiol at 0 °C allows 97.5 +/- 1.2 % RSNO to be present in the final product, biomedical applications would obviously require purification steps, which in the case of SNHT correlated with an additional loss of 15 % RSNO, making it not ideal for any potential real-world biomedical application.

SNTDM was prepared in the literature at 0 °C;<sup>21</sup> however, this was found not to be necessary and comparable yields were obtained in this work at RT. This is likely because SNTDM's stability is not significantly affected by being in solution phase rather than neat (longer durations are not detrimental). This contrasts with SNAP, the common synthetic and very stable RSNO, that is commonly nitrosated at a decreased temperature, due to its diminished stability when dissolved in an aqueous solution.<sup>7</sup> To test the effects of the nitrosating agent's steric hindrance on degree of RSNO formation, different alkyl nitrites were used including n-butyl nitrite, sec-butyl nitrite, iso-propyl nitrite, and *t*-BuNO<sub>2</sub> (see Figure 2.4 and Table 2.3). Surprisingly, under the typical conditions, *t*-BuNO<sub>2</sub> remained comparable if not the most successful nitrosation agent, despite its steric hindrance, even when nitrosating the bulky tertiary thiols SNTDM and SNTPMT.

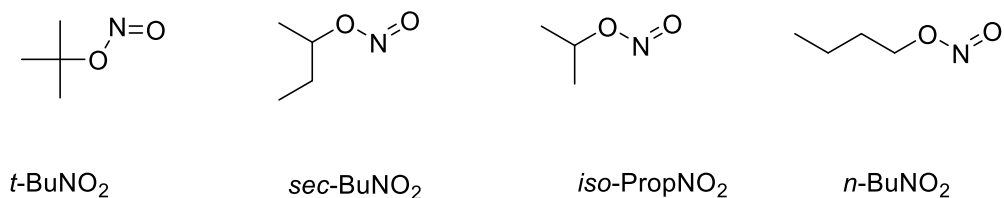


**Figure 2.4.** Nitrosating agents of varying alkyl substitution. Nitrites are the most common class of nitrosating agent.

**Table 2.3.** Time (min) until maximum UV absorption.

RSNO	<i>t</i> -BuNO <sub>2</sub>	<i>sec</i> -BuNO <sub>2</sub>	<i>iPr</i> -NO <sub>2</sub>	<i>n</i> -BuNO <sub>2</sub>
SNTPMT	45	45	40	45
SNTDM	30	30	35	30
SNTBT	10	15	15	5
SNDDT	5	10	5	10

The UV-Vis experiments do not account for the concurrent decomposition that is occurring for these species; however, since three of the tested thiols are tertiary, and thus would be most sensitive to steric effects, the nitrosating agents' structure also should also not play a role in the preparation of the less stable RSNOs. SNDDT is stable enough that during the time period tested, no detectable NO is released (since purification was not performed).

The more hindered RSNOs, SNTDM and SNTPMT, were nitrosated to a greater extent using increased reaction times, requiring approximately 30 and 45 min, respectively, with typical nitrosating agent levels (~1.1 equiv). This is viable for SNTDM and SNTPMT since their heightened stabilities allow longer reaction periods. The maximum RSNO concentration is obtained sooner for the other two species: 5-15 min for SNTBT and 5-10 min for SNDDT. Using 1.1 equiv. *t*-BuNO<sub>2</sub>, the tertiary RSNO, SNTBT, is nitrosated after 10 min, which is longer than SNDDT, the primary RSNO. Although all three are tertiary, SNTDM and SNTPMT likely take longer than SNTBT to reach a maximum RSNO concentration because the molecules themselves are considerably bulkier. For all the tested species, it appears that the thiols' substitution trumps the overall molecular bulk with respect to rate of reaction to form the RSNO. This was indicated by the fact that SNDDT was fully synthesized in 10 min less time compared to SNTBT, despite being bulkier overall (see Figure 2.5).

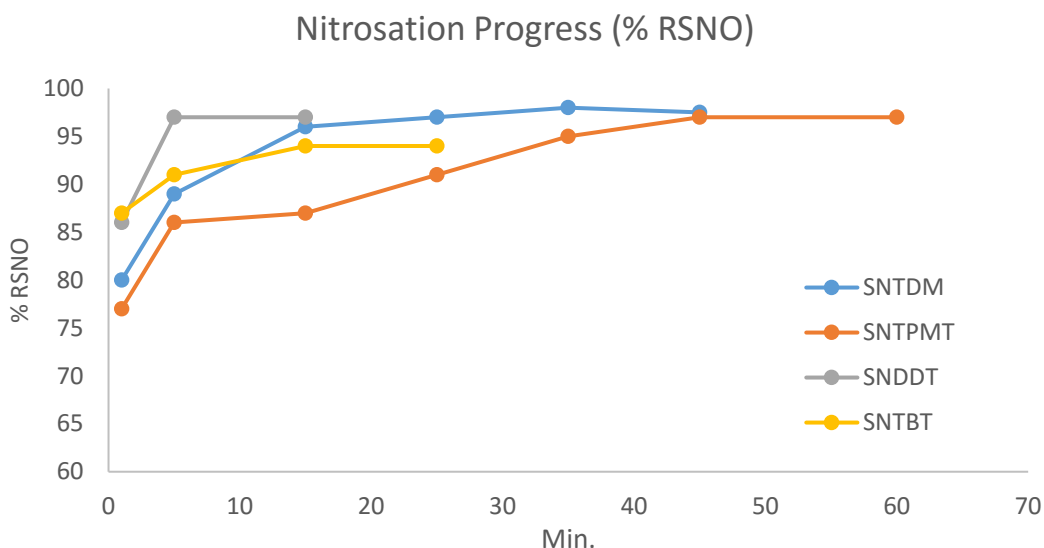
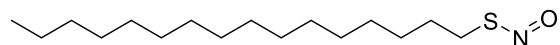


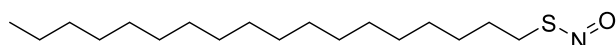
**Figure 2.5.** Nitrosation progress as indicated by the RSNO concentration in reaction mixture. Nitrosations used 1.1 equiv. of  $t\text{-BuNO}_2$ .

While the majority of nitrosations are so rapid that a drastic color change is noted immediately, nitrosation to form SNCT and SNODT was found to be harder to observe due to a less intense color change. This makes any qualitative indication of an approximate nitrosation time impossible (see Figure 2.6 for their structures). Equimolar or a slight excess of nitrosating agents are predominately used in the literature, but very slow nitrosation was observed in the case of SNCT, and the reaction actually appeared to “stall” after 2 h, with only 73 % of the SNCT formed (compared to that expected). This observed conversion was not lower due to decomposition, as after adding additional  $t\text{-BuNO}_2$  additional NO was produced. SNHDT was not monitored by  $^1\text{HNMR}$ ; however, a very slow color change was observed as well.

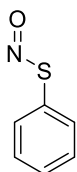
An increased amount of nitrosating agent was then used and the reaction monitored by  $^1\text{HNMR}$ . Whereas 1.2 equiv. of  $t\text{-BuNO}_2$  produced only 73% RSNO after 2 h, using 20 equiv. resulted in a complete nitrosation in under 5 min (see Figure 2.7). The increased levels of  $t\text{-BuNO}_2$  are viable for the reactions studied herein given the fact excess  $t\text{-BuNO}_2$  can be readily removed by rotary evaporation. SNCT and SNODT’s behavior following nitrosation are discussed in sections 2.3.7 and 2.3.8, below.



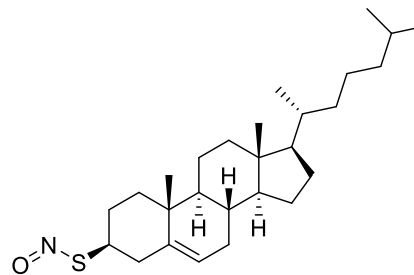
S-nitrosohexadecanethiol (SNHDT)



S-nitrosooctadecanethiol (SNODT)



S-nitrosobenzenethiol (SNBzT)



S-nitrosocholesterolthiol (SNCT)

**Figure 2.6.** Additional lipophilic RSNOs. SNHDT, SNODT, and SNCT required longer nitrosation periods using the typical 1.1 equiv t-BuNO<sub>2</sub> and also displayed less intense colors. SNBzT was rapidly nitrosated and appeared stable; however, further research was not pursued given its noxious odor.

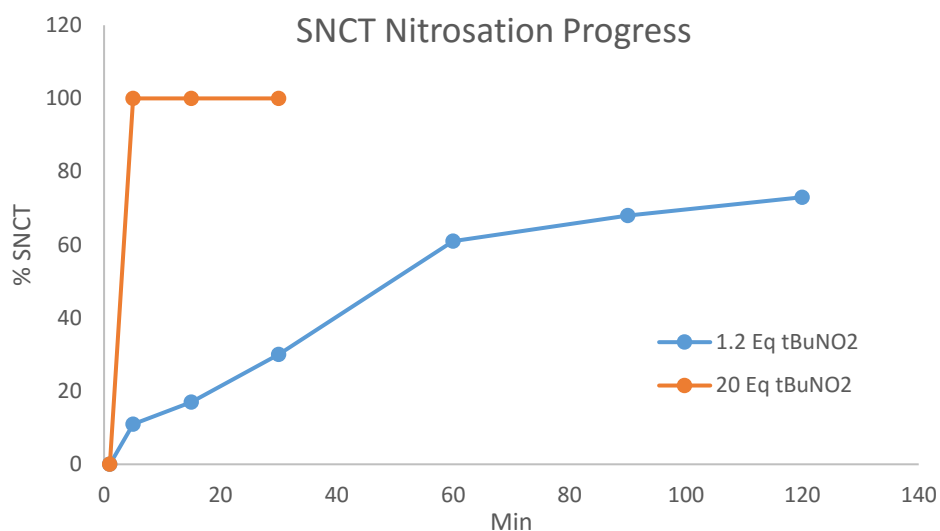


**Figure 2.7.** The increased equivalents of t-BuNO<sub>2</sub> greatly enhances the reaction rate of nitrosation of SNCT and the overall yield of the reaction.

In summary, it has been found that a range of reaction conditions are similarly effective regardless of the thiol being nitrosated to produce a variety of lipophilic RSNO species. Solvent plays a minimal role in nitrosating efficiency and consequently the more volatile ones are ideal



due to their facile removal. *t*-BuNO<sub>2</sub> proved to be an optimal or comparable nitrosating agent for both the starting primary and tertiary alkyl thiols that were converted to RSNOs. Reduced temperatures were found to help preserve RSNO levels during nitrosation, however, this factor is only beneficial when working with the less stable (and less useful) RSNO species. Reaction times were determined to be dependent on the specific thiol with the tertiary and bulkier thiols requiring longer reaction periods. Increasing the rate of nitrosation, and thus reducing decomposition for the less stable species, is best achieved via use of excess nitrosating agent. The following species returned >90% RSNO following their synthesis and purification, making them the most viable candidates for potential biomedical applications: SNTDM, SNTPMT, SNTBT, SNDDT, SNUDT, and SNTD.

### **2.3.2 Qualitative Stability Studies: RSNO Identity**

Initial stability studies can indicate the feasibility of further application-based experiments as well as draw conclusions regarding how different structures of the various alkyl RSNOs' influence stability. For some of the RSNOs, stability can simply be monitored qualitatively via the characteristic color change corresponding to NO release (red/green → white). While the stability of any RSNO is dependent on exposure to light/heat, if any of the RSNOs prepared in this work are drastically unstable under ambient light/temperature, the effects of additional conditions were not investigated in further detail.

Qualitative decomposition studies indicated that the following RSNOs (see Figure 2.8) would have minimal value for further application testing (storage stability, leaching, long-term NO release, and anti-platelet studies).

### **2.3.3 Preliminary Stability Studies: Alkyl Substitution**

Any correlation between substitution at the site of the nitroso functionality and the relative RSNOs' stability, as indicated by the % recovery and preliminary studies, was not clearly

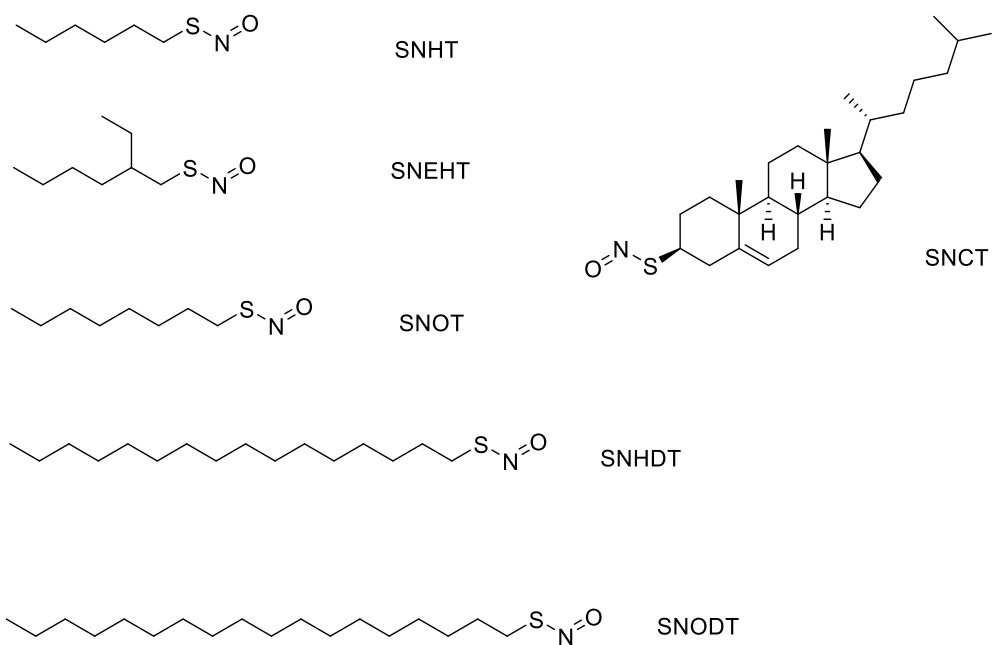


**Figure 2.8.** RSNOs with considerable instability as indicated by rapid decomposition (color loss) under ambient conditions

differentiated between species of varying structure and atomic content. For example, although SNHT and SNDDT are both primary RSNOs, SNHT has released 8 % more NO after purification under ambient conditions. Due to the fact that SNDDT, SNUDT, and SNTDM have comparable atomic content (11 or 12 saturated carbons), molecular masses, and phase at RT, their primary, secondary, and tertiary nitroso groups, respectively, are well-suited for comparing the effects of alkyl substitution on the lipophilic RSNOs' stability (see Figure 2.9).<sup>18</sup> This is also useful given the fact they lack additional heteroatom-functional groups. Initially, it was hypothesized the 3 different RSNOs could provide 3 unique NO-release profiles, allowing NO release specifically tailored devices useful for various applications such as RSNOs that release a quick burst of NO for facial acne ointments, or delayed NO release for biodegradable, antibacterial stents.

Solutions of the three RSNOs were evaluated for the relative effects of light exposure. When all three were exposed to direct sunlight, NO release increased accordingly, as expected from a continuum hv source. Unexpectedly, a discrepancy was noted between the supposed stabilizing effects due to the alkyl substitution: The stabilizing effect was evident between SNUDT and SNDDT, with the secondary RSNO having released 9% less NO after 6 hours of light exposure.

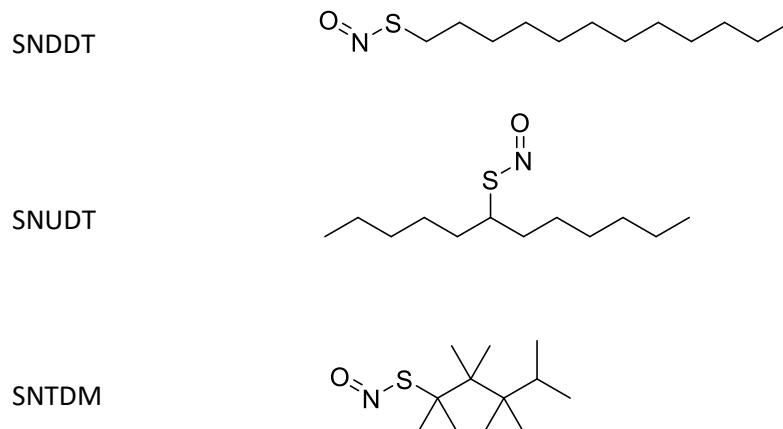


**Figure 2.9.** SNDDT (231 g/mol), SNUDT (217 g/mol), and SNTDM (231 g/mol) share similar molecular masses, and minimal functional group thus facilitating a direct comparison of the effects of their primary, secondary, and tertiary alkyl substitution.

Whereas 66 and 57% of SNUDT and SNDDT remained, respectively, only 9% of the tertiary RSNO, SNTDM, was present in the solution after this time.

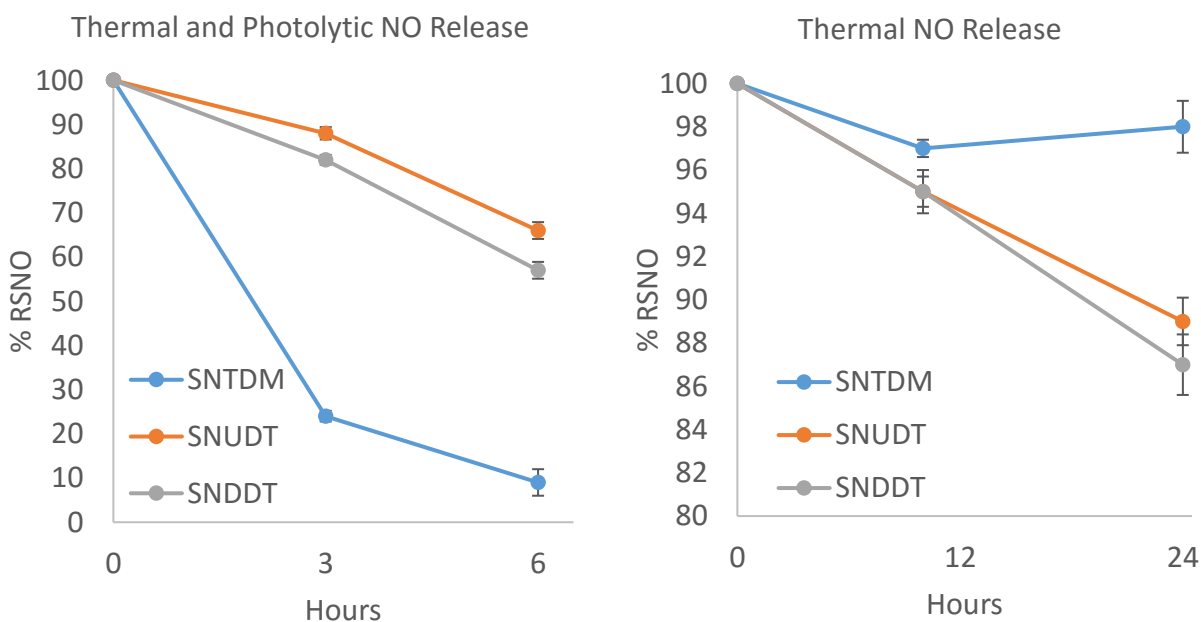


**Figure 2.10.** SNTDM, SNUDT, and SNDDT's response to stimulation by heat/light, and heat as indicated by the remaining % of initial RSNO. Thermal degradation was monitored at RT, and the photo-release was accomplished using a 100 W halogen bulb as the light source.

The same three RSNOs were tested under identical conditions but without light exposure. The species were markedly more stable, and after 24 h each sample had significantly more RSNO remaining than after 6 h of light exposure. By far the most significant observation, however, is that SNTDM is considerably *more* stable than SNUDT and SNDDT. So although the tertiary alkyl substitution decreased the rate of thermal decomposition, the stabilizing effects from that alkyl substitution were less significant than the other structural differences (methyl groups) in regard to photo-induced decomposition. SNTDM's fascinating propensity for photolytic NO release will be further explored in Chapter 4. Although the average concentrations of SNTDM, SNUDT, and SNDDT exhibit the expected trend for thermal induced NO release after 24 h, within error, there is no statistical difference between SNUDT and SNDDT. There is a 10% difference between SNTDM and SNUDT, however, only a 2% difference between SNUDT and SNDDT.

Silicone rubber films containing 1 wt% SNTDM, SNUDT, and SNDDT were tested using an NOA to monitor their real-time NO release profiles (see Figure 2.11). Relative NO release curves correlated with the stability from Figure 2.10's UV-Vis measurements. Lower wt% loaded films were used, compared to other experiments, to minimize any potential leaching that would

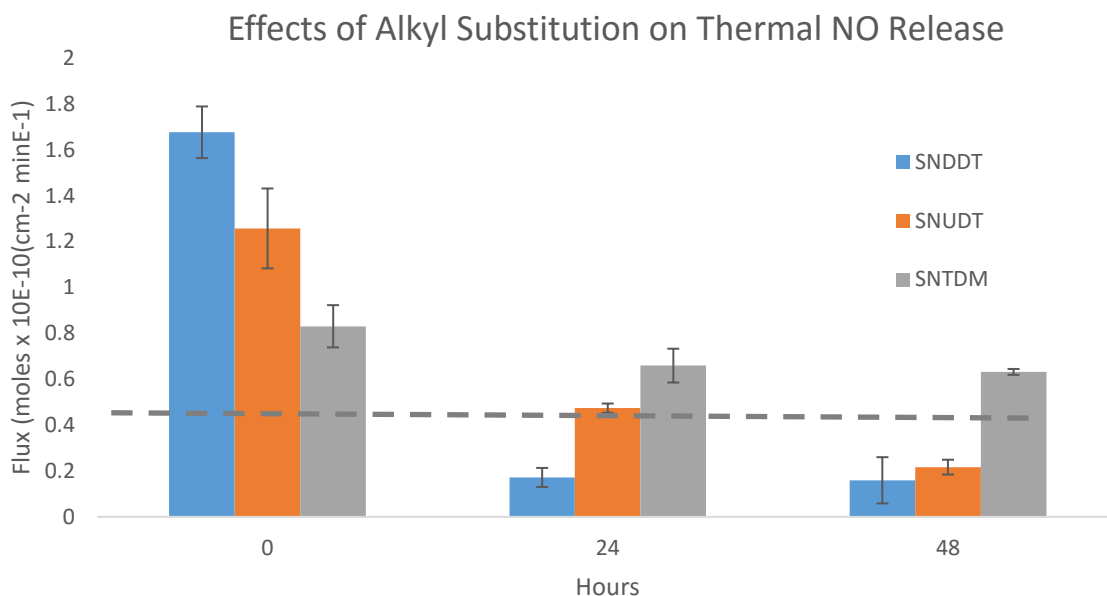


**Figure 2.11.** NO release flux from SR incorporated with SNTDM, SNUDT, and SNDDT over 3 days. The dotted line represents the lower physiological threshold for NO release from endothelial cells.

misrepresent the amount of RSNO remaining and thus the NO flux. After < 1 d, the SNDDT films exhausted their NO reservoirs. SNTDM, SNUDT, and SNDDT demonstrated NO release within the physiological range of endothelial cells ( $0.5\text{-}4.5 \times 10^{-10} \text{ mol cm}^{-2} \text{ min}^{-1}$ ) for 3, 2, and <1 d, respectively.<sup>23</sup> A direct correlation between the RSNOs' alkyl substitution and NO release lifetime is apparent.

#### **2.3.4 Preliminary Stability Studies: Phase Dependence**

To determine if an RSNO's stability is dependent upon its phase, SNHDT (MP~20 °C) was tested for NO release on a NOA at both ambient (~25 °C) and slightly reduced temperatures (~15 °C). The impact of phase effects is inherently dependent on the molecules' functional groups/mass/etc. SNHDT works well for this experiment, because its melting point phase transition temperature lies very close to RT and it does not require significant input of heat to trigger melting—which would rapidly release NO from the other RSNOs with higher or lower melting points and increase the difficulty of drawing conclusions. Reducing an RSNO's storage temperature is also expected to slow its NO release, regardless of phase. Consequently, it was important to observe the effects of temperature change independently of phase. SNHDT's NO release was observed at 1, 8, 15, 22, 30, and 37.5 °C. RT and PT temperatures are exact; however, the intermediate temperatures are approximate and were created by adding warm water to cold while monitoring solution temperature with a thermometer. Due to the molecule's relative instability, constant release values are not easily obtainable; however, the release curves (Figure 2.12) provide a valid comparison. The trend between temperature and NO release is evident as shown in Figure 2.12, although the changes in NO release only have small variations between the range of temperatures examined. The change in NO release observed between the solid at 15 °C and the liquid at 22 °C is not more substantial than the same-phase transitions. One difference, although slight, is an increase in the “burst release” of NO in the solid to liquid phase change. This phenomenon is common among RSNOs<sup>19</sup> and may have some dependence on the liquid vs solid phase of the species. Intermolecular interactions are likely predominately Van der Waal's forces, which are weak enough to not show significant effects on the NO release. Molecules that

would partake in hydrogen bonding would almost certainly exhibit a greater phase stability effect.

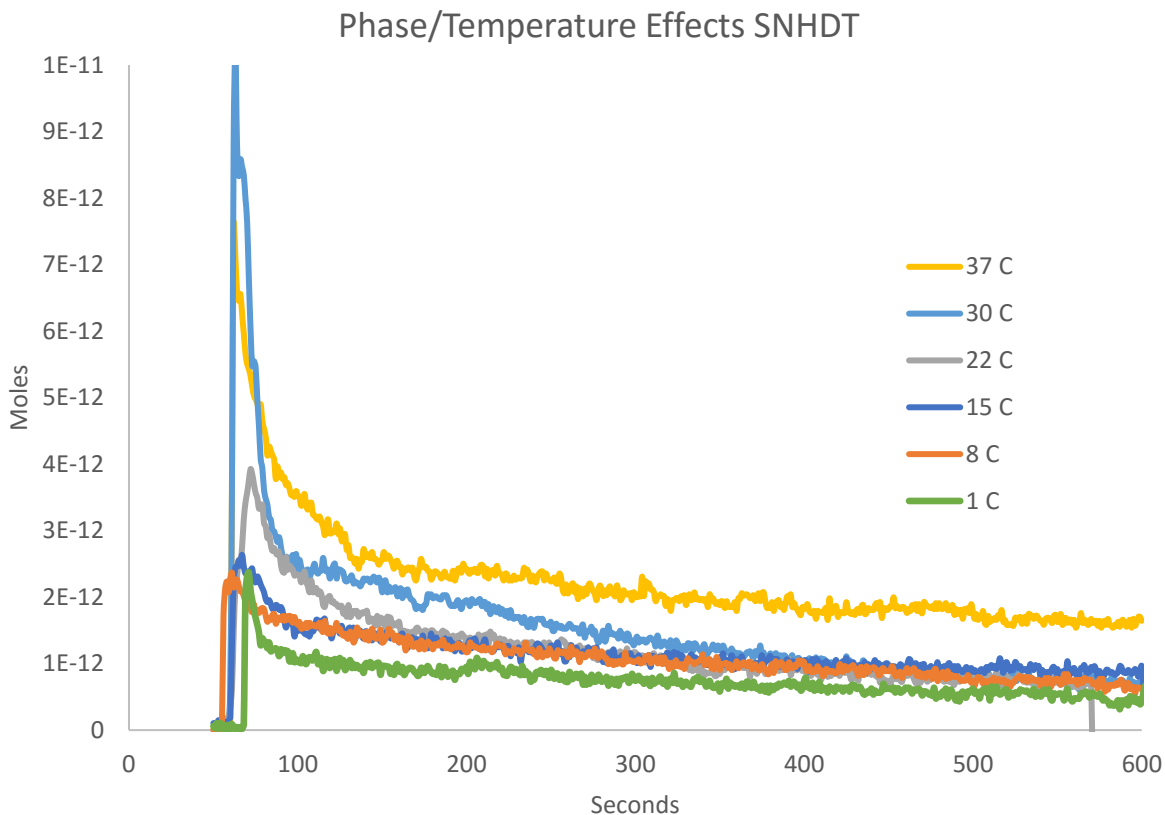


**Figure 2.12.** The relationship between temperature and NO release from both the solid and liquid phases of SNHDT.

### 2.3.5 Preliminary Stability Studies: Molecular Mass

A distinct trend was observed between the % RSNO recovered following purification, and the stability following storage (3 h). This trend, however, was determined to not be a direct correlation with the RSNOs' mass since SNHT has the lowest mass, but not the least stability (see Figure 2.13).

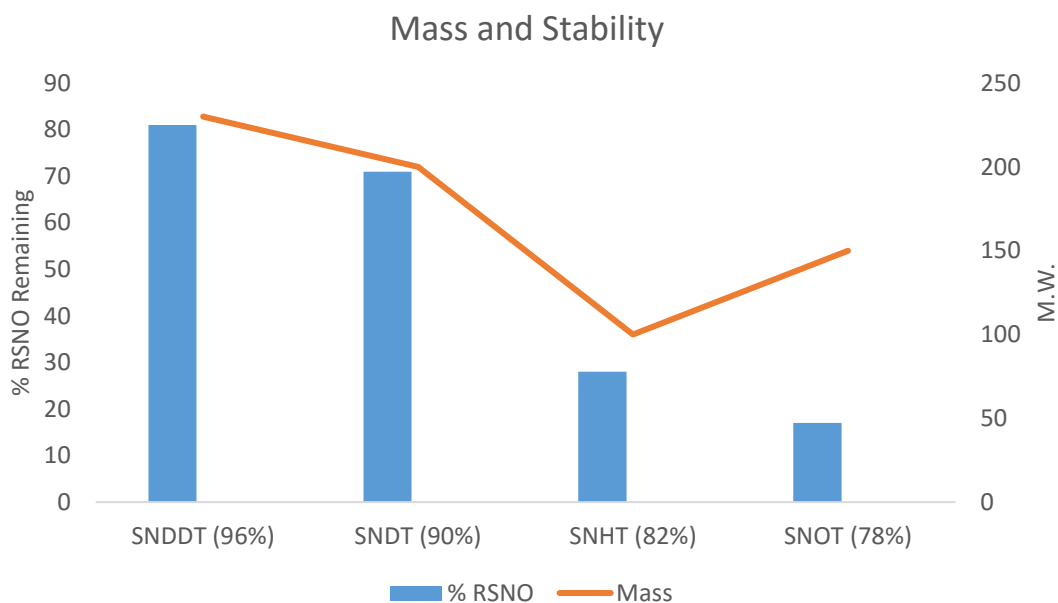


**Figure 2.13** Testing for correlation between the RSNOs' mass and stability. Results were indicated by the % remaining following storage for 3 h at RT in absence of light. Parentheses indicate the amount of RSNO following purification (which was accounted for).

### 2.3.6 *S,S*-Dinitrosolipoic Acid (SDNLA) Results

Lipoic acid and its reduced form, dihydrolipoic acid, are physiological sulfur-containing compounds that are antioxidants (see Figure 2.14).<sup>24</sup> Lipoic acid has been approved by the FDA and is sold as an over-the-counter antioxidant. We synthesized *S,S*-dinitrosolipoic acid to evaluate its stability given the fact that the RSSR decomposition product is physiologically safe. The RSNO was successfully prepared as indicated by the downfield shifts of the protons on the carbons adjacent to the sulfurs, "2a" and "4a", as well as the alpha protons relative to the carboxylic acid "6a" (see the <sup>1</sup>HNMR in Figure 2.14). The thiol's protons are also absent following nitrosation as indicated by the disappearance of shifts "1a" and "5a". SNAP's high stability is partially attributable to intramolecular stabilization involving the carboxy and/or acetamide functional groups. Consequently, we tested SDNLA in the freezer, cupboard, and shelf to observe its stability. After 1 d, NO release was not detected from the cupboard and shelf samples,

indicating complete decomposition. Following 1 wk of freezer storage the NO release was barely detectable as well. SNAP has practically zero decomposition during comparable periods of similar exposures.

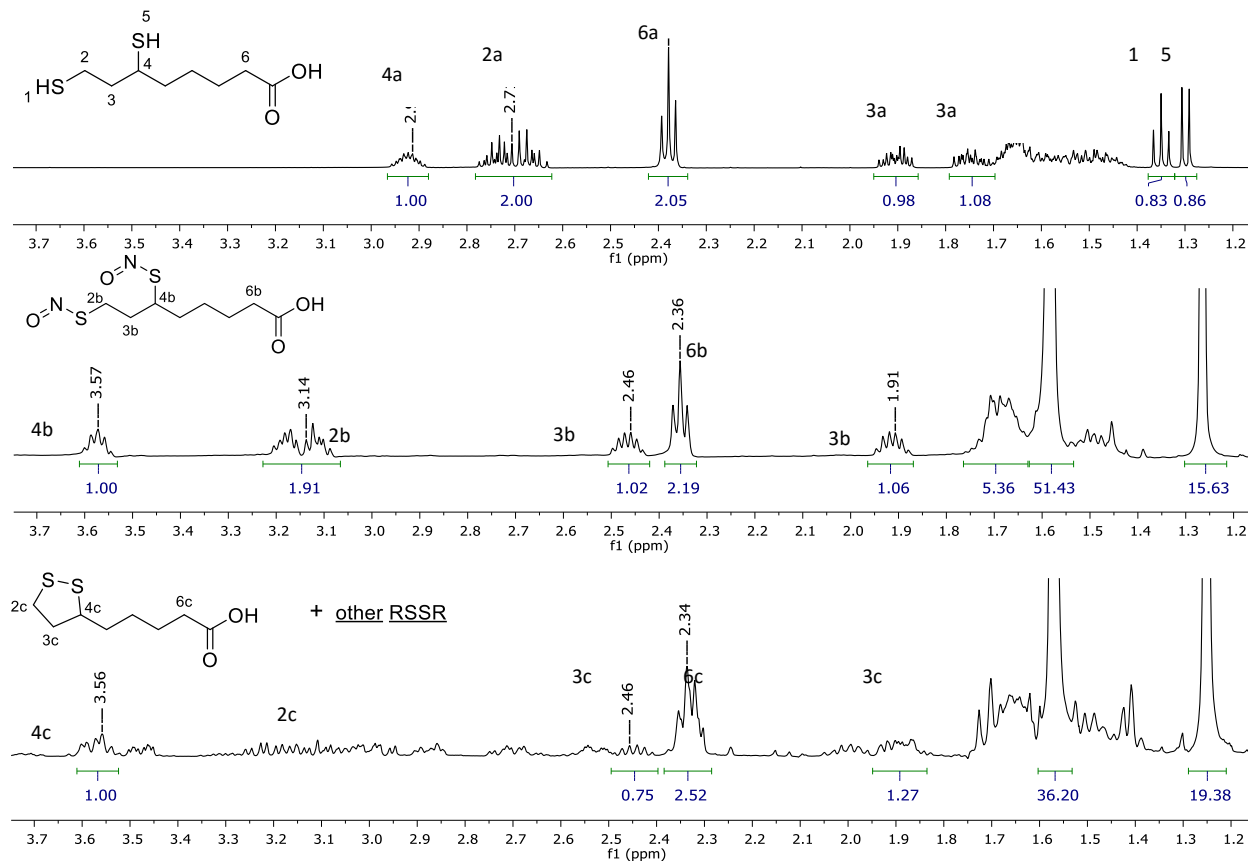


**Figure 2.14.** The reduced form of liponic acid (a) forms a di-nitroso compound (b) before subsequently decomposing to oxidized liponic acid (c) with additional side products—likely the result of intermolecular disulfide formation.

Even though SDNLA contains a secondary nitroso group it rapidly releases NO. The proximity of liponic acid's nitroso groups likely facilitates this RSNO's instability, since the intramolecular disulfide formation results in a five-membered ring. Additionally, as indicated by the appearance of many additional NMR peaks in Figure 2.14c, NO release also occurs from intermolecular disulfide formation. These results were not particularly promising; however, the RSNO was incorporated into SR films to see if the lifetime could be extended from SR bonding or crystallization within the polymer phase. Following the standard preparation conditions and times only 17% RSNO remained, thus indicating that, unfortunately, SDNLA is not a viable RSNO



for biomedical devices. In the future, synthesizing lipoic acid analogs with the thiols at varying distances from one another may serve as a means to provide species with varying NO release profiles; *i.e.* nitroso groups at carbons 5 and 10 could provide a more stable RSNO since the NO release would result in a less favorable 7-membered ring.

### 2.3.7 S-Nitrosocholesterolthiol (SNCT) Results

SNCT has not previously been reported in the literature. It is an analog of an abundant lipophilic physiological molecule (cholesterol) and a secondary RSNO, thus we felt investigating its properties was valuable. Nitrosation was performed using typical conditions; however, the reaction rate necessitated increased *t*-BuNO<sub>2</sub> concentration. Using 1.2 eq *t*-BuNO<sub>2</sub> produced only 30% product after 30 min while 20 eq *t*-BuNO<sub>2</sub> resulted in complete conversion in less than 5 min. While the upfield and strictly aliphatic region is rather convoluted, pure SNCT was obtained and confirmed by the downfield shift of the proton adjacent to the thiol group, "1". The alkene's proton, "2", can also be observed to shift (see Figure 2.15).

NO release was not observed from a 5 mM SNCT/CDCl<sub>3</sub> solution after 1 h at RT without light as indicated by <sup>1</sup>HNMR. After 3 h of storage at PT, almost 50% had decomposed. Although unstable inherently, we discovered SNCT exhibits decreased stability in the solid phase. Removing the CHCl<sub>3</sub>, *t*-BuNO<sub>2</sub>, and *t*-BuOH via rotary evaporation (<10 min, RT, ambient light) yielded a pink solid. Unfortunately, rapid decomposition was immediately noted by the pink→white color change (<5 min, RSSR) indicating that SNCT is considerably less stable in the solid form. The NO measured during complete decomposition indicated only 3% RSNO remained.

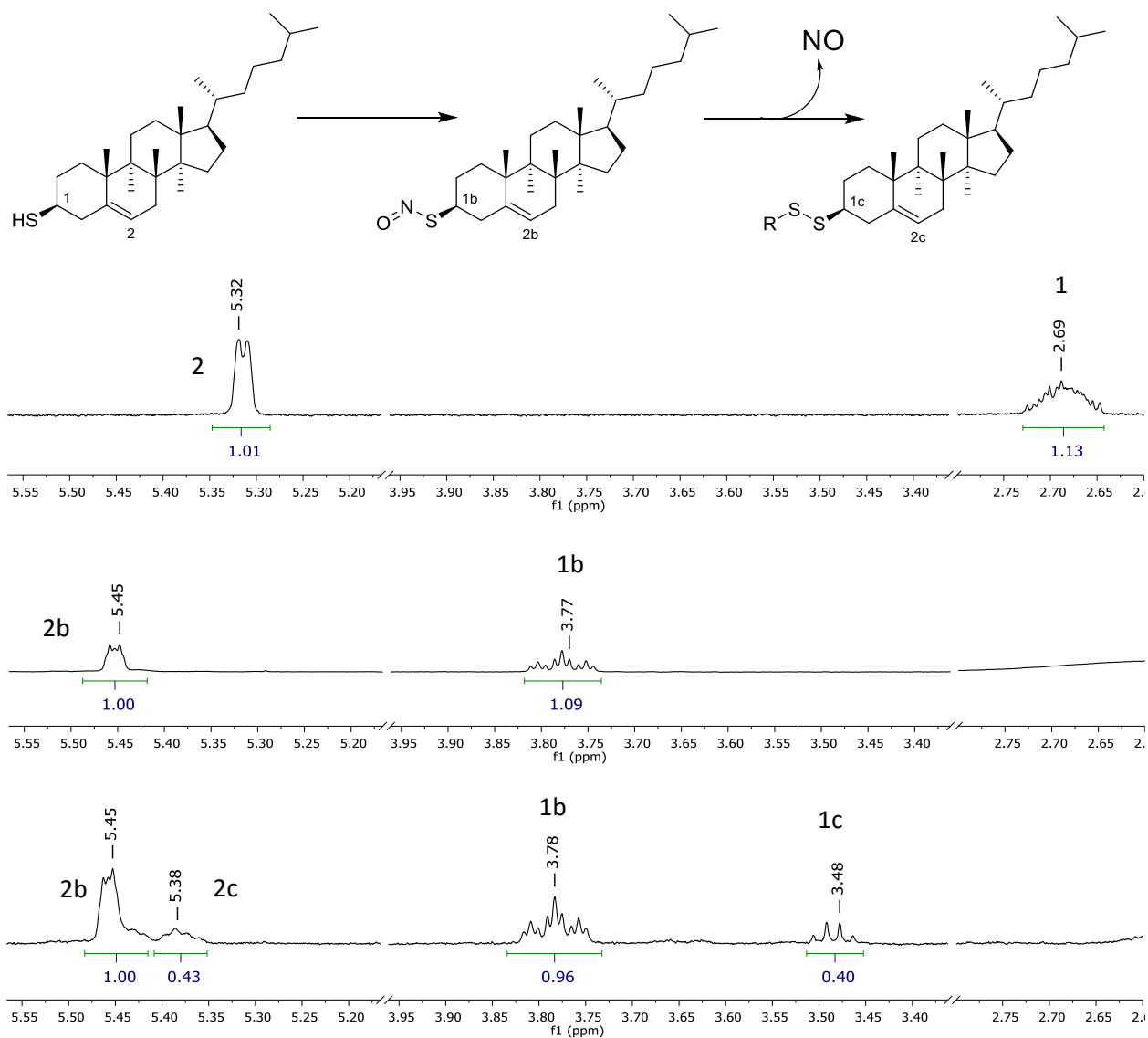


**Figure 2.15.** <sup>1</sup>H NMR spectra for the downfield region of thiocholesterol, SNCT, and a partial decomposition product (SNCT and RSSR). The protons adjacent to the sulfur shift downfield upon nitrosation, and upfield following NO release.

### 2.3.8 S-Nitrosooctadecanethiol (SNODT)

SNODT's nitrosation was observed via <sup>1</sup>H NMR, and like SNCT, required excess *t*-BuNO<sub>2</sub>. It too exhibited a substantially higher rate of NO release as a solid, thus making it not practical for practical biomedical applications. Following purification, accounting for the NO release as

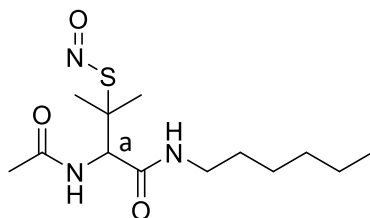
measured via the NOA, indicated that only 8% of SNODT remained. Although SNODT was not investigated further beyond this point, interestingly, a unique decomposition pathway may have occurred as suggested by the appearance of otherwise inexplicable NMR shifts (data not shown).

### 2.3.9 S-Nitrosotriphenylmethanethiol (SNTPMT) Initial Observations

SNTPMT, like SNODT and SNCT, is a heavier solid RSNO with their MWs being 305, 315, and 431 g/mol, respectively. We were initially curious whether it too would show substantially less stability in the solid phase. After isolating the green crystals, no visible loss of color was observed even after several days of exposure to sunlight, contrasting greatly with the other two RSNOs. Its remarkable stability will be further discussed/examined in Chapter 4.

### 2.3.10 S-(3-Acetamido-4-(hexylamino)-2-methyl-4-oxobutan-2-yl) nitrothioite (SNAP-NHC<sub>6</sub>H<sub>13</sub>)

SNAP is one of the most promising RSNOs studied to date, largely due to its considerable stability with regard to thermal and photolytic NO release. One downside is its propensity to leach from polymers given its LogP=0.08.<sup>7,19</sup> In attempt to ameliorate the leaching while utilizing SNAP's stability, we prepared a novel analog, SNAP-NHC<sub>6</sub>H<sub>13</sub>, via a 3-step synthesis (see Figure 2.16) and characterized this species by <sup>1</sup>HNMR (see Figure 2.17). Downfield shifts of the doublet "a" from 4.4 to 4.6 ppm, or the amide protons confirmed the presence of the nitrosation product.



S-(3-acetamido-4-(hexylamino)-2-methyl-4-oxobutan-2-yl) nitrothioite

**Figure 2.16.** SNAP-NHC<sub>6</sub>H<sub>13</sub>, a lipophilic SNAP derivative was prepared to potentially decrease its leaching. Downfield shifts of the doublet "a" from 4.4 to 4.6 ppm can be seen in Figure

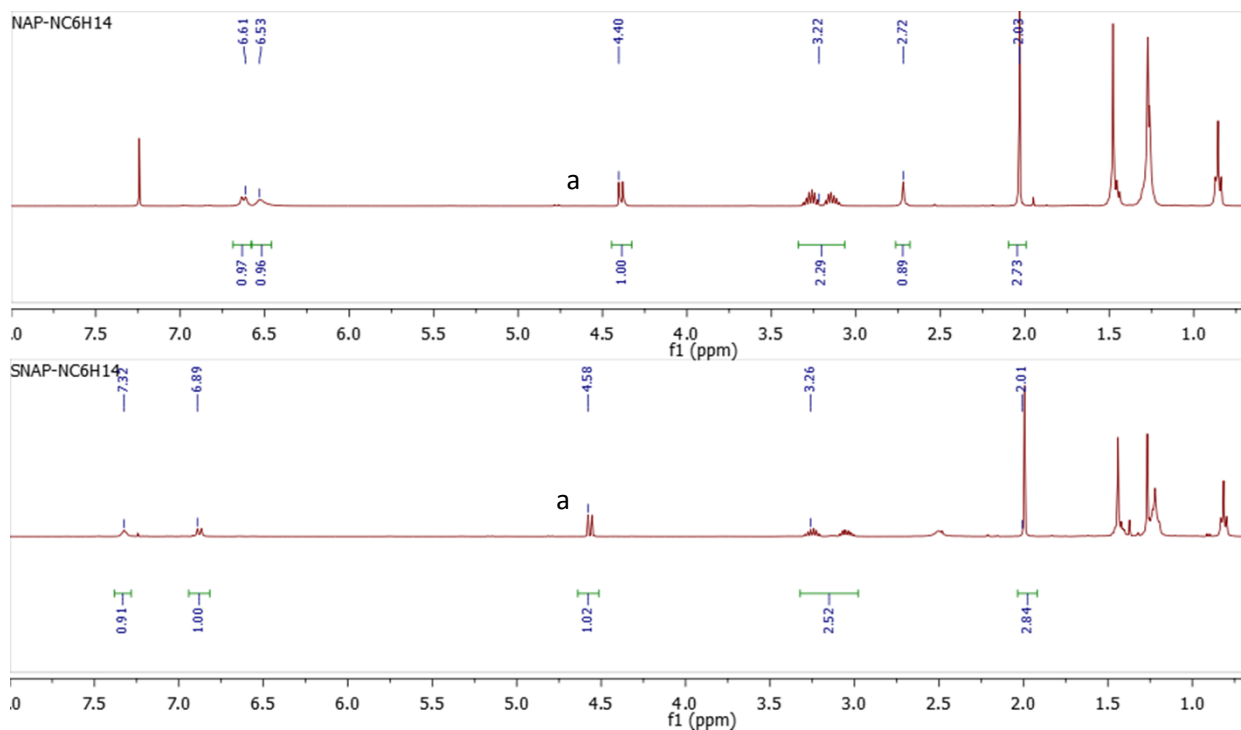


**Figure 2.17.** <sup>1</sup>H NMR of the thiol precursor, NAP-NHC<sub>6</sub>H<sub>13</sub>, and the novel RSNO, SNAP-NHC<sub>6</sub>H<sub>13</sub>, following synthesis. Downfield shifts of the doublet “a” from 4.4 to 4.6 ppm indicate the presence of the nitrosated product.

### 2.3.11 Extended Environmental/Storage Stability Studies

To be useful for biomedical applications, RSNOs must possess reasonable stability for practical storage conditions. Within a medical setting, RSNO-containing medical devices could potentially be stored in a cupboard, refrigerator, or freezer. Given a RSNO’s thermal and photo-induced NO release, freezer storage is almost always most promising; however, it’s useful to understand the effects of various environments on devices’ NO-release and RSNO degradation. These experiments serve to provide a general comparison of the RSNOs’ stability with regard to variations in temperature, light exposure, and specific polymer. Different polymers are known to provide unique stabilizing or destabilizing effects. For example, Brisbois *et. al.* demonstrated that 10 wt% SNAP in E2As polymer (a co-polymer of polyurethane with poly(dimethylsiloxane)

and poly(hexamethylene oxide) could provide a physiological flux of NO for 1 and 2 d longer than 10 wt% SNAP in SR and CS, respectively, when exposed to PT and a 100 W floodlight.<sup>7</sup>

The preparation time for RSNO containing polymers can potentially be detrimental to the total NO loading. Preparation often requires drying overnight or even longer depending on the polymers' thickness and number of topcoats. Casting films containing 5 wt% RSNO resulted in minimal loss for the most stable species, SNTDM and SNTPM, with 10% or less lost for each of the polymers tested. In contrast SNTBT lost 32% in SR and 24% in E2As and CS. Following preparation, 62% of SNDDT's NO had been released in SR and 66% in E2As and CS. SNTBT and SNDDT's concentrations were increased for the casting process as indicated in Table 2.4. This resulted in all of the polymer/RSNOs' films to be more equal in their RSNO loading following preparation. Although starting RSNO levels were similar, the SNTBT and SNDDT films contained significantly higher levels of their RSSR decomposition products which likely resulted from increased leaching into aqueous solutions in contact with the film surface. Following preparation, films were used for various experiments. Some films were immediately carried onto stability testing, while others were prepared for NO-release or leaching studies.

**Table 2.4.** Determining RSNO/polymer ratios to improve consistency in wt% loading.

	SR	CS	E2As		RSNO/polymer (mg)	SR	CS	E2As	
SNTDM	4.7	4.5	4.5	→	SNTDM	10:190	4.7	4.5	4.5
SNTPMT	4.6	4.7	4.6		SNTPMT	10:190	4.6	4.7	4.6
SNTBT	3.4	3.8	3.8		SNTBT	13:187	4.4	4.6	4.7
SNDDT	1.9	1.7	1.7		SNDDT	13:187	4.8	4.9	4.6

SR films with 5 wt% SNTDM, SNTPMT, SNTBT, and SNDDT were stored in a -20 °C freezer, RT cupboard, and a RT shelf approximately 3 m from a westward facing window (see Figure 2.18). All RSNOs showed the slowest NO release under freezer storage conditions, as expected. Increasing to RT with no light (cupboard) decreased their stability.

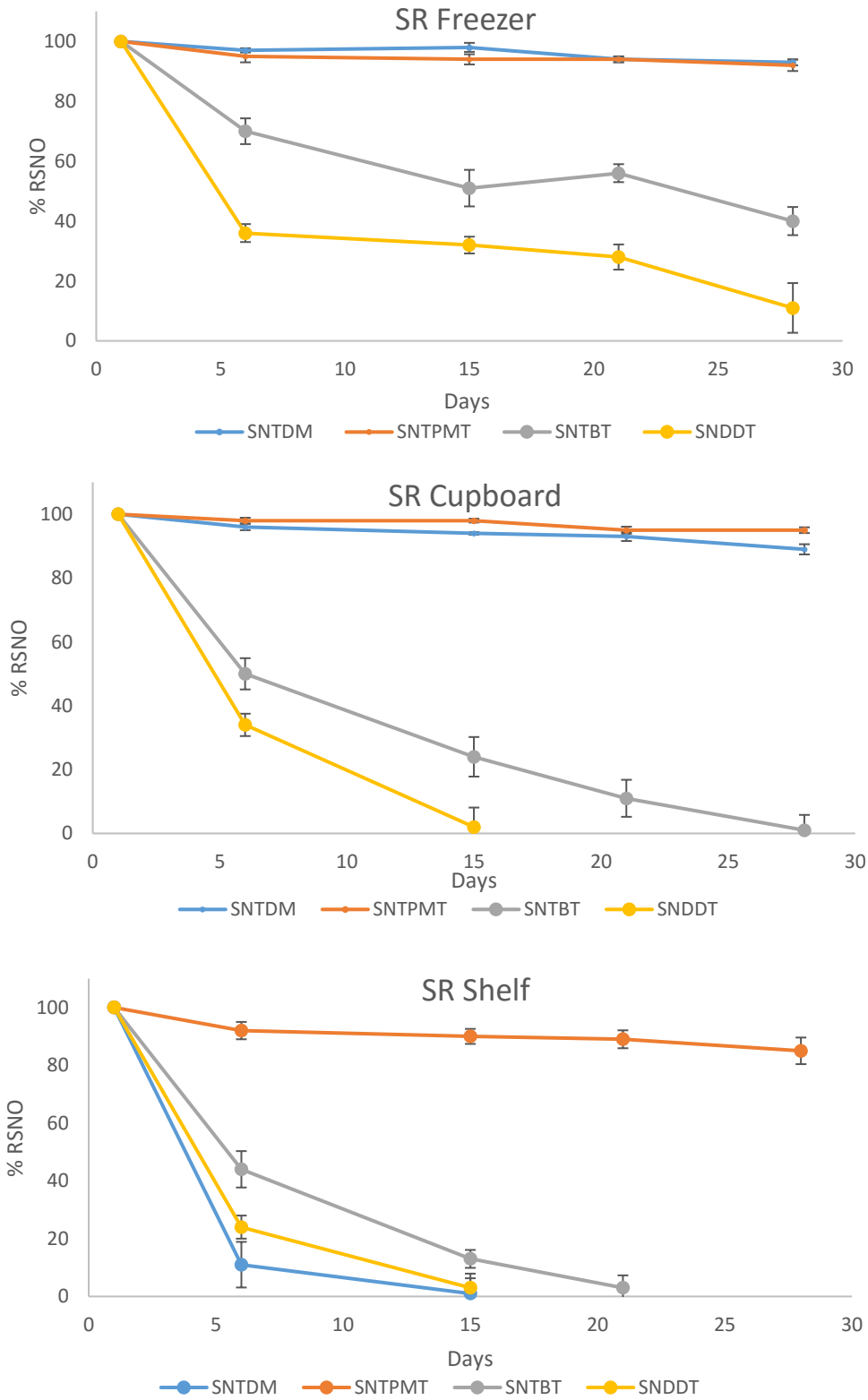


**Figure 2.18.** SR films prepared with 5 wt% SNTDM, SNTPMT, SNTBT, and SNDDT stored in a (a) freezer, (b) cupboard, and on a (c) shelf. n=3

In both environments SNTDM and SNTPMT were substantially more stable than SNTBT and SNDDT, and comparable to one another within error. During shelf storage, as observed during the preliminary studies, SNTDM's NO release greatly increased, and after six days 89% of the RSNO had decomposed. During the same duration even SNDDT, the primary RSNO, had less NO (< 76%) (see Figure 2.18).

5% SNTDM and SNTPMT were doped into SR, CS, and E2As to determine whether the polymers offered any stabilizing effects (see Figures 2.19 and 2.20). Both of the RSNOs exhibit high stability in all three polymers as indicated by more than 90% of their NO intact after 4 weeks of freezer storage. SNAP doped films were stored as well to provide a comparison. Interestingly, SNTDM demonstrated the greatest stability in SR and the lowest in CS. The opposite trend/correlation held true for SNTPMT.

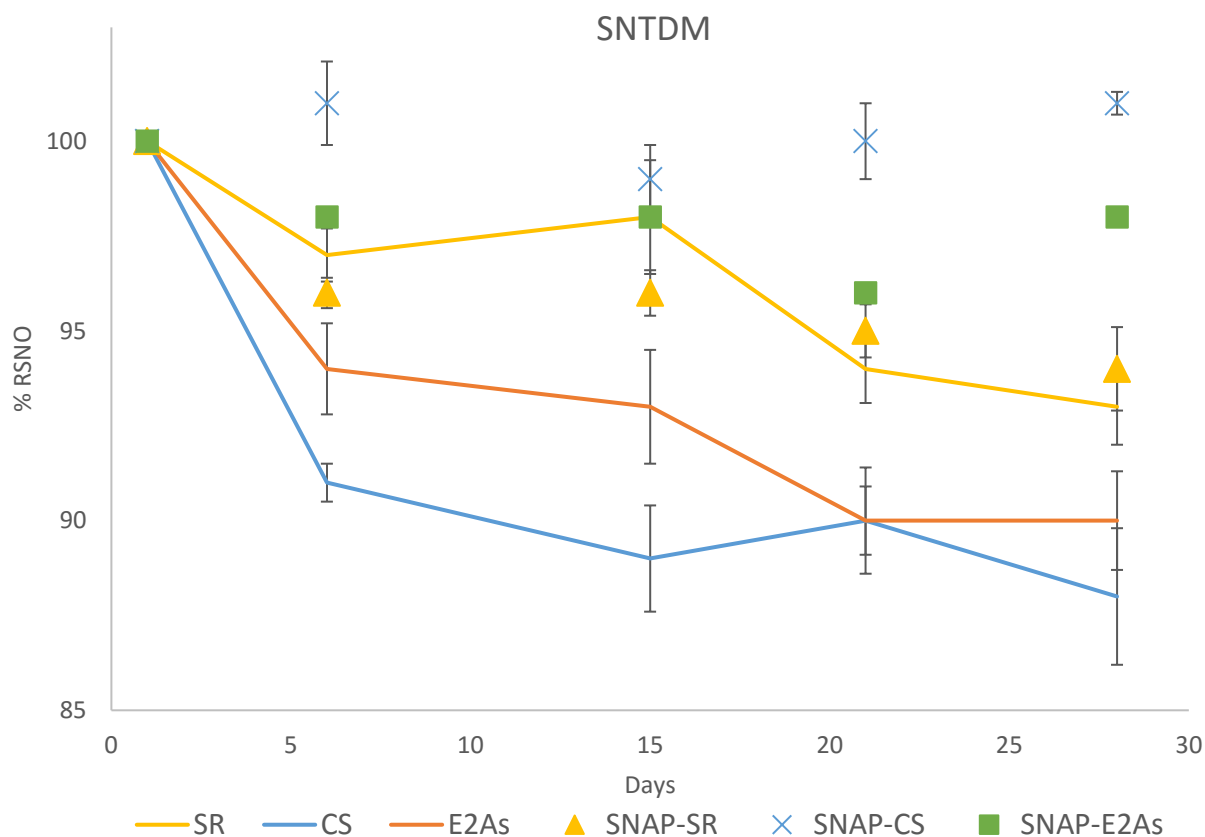


**Figure 2.19.** 5 wt% SNTDM and SNAP incorporated into SR, CS, and E2As and stored at -20 C for 1 month. n=3

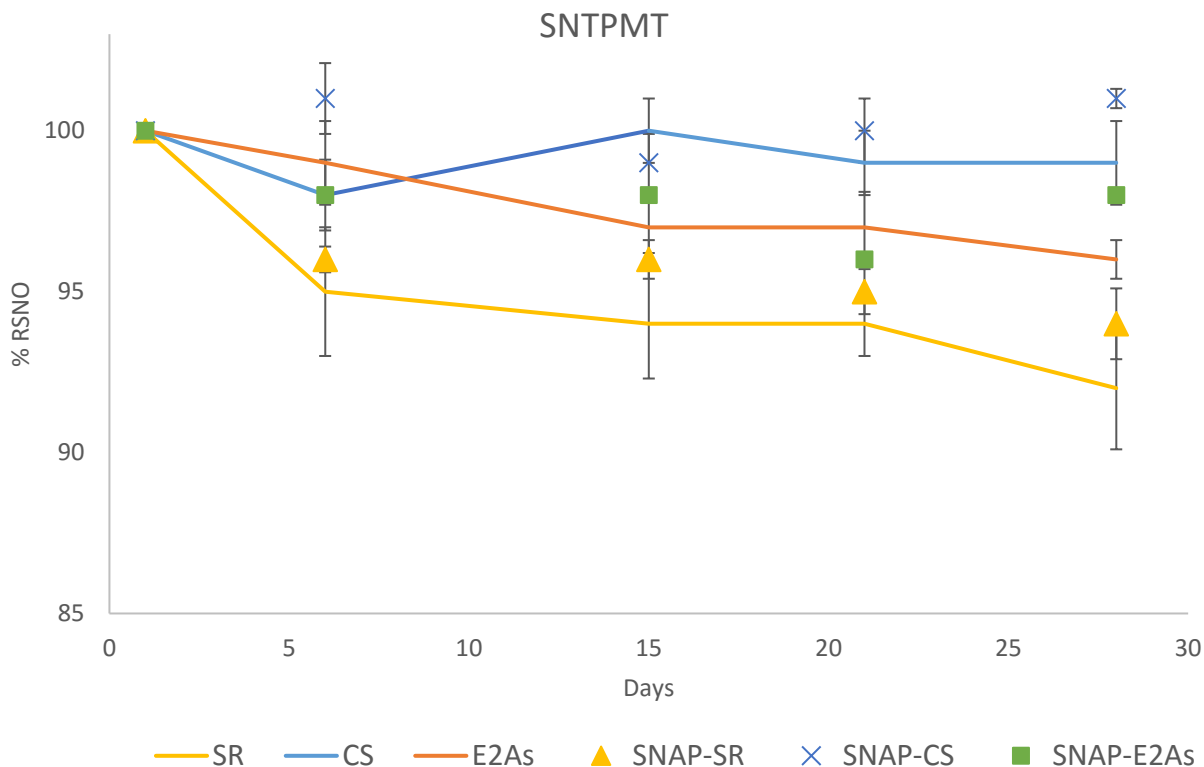


**Figure 2.20.** 5 wt% SNTPMT and SNAP incorporated into SR, CS, and E2As and stored at -20 °C for 1 month. n=3

SNAP demonstrated better stability than STDTM in both E2As and CS; it contained 8 and 13% more RSNO, respectively. In SR, SNTDM, SNTPMT, and SNAP retained comparable amounts of NO intact after 4 weeks. Although comparable during the initial three weeks, 2% more SNAP remained than SNTPMT in E2As films after the fourth week.

As heat and light are known to be two major stimuli for RSNOs' NO release, we expected their storage stability to be greatest in a -20 °C freezer, followed by 4 °C refrigerator, RT cupboard, ambient/shelf, and least in a sunny windowsill, respectively. Indeed, the individual samples followed the expected trend; however, the stability between the three species did not follow an anticipated linear trend as hypothesized because their major structural variation was solely substitution at the site of the nitroso- functionality. Instead we noticed that the tertiary RSNO, SNTDM, is significantly more stable under many conditions, whereas the primary and secondary species were quite comparable.



SNAP-NHC<sub>6</sub>H<sub>13</sub> was very unstable in all conditions tested. In fact, even when stored in the freezer (-20 °C, dark), all three doped polymers prepared with this species had nearly decomposed within one month (data not shown). SNAP, on the other hand, maintains nearly quantitative levels during the same duration. The fact that SNAP-NHC<sub>6</sub>H<sub>13</sub> is an oil in its pure, isolated form, as opposed to SNAP which is a crystal, is hypothesized to account for this phenomenon.

### 2.3.12 Leaching Studies

Five wt% films doped with SNTDM, SNTBT, SNTDPM, and SNDDT were evaluated for their leaching from three polymer phases: SR, E2As, and CS which were stored in a soaking solution of PBS/EDTA at 37.5 °C. As repeatedly reported in the literature, doped molecules commonly leach most significantly during the initial time periods following submersion/exposure to aqueous buffer solutions.<sup>5,7,19</sup> This is likely caused by water uptake into the polymer which then displaces the RSNO compound. Fortunately, this is not problematic with the studied systems given the RSNOs' decreased aqueous solubility. For example, assuming the logP gives a reasonable representation of the RSNOs partition between the lipophilic polymer and surrounding aqueous solution, it would require a 1,000,000:1 water:octanol volume ratio to displace 50% of the SNTDPM from a polymer (LogP=6.0). Given SNAP's logP=0.08, it would only require approximately a 1:1 volume ratio to displace 50%.

Since the most significant leaching occurs soon after submersion (and thus before significant decomposition) the measured RSNO species represents the majority of the leached content. This is sufficient for shorter-term devices; however, for more stable RSNOs, and biomedical devices potentially used for longer applications, accounting for leached RSSR will give a more accurate depiction of the total leached species. The RSSR concentration will also be monitored in Chapters 3 and 4.

The % of leached RSNO for SNTDM, SNTDPM, and SNDDT was substantially lower than SNAP in each polymer over the entire soaking duration (see Figure 2.21). Between the most lipophilic compounds, SNTDM, SNTDPM, SNDDT, and the tested polymer systems, there was no

apparent trend between the logP values and total % leached.

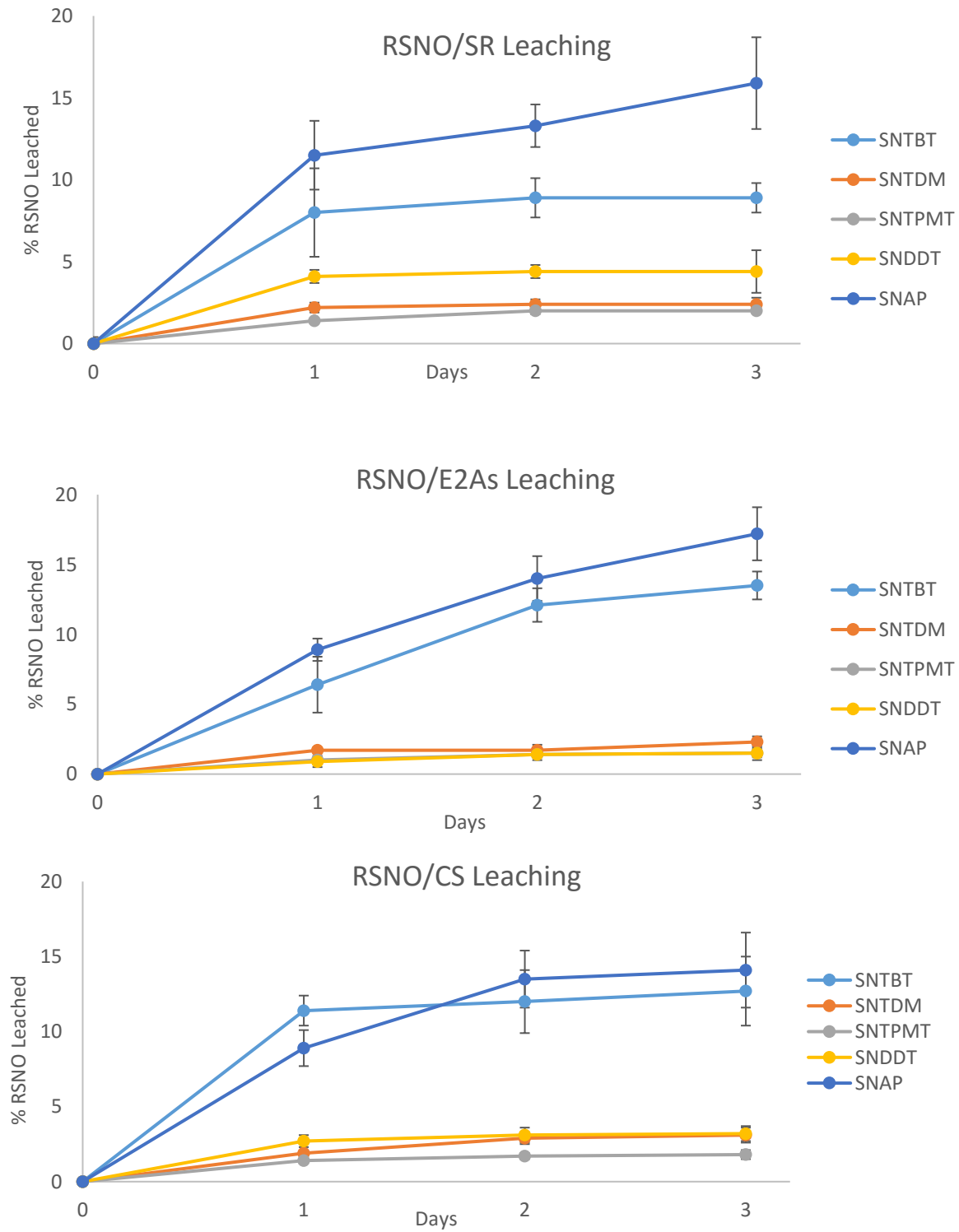


**Figure 2.21.** The % of leached RSNO from (a) SR, (b) E2As, and (c) CS films doped with 5 wt% SNTDM, SNTPMT, SNDDT, SNTBT, and SNAP.

Comparing the total leached values after 3 d of soaking at 37.5 °C, SNTDM, SNTPMT, and SNDDT had approximately 14%, 15%, and 12% less leached RSNO than SNAP from SR, E2As, and CS, respectively. There was a clear difference between the least lipophilic compound, SNTBT, and more lipophilic compounds. In fact, in E2As and CS, SNTBT leached nearly the same as SNAP during the tested duration: 15% and 13%, respectively.

Whereas SNAP, SNTDM, and SNTPMT's leaching values are accurate (due to their substantial stability), SNDDT and SNTBT's leaching is likely greater than the RSNO values reported

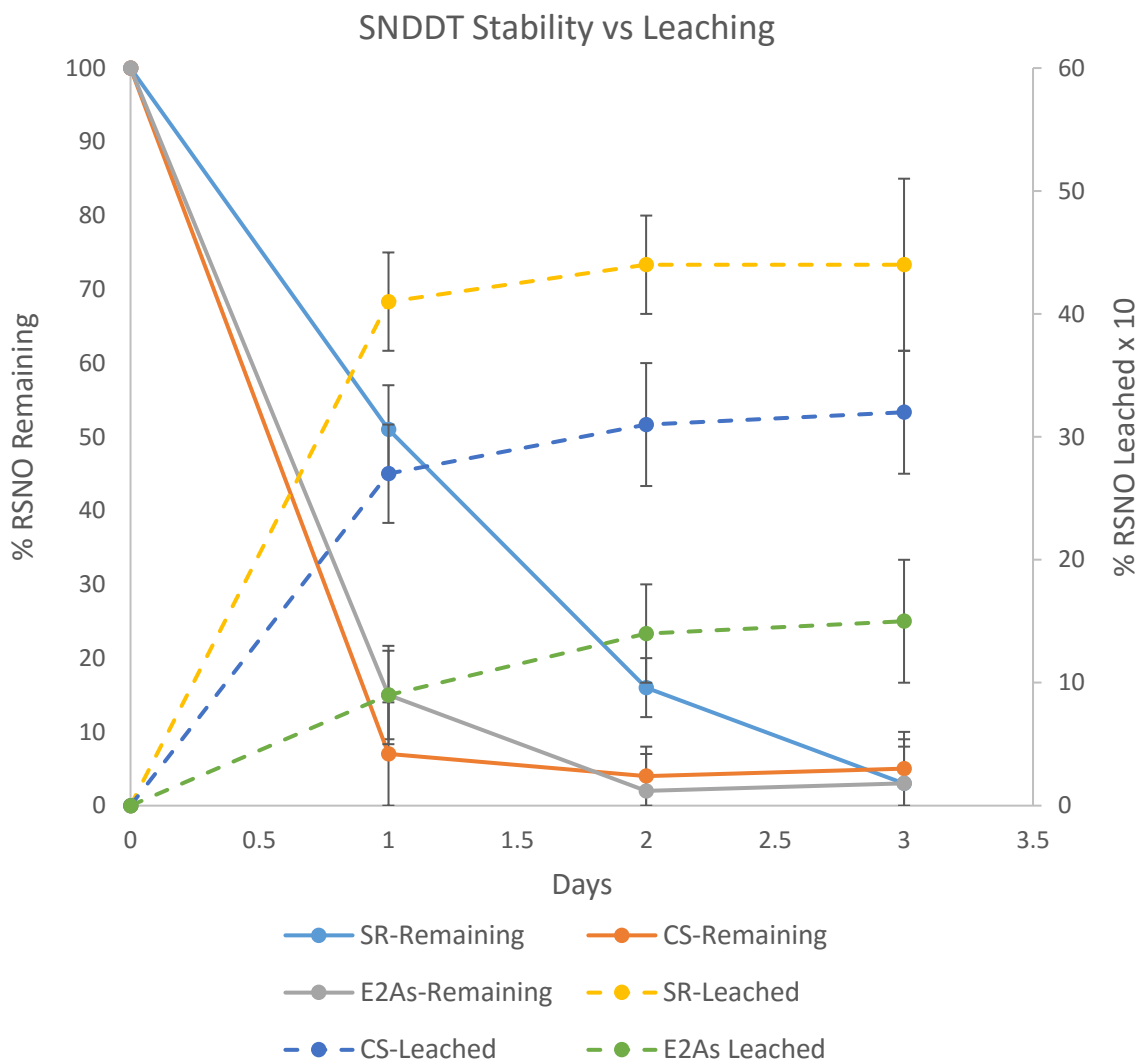


**Figure 2.22.** SNDDT's low stability likely causes the leached RSNO concentration to not accurately reflect the total leached content.

in the figures above. This is demonstrated in Figure 2.22 with SNDDT. After 1 day, 4% SNDDT had leached into the PBS while 50 % of the RSNO had already decomposed. It is likely that some of the 50 % that had decomposed (now a disulfide) had also leached into the PBS soaking solution and is not detected by UV absorption. Additionally, some RSNO may have leached and then decomposed, once again confounding the total leached content.

### **2.3.13 Long-Term NO Release**

Biomedical devices require replacement so as to reduce the risks of a blood clot or infection associated with thrombosis or biofilm formation, respectively. Extending the duration of a biomedical device's use is advantageous since replacing it can introduce bacteria into the patient and increase the risk of infection.<sup>3,7</sup> Prolonging a device's use can also reduce costs and minimize a patient's discomfort.<sup>19</sup> Biomedical grade polymers that release NO have the potential for extended implantations since NO deters thrombosis and biofilm formation.<sup>7</sup>

SNTDM, SNTPMT, and SNAP were incorporated into SR, E2As, and CS films, and their NO release monitored periodically during prolonged exposure to physiological conditions which emulate an intravascular or lower urinary-tract environment (dark, 37 C°) (see Figure 2.23). SNAP's NO release from each of the polymers has previously been published and agrees well with the results observed here.<sup>1,3,7,9</sup> SNTDM and SNAP both released NO at or above the lower-threshold physiological NO flux of endothelial cells ( $0.5 \times 10^{-10} \text{ mol cm}^{-2}\text{min}^{-1}$ ) for 1 month.<sup>1</sup> Whereas SNTPMT/E2As films also released NO for approximately 1 month, SR and CS films containing 10 wt% SNTPMT exhibited superior lifetimes, lasting at least 41 d at or above 0.5 flux. This duration of NO release at or above 0.5 flux has not previously been observed from a polymer loaded with 10 wt% of any RSNO species.

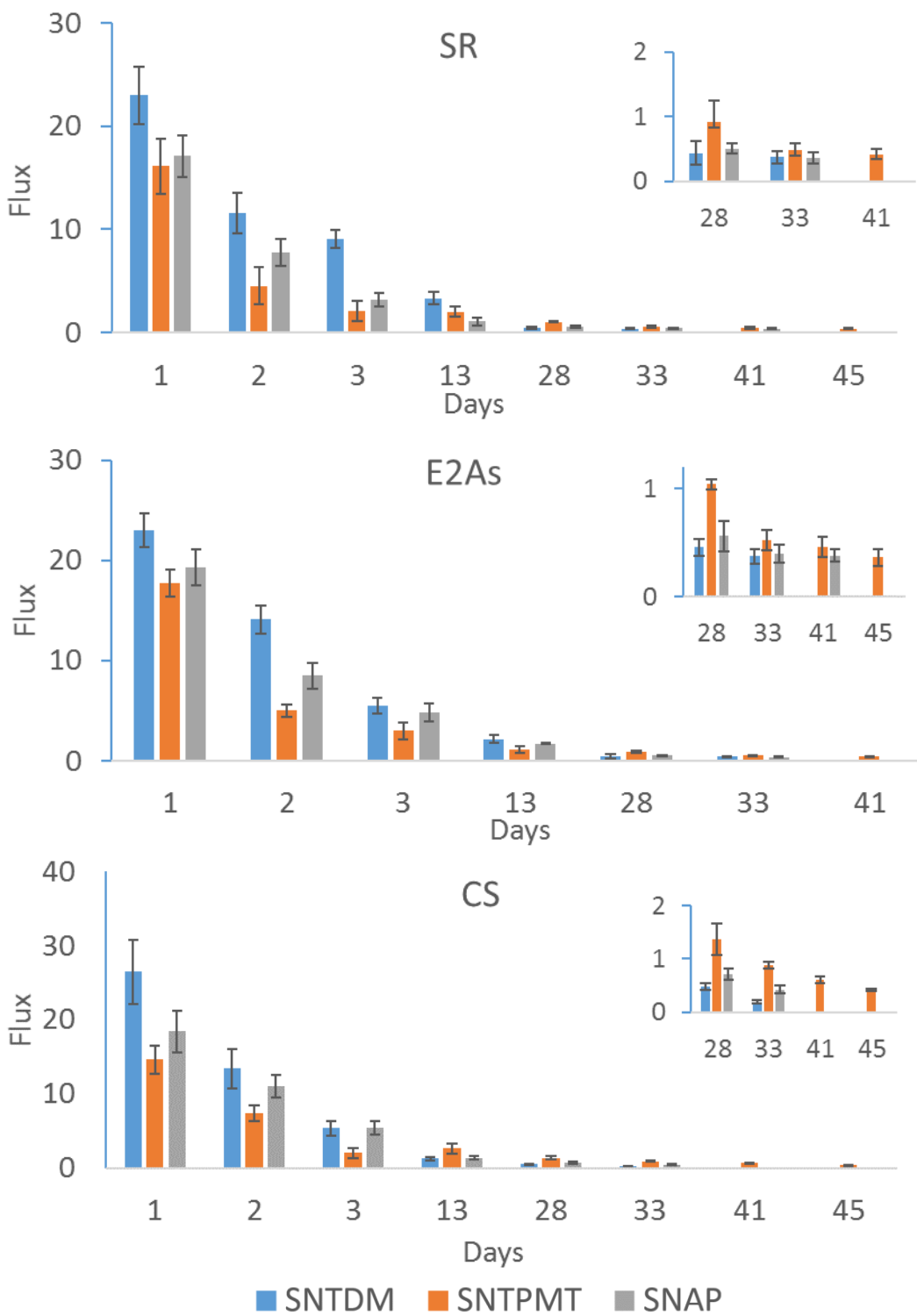


**Figure 2.23.** NO release measurements from 10 wt% SNTDM, SNTPMT, and SNAP in SR, E2As, and CS films stored at 37C in the dark over time. n=3

### 2.3.9 Platelet Adhesion Studies

Thrombus formation on biomedical devices is attributable to serious health concerns such as blood clots/embolisms. Additionally, a thrombus can impact device function, especially if that device is used for bio-analyte sensing or requires blood flow over its surface. Platelet adhesion is one of the fundamental early steps of the thrombosis mechanism, and scientists have previously demonstrated NO's ability to prevent it.<sup>14</sup> Research in the Meyerhoff group demonstrated that a PVC polymer doped with low levels of DBHD (0.5-4 wt%), a diazeniumdiolate type NO donor, can reduce platelet adhesion by 79%.<sup>14</sup> We hypothesized that the RSNO species demonstrating the best stability, NO-release, and minimal leaching from the studies reported in this chapter could potentially decrease platelet adhesion on biomedical grade polymers.

A 96-well plate was coated with a homogeneous polymer/RSNO/THF solution. Given their promising NO release properties, SNTDM and SNTPMT were used as the RSNOs in this study and both species were incorporated into CS, E2As, and SR films. After drying, the wells were exposed to PRP solutions and platelets were allowed to potentially adhere to the polymer. After removal of the PRP solution, adhered platelets were exposed to a surfactant solution to damage their cellular membrane, resulting in the release of lactate dehydrogenase (LDH). The solution of LDH, an oxidoreductase enzyme, was exposed to NAD<sup>+</sup> which was consequently reduced to NADH (see Figure 2.24). NADH is readily detectable via its absorbance at 450 nm. Because NO release reduces the presence of adhered platelets, the hypothesis was that RSNO/polymer wells would have less platelets, and thus less NADH present.<sup>14</sup>

Pure polymer controls when exposed to PRP/surfactant provided a representation of their inherent propensity to adhere with platelets. 40% more platelets adhered to silicone rubber than E2As, while 31% more adhered to SR than CS. Within error, CS and E2As have comparable levels of adhered platelets (see Figure 2.25).

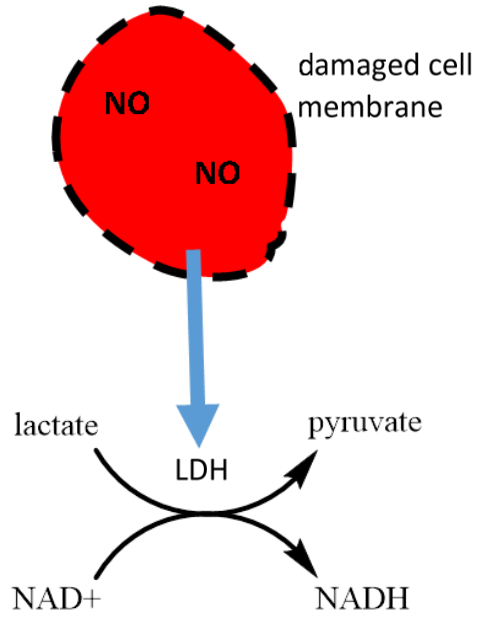


**Figure 2.24.** Adhered platelets when lysed with a surfactant release LDH that in turn reduces NAD<sup>+</sup> to NADH, the molecule tested.

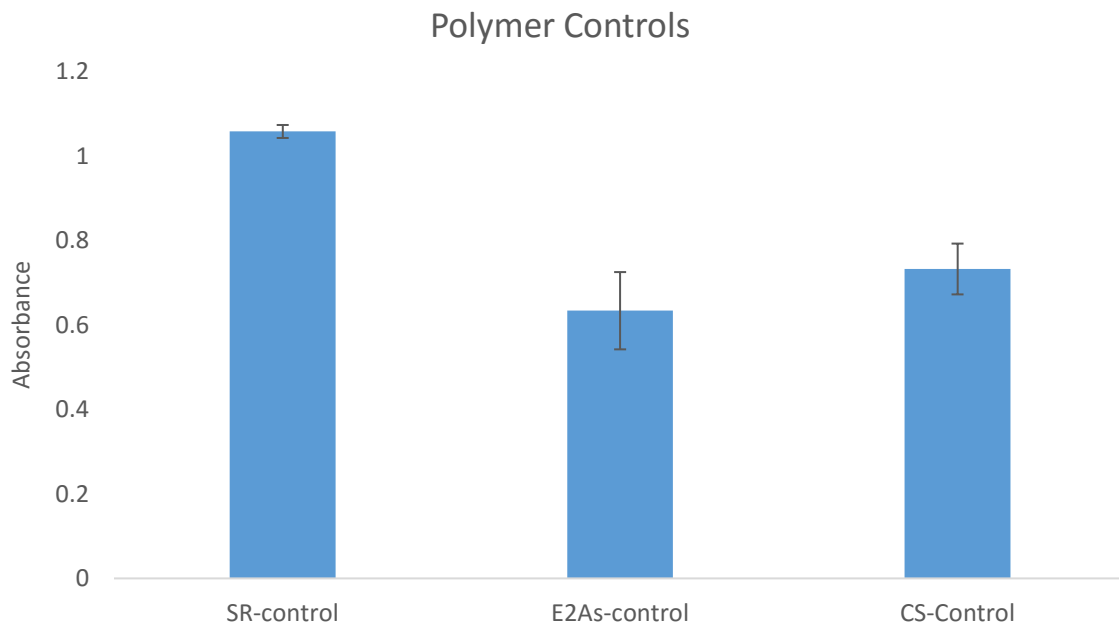


**Figure 2.25.** Control polymers inherent platelet adherence represented as a relative comparison of absorbance. N=3

1, 5, and 10% of the RSNOs were doped into SR, and each showed a direct correlation between increased RSNO levels and antiplatelet effects, as predicted (see Figure 2.26). For every wt% tested, SNTDM and SNTPMT prevented more platelet adhesion than SNAP. SNTDM and SNTPMT performed comparably with 1 wt% loading as both had 86% less platelets than the SR controls. With 10 wt% loading, SNTDM/SR had only 3% the platelets as were found attached to the controls—a very low number. SNAP/SR had 16% the number of activated platelets as the SR controls.

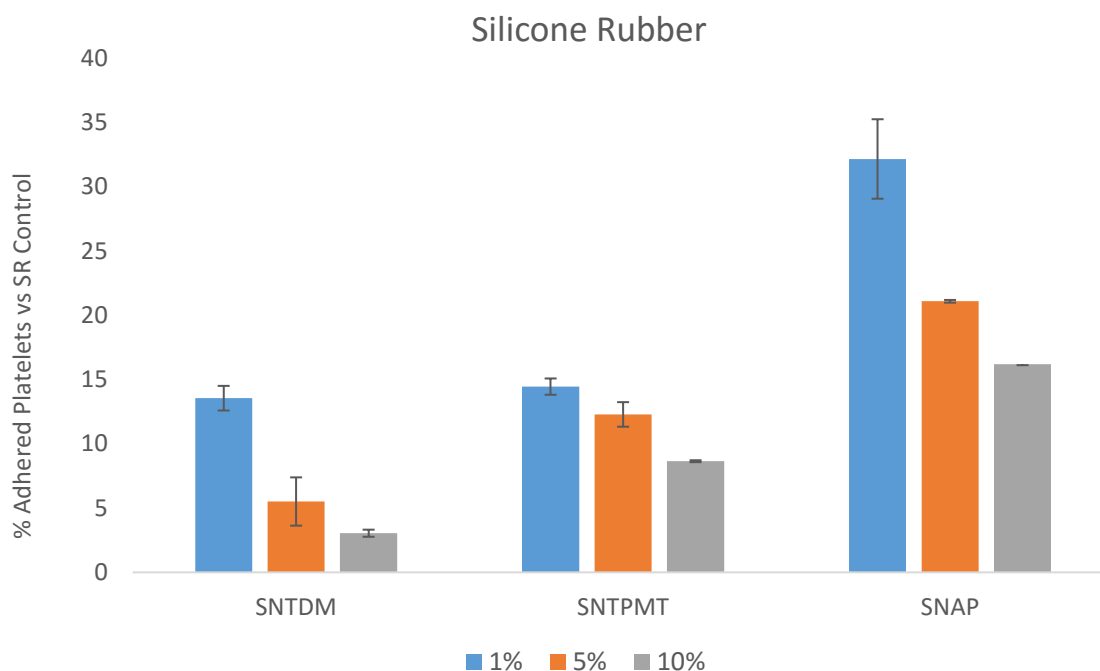


**Figure 2.26.** SNTDM, SNTPMT, and SNAP’s effect on platelet reduction at 1, 5, and 10 wt% in SR (n=3). % of adhered platelets are relative to controls (see Fig. 2.24).

For the E2As polymer, only 5 and 10 wt% loadings were tested due to limited blood availability (see Figure 2.27). Again, SNAP and SNTDM demonstrated direct correlations between increased RSNO load and reduced platelet adhesion. They performed similarly under the tested conditions. SNTPMT performed uniquely; however, and upon increasing from 5% to 10 wt% loading the number of adhered platelets more than doubled. Despite this, the levels of activated platelets were still 48% below that of the E2As control polymers. Again, SNTPMT/CS wells exhibited a reverse relationship between the RSNO levels and any platelet reduction (see Figure



2.28). This time, increasing from 5% to 10 wt% resulted in 90% *more* adhered platelets relative to the control, nearly doubling the levels. SNAP's adhered platelets also increased going from 5

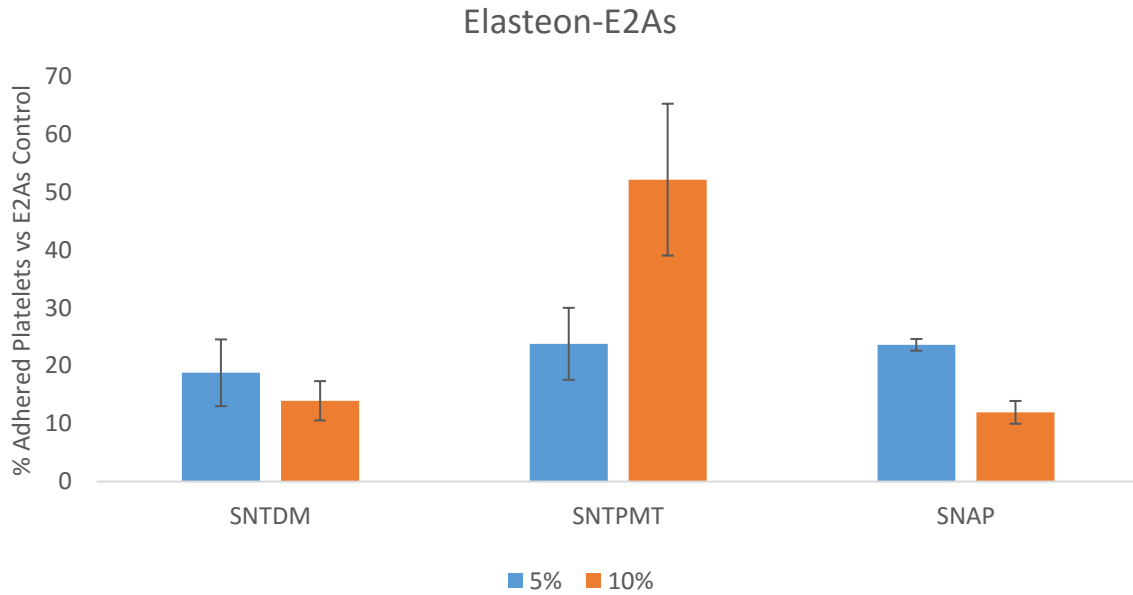


**Figure 2.27.** SNTDM, SNTPMT, and SNAP's effect on platelet reduction at 1, 5, and 10 wt% in E2As (n=3). % of adhered platelets are relative to controls (see Fig. 2.25).

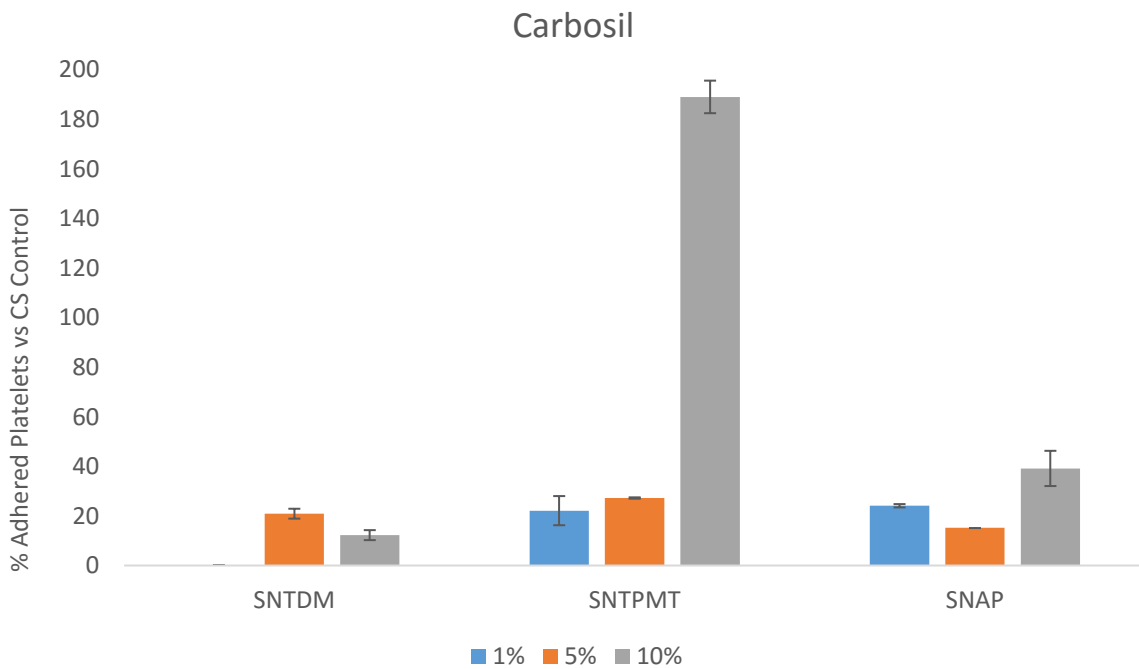


**Figure 2.28.** SNTDM, SNTPMT, and SNAP's effect on platelet reduction at 1, 5, and 10 wt% in CS (n=3). % of adhered platelets is relative to controls (see Fig. 2.25).

to 10 wt%, increasing by 24%; however, levels still remained 61% lower than the control. SNTDM's 5 and 10 wt% wells reduced platelet adherence on CS by 21 and 12% relative to the controls, respectively.

While the experiments indicate the relative effects of each RSNO/polymer, it is important to keep in mind that the number of decreased platelets does not mean there are necessarily less platelets overall since each polymer has a different level of platelets attached to the control films (see Figure 2.25). In future studies a coulter counter will be used to provide a quantitative analysis of the specific platelet counts. SNTPMT's unexpected behavior could be partially attributed to its solubility. Any precipitated solid could affect the polymers' surface texture (increased roughness), an attribute known to correspond with increased platelet adhesion. This explanation likely fits with the SNAP-doped CS films as well, particularly since *Wo et al.* previously demonstrated that SNAP crystals are present in such films when SNAP is present at or above 5 wt%.<sup>9</sup> In the future, SEM images will determine if the polymer surface is in fact affected in the case of the presence of SNTPMT within the polymers.

## 2.4 Conclusions

In this chapter, the potential of many lipophilic alkyl and aryl RSNOs' was evaluated for use in biomedical applications. Preliminary studies indicated that nitrosations of most of the species examined are nearly quantitative under the tested conditions, regardless of the thiols' substitution, molecular mass, nitrosating agent, and solvent. Despite this it was impossible under the tested conditions to obtain some of the RSNOs following purification. The secondary and tertiary RSNOs required longer nitrosation times under the typical ~1.1 equiv. *t*-BuNO<sub>2</sub> concentrations. This proved to be detrimental to the less stable species and resulted in undesirable premature NO release. Increasing the equivalents of nitrosating agent allowed quicker nitrosations and thus can be employed given the typical purification methods, which remove the excess nitrosating agents. Despite the increased nitrosation rates, the least stable RSNOs are not suitable for biomedical applications given their instability during isolation.

Preliminary studies examined the effects of the RSNOs' inherent chemical characteristics and their corresponding NO release behavior. Increased alkyl substitution correlated with enhanced thermal stability, as has previously been demonstrated with RSNOs bearing similar structures. A substantial anomaly was observed, however, with regards to the tested RSNOs' photoactivation as SNTDM exhibited extreme sensitivity compared to the SNDDT primary thiol isomer and secondary thiol SNUDT species. This photo-instability will require devices to be stored in more stringent conditions; however, it may prove promising in the development of devices and applications utilizing light-induced NO release (e.g., topical phototherapy for wound healing or acne treatment, etc.).

SNHDT's solid or liquid phase appeared to play a minimal role in the RSNO's stability as no significant change was noted upon freezing the molecule, except a slight increase in the initial NO "burst release". This trend may also apply for other RSNOs with minimal heteroatoms; however, RSNOs bearing additional functionality could exhibit different stabilizing effects (hydrogen bonding, etc.) due to their phase. Any trend between the RSNOs' molecular masses and stabilities was not evident with the primary substituted RSNO species that were tested. The larger RSNOs, SNCT and SNODT, demonstrated significant instability, however, and given their more unique structures it is unlikely that their greater mass solely accounts for this behavior.

When doped into SR films, SNTPMT and SNTDM exhibited substantial stability during cupboard and freezer storage. Indeed, both had 90% or above NO loading retained even after 4 weeks of storage under these conditions. 85% of the SNTDM inside the SR films remained after 1 month exposure to sunlight, thus exhibiting a very surprisingly high stability. SNDDT and SNTBT were unstable under the wide range of storage conditions tested. Both RSNO compounds released all of their NO well before the end of the 1 month storage period on the shelf (RT, ambient light and 3 m from window) as well as in the cupboard (RT, dark). Even in the freezer (-20 °C), only 40% and 11% of the SNTBT and SNDDT remained, respectively, in the SR films following 1 month of storage. SNTBT and SNDDT's instability does not make them good candidates for biomedical applications.

SNTDM and SNTPMT were doped into SR, CS, and E2As and compared to SNAP's stability during 1 month of storage in a freezer. SNAP was more stable than SNTDM in all polymers except SR, in which they both retained ~94% NO after 1 month. Films made from E2As and CS contained 10% and 12% more SNAP than the SNTDM counterparts, respectively. SNTPMT demonstrated excellent stability and performed comparably to SNAP in all polymers with the exception of E2As, in which  $95.7 \pm 0.6\%$  SNTPMT vs  $98.4 \pm 0.9\%$  SNAP remained.

Leaching of the RSNO compounds from SR, E2As, and CS polymer membranes was quantitated and compared to SNAP's leaching behavior. SNTDM, SNTPMT, and SNDDT exhibited substantial retention within the hydrophobic polymer. However, both SNAP and SNTBT demonstrated significant leaching into the surrounding aqueous buffer solutions, very likely resulting from their lower LogP values and thus increased aqueous solubility. SNTBT's leaching combined with its decreased stability makes it inferior to SNTDM and SNTPMT for potential biomedical applications.

Finally, the effect of SNTDM and SNTPMT's NO release as assessed via surface platelet adhesion was determined using PRP obtained from citrated porcine blood and compared to that demonstrated by SNAP. SNTDM and SNTPMT performed very well when incorporated into SR polymer films and exhibited less platelet adherence than SNAP at each of the tested wt% levels. At 10 wt% loading, only 3.0 % platelets (relative to control levels) had adhered to the SNTDM/SR polymer. SNTDM outperformed the other RSNOs in CS at 10 wt% and showed only 12% as many adhered platelets as the controls.

The data for SNTDM, SNTPMT, and SNAP's performances during this chapter's most important experiments are summarized in Table 2.5 below. As reported in the literature, many RSNOs often excel in one facet of their performance while they lack in other(s).<sup>18,21,22,25</sup> Due to this, certain RSNOs are better suited for certain applications than others. SNAP, more so than other RSNOs, has consistently proven superior given its relative high stability under both thermal and light exposure.<sup>9</sup> This gives SNAP exceptional storage capacity and provides an extended NO release for biomedical applications, characteristics which have impeded RSNOs' clinical progress. One of SNAPs downfalls, however, has been its leaching from biomedical grade polymers.

Although SNAP is stable, its propensity to leach from the polymer films containing it into aqueous solutions in contact with the surface limits its utility in regard to localized treatments. The most promising new lipophilic RSNOs studied herein, SNTDM and SNTPMT, exhibited substantially lower leaching under all the tested conditions. Preliminary studies show that SNTPMT is at least comparable to SNAP while in the crystalline phase with respect to resistance against decomposition in ambient light and temperature exposure, a characteristic not previously reported in the literature to the best of our knowledge for any RSNO. Future work will further examine SNTPMT's behavior in polymers regarding its longer-term stability to explore if its behavior is comparable to that observed in its crystalline phase. Although SNTDM is less stable than SNTPMT and SNAP under the tested conditions, its increased NO release profile demonstrates greater efficacy towards preventing platelet adhesion.

**Table 2.5.** Comparison of SNTDM, SNTPMT, and SNAP's best results for leaching, stability, long-term NO release, and antiplatelet experiments. Superior results are indicated in bold. Best wt% in the platelet studies are indicated in parentheses.

	SNTDM	SNTPMT	SNAP
Leaching-SR (5 wt%)	<b>2.4 ± 0.4%</b>	<b>2.0 ± 0.2%</b>	15.9 ± 2.8%
Leaching-CS (5 wt%)	3.1 ± 0.5%	<b>1.8 ± 0.3%</b>	14.1 ± 2.5%
Leaching-E2As (5 wt%)	2.3 ± 0.4%	<b>1.5 ± 0.3%</b>	17.2 ± 1.9%
Freezer-SR-4 weeks (5 wt%)	<b>93.1 ± 0.7%</b>	92.0 ± 2. %	<b>94.0 ± 1.1%</b>
Freezer-E2As-4 weeks (5 wt%)	90.2 ± 1.3%	95.7 ± 0.6%	<b>98.4 ± 0.9%</b>
Freezer-CS-4 weeks (5 wt%)	88.0 ± 1.8%	99.0 ± 1.3%	<b>101.0 ± 0.3%</b>
Relative Platelet Adherence (CS)	<b>12.3 ± 2.0% (10)</b>	22.1 ± 5.9% (1)	15.2 ± 0.1% (10)
Relative Platelet Adherence (SR)	<b>3.0 ± 0.3% (10)</b>	8.6 ± 0.1% (10)	16.2 ± 0.1% (10)
Relative Platelet Adherence (E2As)	<b>14.0 ± 3.4% (10)</b>	23.8 ± 6.2% (5)	12.0 ± 2.0% (10)
Long-Term NO Release (CS)	28 d	<b>41 d</b>	28 d
Long-Term NO Release (SR)	28 d	<b>41 d</b>	28 d
Long-Term NO Release (E2As)	28 d	<b>33 d</b>	<b>33 d</b>

## 2.5 References

- 1 E. J. Brisbois, R. P. Davis, A. M. Jones, T. C. Major, R. H. Bartlett, M. E. Meyerhoff and H. Handa, *J. Mater. Chem. B*, 2015, **3**, 1639–1645.
- 2 D. A. Riccio, P. N. Coneski, S. P. Nichols, A. D. Broadnax and M. H. Schoenfish, *ACS Appl. Mater. Interfaces*, 2012, **4**, 796–804.
- 3 A. Colletta, J. Wu, Y. Wo, M. Kappler, H. Chen, C. Xi and M. E. Meyerhoff, *ACS Biomater. Sci. Eng.*, 2015, **1**, 416–424.
- 4 J. M. Tullett, D. D. Rees, D. E. G. Shuker and A. Gescher, *Biochem. Pharmacol.*, 2001, **62**, 1239–1247.
- 5 A. B. Seabra, L. L. da Rocha, M. N. Eberlin and M. G. de Oliveira, *J. Pharm. Sci.*, 2005, **94**, 994–1003.
- 6 A. B. Seabra and M. G. De Oliveira, *Biomaterials*, 2004, **25**, 3773–82.
- 7 E. J. Brisbois, H. Handa, T. C. Major, R. H. Bartlett and M. E. Meyerhoff, *Biomaterials*, 2013, **34**, 6957–66.
- 8 J. P. Kinsella, G. R. Cutter, W. F. Walsh, D. R. Gerstmann, C. L. Bose, C. Hart, K. C. Sekar, R. L. Auten, V. K. Bhutani, J. S. Gerdes, T. N. George, W. M. Southgate, H. Carriedo, R. J. Couser, M. C. Mammel, D. C. Hall, M. Pappagallo, S. Sardesai, J. D. Strain, M. Baier and S. H. Abman, <http://dx.doi.org/10.1056/NEJMoa060442>, 2009.
- 9 Y. Wo, Z. Li, E. J. Brisbois, A. Colletta, J. Wu, T. C. Major, C. Xi, R. H. Bartlett, A. J. Matzger and M. E. Meyerhoff, 2015.
- 10 R. J. Singh, N. Hogg, J. Joseph and B. Kalyanaraman, *J. Biol. Chem.*, 1996, **271**, 18596–18603.
- 11 M. M. Veleparampil, U. K. Aravind, C. T. Aravindakumar, M. M. Veleparampil, U. K. Aravind and C. T. Aravindakumar, *Adv. Phys. Chem.*, 2009, **2009**, 1–5.
- 12 L. Grossi and P. C. Montecchi, *Chemistry*, 2002, **8**, 380–7.
- 13 H. Handa, T. C. Major, E. J. Brisbois, K. A. Amoako, M. E. Meyerhoff and R. H. Bartlett, *J. Mater. Chem. B. Mater. Biol. Med.*, 2014, **2**, 1059–1067.
- 14 Y. Wu, Z. Zhou and M. E. Meyerhoff, *J. Biomed. Mater. Res. A*, 2007, **81**, 956–63.
- 15 R. A. Smaldone and J. S. Moore, .
- 16 C. W. Mccarthy, J. Goldman and M. C. Frost, .
- 17 D. L. H. Williams and D. L. H. Williams, in *Nitrosation Reactions and the Chemistry of Nitric Oxide*, 2004, pp. 137–160.

- 18 B. Roy, A. du Moulinet d'Hardemare and M. Fontecave, *J. Org. Chem.*, 1994, **59**, 7019–7026.
- 19 A. R. Ketchum, M. P. Kappler, J. Wu, C. Xi and M. E. Meyerhoff, *J. Mater. Chem. B*, 2016.
- 20 D. L. H. Williams and D. L. H. Williams, in *Nitrosation Reactions and the Chemistry of Nitric Oxide*, 2004, pp. 117–135.
- 21 N. M. Giles, S. Kumari, B. P. Gang, C. W. W. Yuen, E. M. F. Billaud and G. I. Giles, *Chem. Biol. Drug Des.*, 2012, **80**, 471–478.
- 22 S. Kumari, I. A. Sammut and G. I. Giles, *Eur. J. Pharmacol.*, 2014, **737**, 168–176.
- 23 M. W. Vaughn, L. Kuo and J. C. Liao, *Am. J. Physiol.*, 1998, **274**, H1705–14.
- 24 L. Packer, E. H. Witt and H. J. Tritschler, *Free Radic. Biol. Med.*, 1995, **19**, 227–250.
- 25 H. Al-Sa'doni and A. Ferro, *Clin. Sci. (Lond)*., 2000, **98**, 507–20.

## CHAPTER 3.

### THE PREPARATION AND CHARACTERIZATION OF NITRIC OXIDE RELEASING SILICONE RUBBER MATERIALS IMPREGNATED WITH *S*-NITROSO-*TERT*-DODECYL MERCAPTAN

#### 3.1 Introduction

As indicated by the results presented in Chapter 2, *S*-nitroso-*tert*-dodecyl mercaptan (SNTDM) possesses traits that are promising for the RSNO's future use in biomedical applications including long-term NO release, minimal leaching (from hydrophobic polymers), reasonable storage stability, and antiplatelet activity. Continued investigation of this molecule within this chapter involved development of a solvent swelling technique to effectively impregnate the SNTDM into catheters. The NO release behavior was determined in unique environments and the performance optimized for antimicrobial studies with *S. aureus*. The effects of an EtO sterilization technique on RSNO concentration were also tested as well given that that the conditions can be detrimental to the RSNO inside. This chapter was published in The Journal of Materials Chemistry B (2016, **4**, 422-430).

Silicone rubber (SR) has become one of the most common polymers used to prepare biomedical devices since it was first introduced to the medical field in the 1940's. Its low compression set, robust mechanical properties, chemical and temperature resistance, as well as intrinsic flexibility for melding and extrusion processes have allowed its use for numerous health care applications including shunts, implants, medical adhesives, and catheters. Silicone rubbers



have demonstrated greater biocompatibility and biodurability for certain applications compared to other common polymeric materials. Polyurethanes lack stability over as broad a temperature range compared to polydimethylsiloxanes, which potentially limits sterilization techniques or storage conditions. Exposure to organic solvents such as acetone and isopropyl alcohol, which are commonly found in adhesives and disinfectants, can solubilize polyurethanes and lead to surface cracking. Unlike polyurethanes, silicone rubber catheters are resistant to hydrolysis due to their high crosslinking. Silicone rubber's lower compression set provides increased flexibility and resistance to deformation. PVC commonly requires plasticizers, which are known to leach from the materials during use. Silicone rubber's stability also lends itself to sterilization by ethylene oxide (EtO), a process often used to sterilize biomedical devices prior to medical procedures.<sup>1-5</sup>

Despite these characteristics, introducing any foreign material such as an intravenous or urinary catheter within a patient can cause health complications including urinary tract or bloodstream bacterial infections.<sup>2</sup> Although progress has been made in preventing catheter-related bloodstream infections (CRBIs), such complications remain prevalent and are estimated to cost between 670 million and 2.68 billion dollars annually in the United States alone.<sup>6</sup> Urinary tract infections (UTIs) are the most common, with catheter-associated infections accounting for approximately 75% of occurrences.<sup>7</sup> Microbial biofilms commonly form on the surfaces of biomedical devices. Bacteria release extracellular polymeric substances that form a hydrated matrix. Bacteria within a biofilm community undergo significant phenotypic changes while in the matrix. Bacteria present within a biofilm demonstrate antibiotic resistance due to adaptive stress responses and poor antibiotic penetration, as well as protection from the host's immune system.<sup>8-10</sup> *Staphylococcus aureus* is the most common cause of nosocomial bloodstream infections, specifically those associated with biofilm formation on indwelling biomedical devices.<sup>11</sup> It can cause a range of illnesses, from skin infections to life-threatening diseases like bacteremia or sepsis. Given this and the ever-growing concern of antibiotic-resistant bacteria like methicillin-resistant *Staphylococcus aureus* (MRSA), developing effective ways to combat infections by this organism is crucial.<sup>6-11</sup>

Many methods have been studied to improve device biocompatibility such as surface modification, passive or bioactive coatings, and silver incorporation, each with their own advantages and disadvantages.<sup>12-15</sup> Indeed, Ag<sup>+</sup> eluting urinary catheters have not solved the problem given that The Healthcare Infection Control Practices Advisory Committee (HICPAC) states that silver-alloy coated catheters lead to similar infection rates compared to the conventional silicone ones. Further, they have stated that routine irrigation of the bladder with conventional antimicrobials (antibiotics) is not recommended as it increases antimicrobial resistance.<sup>9,10</sup> Recent work from our group has aimed to increase the biocompatibility and antimicrobial activity of medical grade polymers through the incorporation of nitric oxide releasing molecules.<sup>16-19</sup>

Nitric oxide (NO) is an endogenous molecule that exhibits a diverse range of benefits including its antimicrobial, antithrombotic, and vasodilatory properties, all of which have use in improving the biocompatibility of medical devices. NO releasing polymers can provide treatment at localized sites, thus minimizing side effects and complications experienced with use of systemic or local antibiotics (e.g., drug interactions) and the ever growing concern of antibiotic resistant bacteria.<sup>17-19</sup> Due to its propensity to readily oxidize, NO should be released from biomedical devices in controlled amounts, for specific durations, and at discrete locations. Regev-Shoshani *et al.* successfully demonstrated that Foley catheters impregnated with NO gas could prevent *E. coli* colonization and biofilm formation; however, they acknowledge the model does not immediately translate to clinical environments in which catheters are exposed to high urine flow.<sup>20</sup> Catheters exposed to dynamic urine flow for 24 h showed diminished bactericidal effects in the surrounding solution.<sup>20</sup> Although antimicrobial activity was demonstrated for 24 h following 1 week of storage,<sup>20</sup> retaining NO within polymers would be difficult for extended periods of storage without pressurized containers. Given NO's reactivity and the difficulties associated with the controlled delivery of this gas, various classes of NO donor molecules have been studied for potential use as an NO reservoir within polymers including diazeniumdiolates, S-nitrosothiols (RSNOs), metal nitrosyl compounds, and other nitrogen oxides.

Some RSNOs are physiological NO donors, with endogenous species including S-nitrosocysteine (CysNO), S-nitrosogluthathione (GSNO) and S-nitrosoalbumin present within the

human blood stream. Given these donors' inherent biocompatibility, they have been thoroughly studied as a means to create controllable NO delivery from materials; however, each has limitations including low stability towards thermal and photolytic decomposition. These traits make device preparation and storage difficult. Further, high water solubility enhances extraction out of the polymeric materials when in contact with blood or urine. Nonetheless, various exogenous NO donors have been incorporated into biomedical polymers in attempt to utilize NO's effects, one of the most promising RSNOs being *S*-nitroso-*N*-acetyl penicillamine (SNAP).<sup>21-23</sup> Indeed, our group recently demonstrated SNAP's ability to release NO over long durations (>3 weeks) and decrease thrombus formation at localized treatment sites.<sup>17</sup> Additionally, Colletta *et al.* recently reported that silicone rubber Foley catheters impregnated with SNAP were able to decrease *Staphylococcus epidermidis* and *Proteus mirabilis* levels for 2 weeks relative to controls. One limitation, however, is that an appreciable amount of SNAP, and likely its dimer, leach from the polymers.<sup>18</sup> Leaching decreases NO's efficacy at the localized polymer site and can cause NO's effects at unintended locations within the body.

Since scientists discovered NO to be the endothelial derived relaxing factor in 1987, researchers have continued to synthesize and develop a library of numerous NO donors, each bearing characteristics potentially suitable for unique medical applications.<sup>21,22</sup> Lipophilic alkyl RSNOs have previously been synthesized, however, they have not seriously been considered as potential medical sources of NO until recently.<sup>24-26</sup> Currently, *S*-nitroso-*tert*-dodecyl mercaptan (SNTDM) is the most promising alkyl RSNO we have studied to date. Giles *et al* demonstrated SNTDM's potential for photoactivated vasorelaxation, however, to the best of our knowledge this species has not been studied within polymeric environments.<sup>25</sup> SNTDM's highly lipophilic character (LogP=5.31) should increase retention within silicone rubber due to its hydrophobic nature.<sup>27</sup> As an RSNO's stability is largely dependent upon the substitution at the site of the nitroso functionality, we suspected that SNTDM could provide a long-term NO release.<sup>28,29</sup>

Typically, to add NO release to a polymer tubing, it would be desirable to incorporate the NO releasing agent into the extrusion process. However, RSNOs cannot withstand the elevated temperature employed for extrusion.<sup>18</sup> To overcome this limitation we have adapted our recently reported solvent swelling method to impregnate SR tubing with SNTDM, a process which

can be conducted at room temperature. Several solvents have previously been reported to effectively swell silicone rubber with no harm to its properties.<sup>30</sup> It will be shown here that silicone rubber tubing impregnated with SNTDM demonstrates significant NO release duration, reasonable storage stability, minimal leaching when in contact with an aqueous phase, as well as substantial antimicrobial activity toward *S. aureus*.

## 3.2 Experimental

### 3.2.1 Materials

*tert*-Dodecyl mercaptan (TDM), *tert*-butyl nitrite (tBuNO<sub>2</sub>), chloroform (CHCl<sub>3</sub>), diethyl ether (Et<sub>2</sub>O), dimethyl sulfoxide (DMSO), sodium chloride, potassium chloride, sodium phosphate dibasic, potassium phosphate monobasic, ethylenediaminetetraacetic acid (EDTA), copper (II) chloride, cysteine, and magnesium sulfate were purchased from Sigma Aldrich (St. Louis, MO). Dow Corning RTV 3140 Silicone Rubber (SR) was purchased from Ellsworth Adhesives (Germantown, WI). Standard silicone tubing (1.58 mm I.D, 3.18 mm O.D.) was purchased from Helix-Medical (Carpinteria, CA). All aqueous solutions were prepared with deionized water from a MilliQ system (18 MΩ cm<sup>-1</sup>; Millipore Corp., Billerica, MA). Phosphate buffered saline (PBS) containing 10 mM sodium phosphate, 138 mM NaCl, 2.7 mM KCl, and 100 μM EDTA (pH 7.4) was used as the buffer for all *in vitro* experiments. Luria Bertani (LB) broth and LB agar were obtained from Fisher Scientific Inc. (Pittsburgh, PA). *Staphylococcus aureus* ATCC 45330 was obtained from the American Type Culture Collection.

### 3.2.2 Synthesis of S-nitroso-*tert*-dodecyl mercaptan (SNTDM)

SNTDM was synthesized using a modified version of previously reported methods (see Figure 3.1)<sup>22,23</sup> *tert*-Dodecyl mercaptan was dissolved in anhydrous diethyl ether, before adding 1.1 equivalents of *tert*-butyl nitrite. After 45 min of vigorous stirring, the Et<sub>2</sub>O solution was washed with an excess of DI water and then dried with MgSO<sub>4</sub>. Et<sub>2</sub>O, residual tBuNO<sub>2</sub>, and the *tert*-butanol by-product were removed via rotoevaporation to yield a green/red liquid. SNTDM could be quantified via its absorbance (CHCl<sub>3</sub>, ε<sub>341</sub>=596 M<sup>-1</sup>cm<sup>-1</sup>, DMSO ε<sub>340</sub>=606 M<sup>-1</sup>cm<sup>-1</sup>) using a Lambda 35 UV-Vis spectrophotometer (Perkin-Elmer, MA). Following synthesis, SNTDM was

immediately used for experiments or kept in a -20 °C freezer to be used soon thereafter. Light exposure was minimized during all experiments.

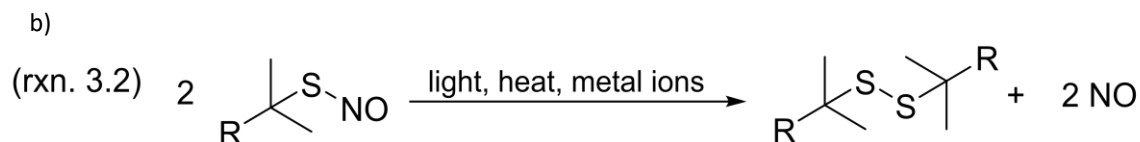
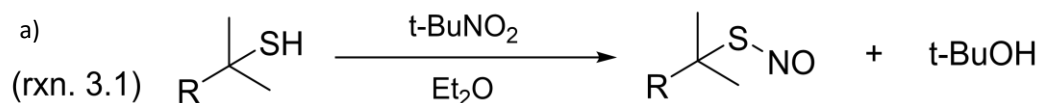


**Figure 3.1.** (a) Nitrosation of *tert*-dodecyl mercaptan (TDM) to yield *S*-nitroso-*tert*-dodecyl mercaptan (SNTDM). (b) Decomposition can be catalysed by light, heat, or metal ions such as Cu (I) to yield the disulfide and 2 equivalents of nitric oxide (NO). R=C<sub>9</sub>H<sub>19</sub> isomer.

### 3.2.3 Stimulated SNTDM decomposition

A 100 W halogen floodlight (GE model 17986) was used as a broad spectrum light source to facilitate photo-decomposition of the SNTDM doped materials. The technique was employed for various experiments requiring quick conversion to the disulfide and measuring the initial amount of RSNO present. The rate of decomposition was at times also stimulated by addition of a 50 mM CuSO<sub>4</sub>/cysteine solution. DMSO was required as a co-solvent to ensure SNTDM solubility.

### 3.2.4 UV-Vis spectroscopy

Following SNTDM's synthesis, determination of the molar absorptivity at 341 nm (CHCl<sub>3</sub>) and 340 nm (DMSO) allowed the concentration to be determined during subsequent experiments. Pure SNTDM was decomposed via photo-irradiation to form DTDD and the molar absorptivity determined to be ε<sub>275</sub>=418 M<sup>-1</sup>cm<sup>-1</sup> (see Figs. 3.1 & 3.2).

### 3.2.4 Chemiluminescence NO release measurements

Samples were placed in a glass sample cell and NO release was measured by a Sievers chemiluminescence Nitric Oxide Analyzer (NOA) 280 (Boulder, CO). Conditions varied depending on the experiment. Clear or amber cells were used to control light exposure, and a water bath

provided variable temperatures. If required, the RSNO/SR sample was submerged in PBS (pH=7.4, 100  $\mu$ M EDTA). NO was purged from the buffer and/or headspace into the detection chamber using N<sub>2</sub> sweep-gas.

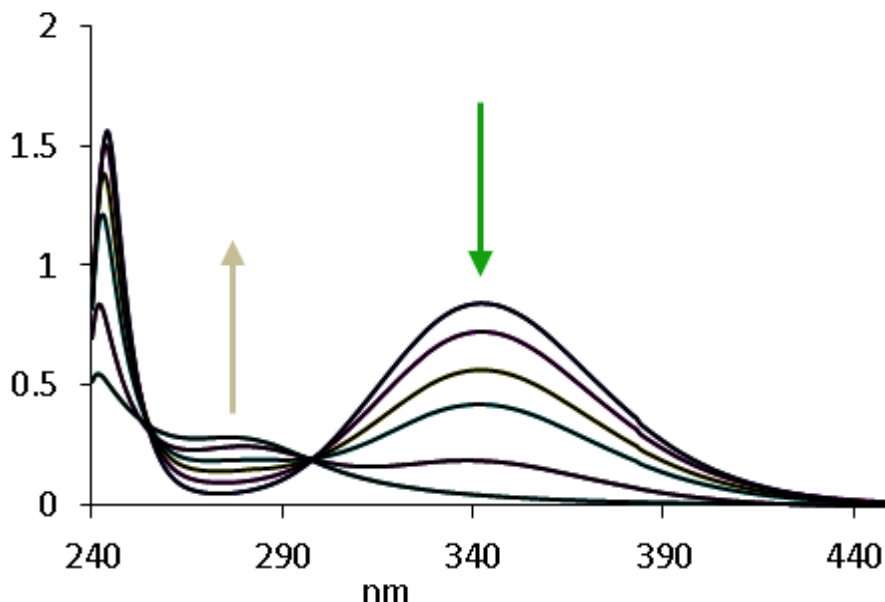


**Figure 3.2** Spectra displaying the inverse relationship between SNTDM (341 nm) and DTDD (275 nm) absorbances during decomposition.

### 3.2.5 Swelling

Segments of commercial silicone rubber tubing were submerged in vials containing a SNTDM/CHCl<sub>3</sub> solution. After stirring/soaking in the dark, the pieces were removed, briefly rinsed with a lower solubility solvent, dried with a Kim-wipe, placed in clean vials and allowed to return to the original length/diameter in the dark before being further drying in a vacuum oven in the dark to remove residual CHCl<sub>3</sub> (see Figure 3.3). SR segments were 0.5 cm in length unless otherwise specified.

*Loading efficiency:* Tubing segments were impregnated using the swelling method described above. After the tubes had dried, the wt% of impregnated SNTDM was determined by extracting the contents of a weighed piece of SR into CHCl<sub>3</sub> and measuring SNTDM's absorbance at 341 nm and/or accounting for the total released NO via NOA measurements during stimulated decomposition (by photolysis).

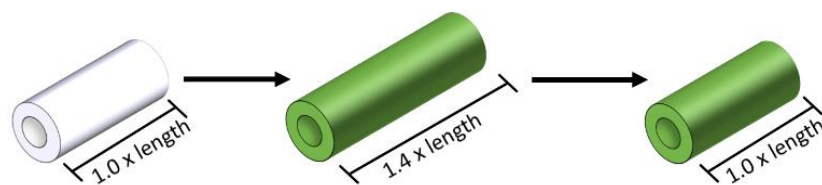


**Figure 3.3** SR tubing segments swelling with SNTDM/solvent solution. Tubing retained SNTDM's color upon impregnation with intensity correlating to wt%. The SR tubing return to original dimensions following solvent evaporation.

### 3.2.6 Characterization of SNTDM/silicone rubber Long term NO release

Samples were tested on an NOA periodically to determine their average NO release/flux. Between measurements, the tubings were soaked in PBS, and stored in a dark 37.5 °C oven to simulate physiological conditions. Prior to each measurement, the soaking solutions were replaced with fresh PBS and saved to test for leaching.<sup>16</sup> All measurements were conducted in triplicate.

### 3.2.7 Leaching measurements

PBS soaking solutions were extracted into CHCl<sub>3</sub>, and the amount of leached RSNO and RSSR was determined via UV-Vis spectroscopy.<sup>28</sup> All measurements were conducted in triplicate.

### 3.2.8 Storage stability studies

SNTDM impregnated SR tubing storage stability was determined in various environments including natural and ambient light, a RT/dark cupboard, 4 °C refrigerator, and in a -20 °C freezer. The RSNO levels were monitored periodically via UV/Vis spectroscopy. Stability testing for polymeric environments was achieved by first extracting the RSNO/RSSR contents into CHCl<sub>3</sub>. Experiments were conducted in triplicate.

### 3.2.9 Effects of ethylene oxide (EtO) sterilization

Three cm length silicone rubber tubing segments (1.58 mm I.D, 3.18 mm O.D.) were impregnated using the technique described above and submitted to the University of Michigan

Hospital sterilization facility. During the procedure, the segments were sequentially exposed to 40-80% humidity for 1 h, EtO gas for 2-3 h (40-80% humidity) followed by exhaust/aeration for 14 h. A temperature of 54 °C was maintained during the entire procedure. The SNTDM content of the tubings was measured using UV-Vis before and after sterilization. The NO flux levels were also measured following the procedure.<sup>29</sup>

### **3.2.10 Antimicrobial and biofilm study**

Three cm SR tubing pieces were impregnated using the above swelling technique, and the open ends were sealed with RTV silicone. The SR pieces were attached to the coupon holders of a CDC biofilm reactor (Biosurface Technologies, Bozeman, MT) using rubber bands. The bioreactor was filled with 10% LB broth and injected with 4 ml of overnight grown bacteria (*S. aureus*) culture. Fresh 10% LB broth was continuously supplied with a flow rate of 100 mL/h via a peristaltic pump while maintaining stirring in the bioreactor over the course of the experiment. All equipment was autoclaved prior to use and the media reservoir replaced as needed. The bioreactor was kept in a dark 37 °C oven. After 7, 14, and 21 d, the SR tubing segments were removed and the portions not touching the rubber bands cut into 2 pieces. One piece was vortexed in 2mL of 10 mM PBS buffer (pH=7.4) to homogenize any biofilm and form a single cell bacteria suspension for plating. The PBS solution was serially diluted, plated on LB agar plate and incubated overnight at 37 °C. The other was stained with Live/Dead BacLight Bacterial Viability Kit (Life technologies, Grand Island, NY) to obtain images via fluorescence microscopy (Olympus IX71, Center Valley, PA) using Fluorescence Illumination System (X-Cite 120, EXFO), filters for SYTO-9 (ex. 488 nm/em. 520 nm), and propidium iodide (ex. 535 nm/em. 617 nm). Experiments were conducted in triplicate.<sup>30,31</sup>

### **3.2.11 Statistical Analysis**

Statistical analysis data for all experiments are reported as mean SEM (standard error of the mean). Statistical significance between the control and SNTDM impregnated SR catheters was determined using a Student's t-test. Values of  $p < 0.05$  were considered statistically significant.



### 3.3 Results and Discussion

#### 3.3.1 Nitrosation and characterization of SNTDM

Nitrosation of thiols has found considerable success using acidified nitrite. *t*-BuNO<sub>2</sub> is commonly employed for the nitrosation of thiols that are not soluble in aqueous conditions, as it readily dissolves in organic solvents, forming a homogeneous solution with the thiol starting material. Yields are typically quantitative and require minimal purification. Following nitrosation, the byproduct, *tert*-butanol along with residual *t*BuNO<sub>2</sub> can be removed by room temperature rotoevaporation. Their relatively low boiling points do not require higher temperatures that would jeopardize RSNO purity and yields. These conditions proved useful for synthesizing SNTDM; however, Et<sub>2</sub>O was used as the solvent rather than the more common DMSO. Et<sub>2</sub>O's low boiling point facilitated removal, which was crucial as neat SNTDM was required for subsequent experiments.<sup>24,25,34,36</sup>

Given RSNOs' inherent thermal and photolytic instability coupled with the often lengthy preparation times for experiments in this research, being able to determine SNTDM's concentration at various time points was paramount. The most common way to measure RSNO concentrations is by detection of their  $n_0 \rightarrow \pi^*$  transition (320-360 nm). Despite this, different molar absorption coefficients are frequently reported for the same RSNOs, as determining them is difficult due to decomposition during experiments. For example, extinction coefficients for GSNO's absorbance at 335 nm have been reported as 586, 767, and 922 M<sup>-1</sup>cm<sup>-1</sup>.<sup>34-40</sup>

Consequently, when determining the molar absorptivity, maximum RSNO purity is essential. The extent of nitrosation was initially determined using chemiluminescence, the known gold standard for quantitative NO (and thus RSNO) measurements.<sup>39</sup> Immediately following purification, a SNTDM/DMSO solution was injected into an NOA cell containing a CuCl<sub>2</sub>, cysteine, water/DMSO solution to facilitate NO release. ~99.8 +/- 3.5 % of SNTDM was accounted for via integration of NO release curves. This agreed well with UV/Vis measurements that were obtained concurrently and showed minimal DTDD to be present following synthesis.

Under thermal or photolytic decomposition, RSNOs dimerize to the corresponding disulfide. By starting with pure SNTDM, and shining a 100 W broad spectrum light to induce decomposition, we are able to quantitatively convert SNTDM to DTDD (2:1 stoichiometry).<sup>17</sup> This inverse relationship can readily be monitored by UV-Vis spectroscopy as seen in Figure 3.2. Consequently, SNTDM and DTDD concentrations can be rapidly determined which facilitates understanding the NO release chemistry, especially the rate of this reaction.

### 3.3.2 RSNO Impregnation of Silicone Tubing

SNTDM has previously shown potential for use as a medicinal NO donor. Giles *et al.* utilized SNTDM's photoactivity to controllably induce vasorelaxation and also induce cell death in A549 lung carcinoma cells. However, to date, SNTDM has not yet been studied for use as a NO donor in polymeric materials.<sup>25,26</sup> After determining suitable methods for RSNO/RSSR characterization, we developed conditions to efficiently impregnate SNTDM into silicone rubber, as it is one of the most common biomedical polymers and shares a nonpolar character with

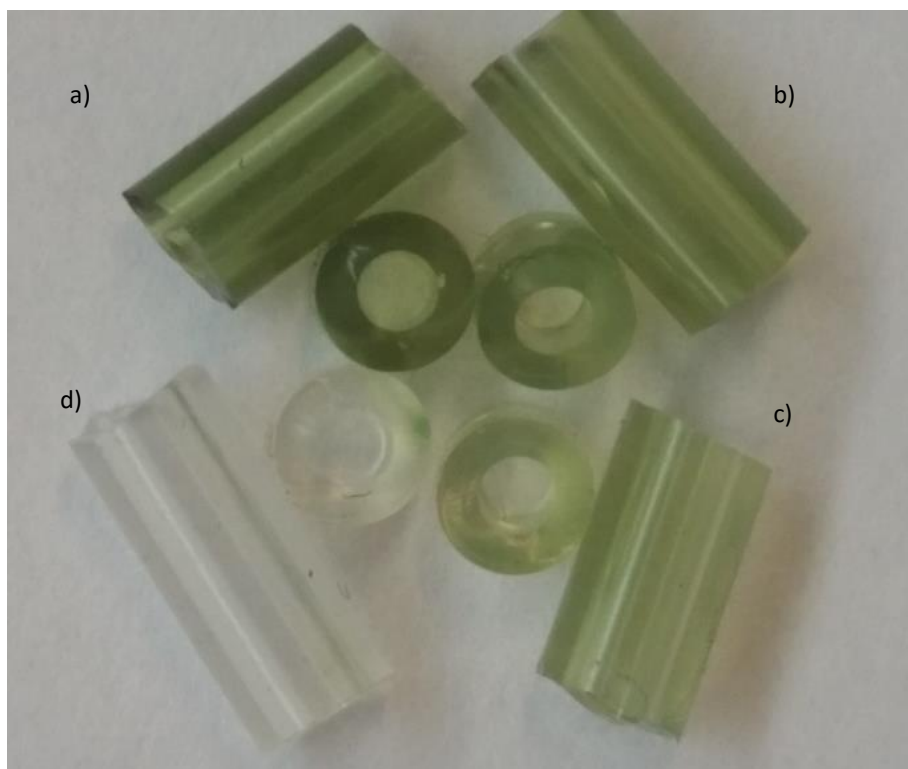


**Figure 3.4** Small segments and cross sections of silicone rubber impregnated with (a) 6.8, (b) 4.0, (c) 1.3, and (d) 0 % SNTDM showing homogenous dispersions (as indicated by color).

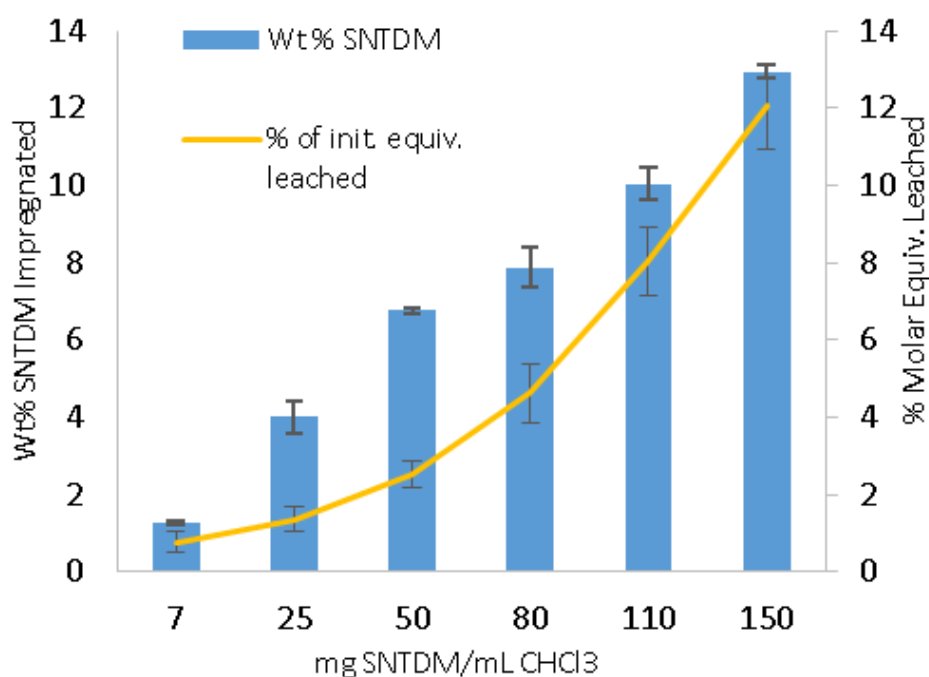
SNTDM/DTDD, thus increasing retention. Silicone rubber tubing was impregnated with SNTDM via a swelling technique using a  $\text{CHCl}_3$  solution. This yielded a translucent green polymer with no visible phase separation (see Figure 3.4).  $\text{CHCl}_3$  is known to be compatible with PDMS and swell the polymer by a 1.39 length ratio.<sup>2,30</sup> The tested tubing swelled by the same ratio, and returned to their original length following solvent evaporation (Figure 3.3). There was no noticeable change to the silicone rubber's mechanical properties following SNTDM impregnation, but more detailed quantitative testing will be required before any definitive conclusions can be made. Previously, Bayston *et al.* impregnated SR with conventional drugs such as rifampicin, trimethoprim, and spiramycin using similar swelling conditions with no detriment to the polymers' mechanical properties.<sup>41</sup> SNTDM's homogeneous impregnation can be observed by the green color that is visible throughout the length and cross section of the tubing (Figure 3.4). This technique provides an effective method for high RSNO loading that is attractive for industrial use.<sup>18,30,43-45</sup>

Impregnation contrasts with dip-coating, another common method, which results in the NO donor being largely concentrated near the polymer's surface.<sup>17</sup> This may yield instability due to the RSNO molecules' close proximity to a higher dielectric solution phase which facilitates decomposition and potentially decreases any polymeric "shielding" to light.<sup>28</sup> Increased RSNO concentration closer to the solution/polymer interface likely encourages leaching as well. Dip-coated catheters frequently require top-coats to increase stability and minimize leaching,<sup>17</sup> a process that increases the catheters' diameters, potentially making them less suitable for certain applications. With a LogP of 5.31, SNTDM's lipophilic nature lends itself to swelling in hydrophobic polymers, whereas more polar RSNOs like S-nitroso-glutathione and S-nitroso-N-acetyl-penicillamine have less affinity for hydrophobic polymers such as silicone rubber.<sup>17</sup>

Different amounts of SNTDM were impregnated by altering the concentration of SNTDM in the soaking solution. Various soaking solutions with differing concentrations (ranging from 7 - 150 mg SNTDM/mL  $\text{CHCl}_3$ ) were examined (see Figure 3.5). SR tubing soaked in a 50 mg/mL solution resulted in 6.8 wt% impregnation. These samples provide a NO flux above physiological levels for more than 3 weeks and exhibit very low leaching.

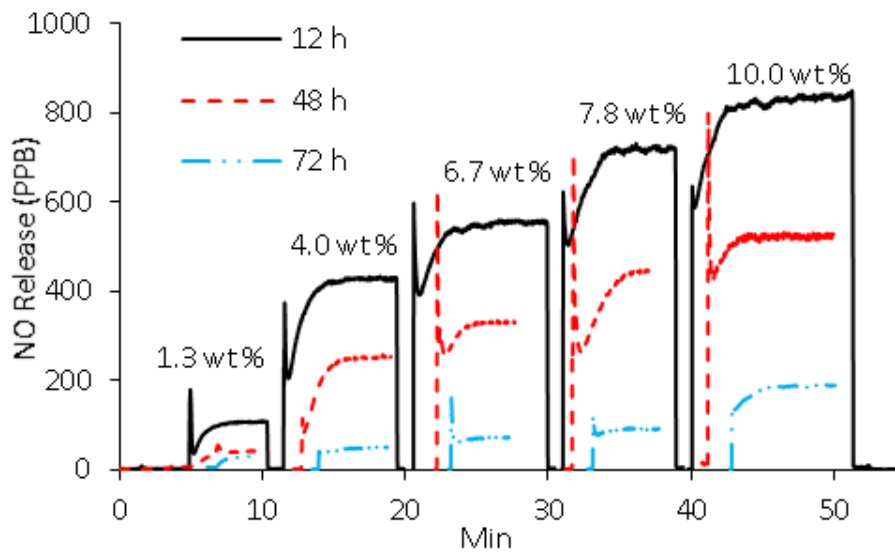
Tubing with 1.3 and 4.0 wt% SNTDM levels leach SNTDM and the disulphide product at only slightly lower rates than the 6.8 wt% loaded SR tubing (see Figure 3.5) and exhibit shorter NO release duration. Therefore, SR tubings impregnated with 6.8 wt% SNTDM were used for the majority of subsequent experiments, as they combined low leaching levels with a longer NO release duration.

Figure 3.6 shows the NO release profile for various SR tubing with different wt% SNTDM loading during the initial days following preparation and soaking at physiological pH and



**Figure 3.5** The soaking solutions' SNTDM concentration affects the amount of impregnation, which in turn relates to leaching. The reported leaching levels are the final cumulative concentrations corresponding to the SNTDM/SR tubing's NO release lifetime.

temperature. All the SNTDM impregnated SR tubings reach a fairly steady-state NO flux after ~10 min. This is in contrast with SR impregnated with SNAP, which requires more than 30 min to achieve a constant flux.<sup>18</sup> The ease of varying the RSNO's concentration within the polymer potentially allows its use for a diverse range of applications.



**Figure 3.6** Initial NO release in parts per billion (ppb) for SR tubing impregnated with various wt% SNTDM (S.A. 0.42 cm<sup>2</sup>). SNTDM/SR adopts a steady-state flux quickly, taking less than 10 min.

### 3.3.3 Long-term NO Release From SR Tubing

Within blood vessels, the levels of NO produced by endothelial cells never reach the surface of IV catheters, etc. owing to the rapid consumption of NO by oxyhemoglobin. Consequently, longer term use of polymeric devices is often associated with increased thrombus and biofilm formation, leading to a greater risk of an embolism and infection.<sup>16,17</sup> By liberating NO at their own surfaces, these risks associated with catheter devices can be reduced, allowing their extended use.<sup>17,18</sup> As shown in Figure 3.7, the SR tubing impregnated with 6.8 wt% SNTDM provides an NO flux exceeding or comparable to physiological levels for more than 26 d under physiological conditions. RSNOs commonly exhibit a “burst release” of NO, as seen in Figure 3.7. In fact, SNAP impregnated silicone Foley catheters were recently reported to have a 4-fold greater NO flux on day 1 than on day 2 (in contrast with SNTDM’s behavior which was less than a 2-fold difference).<sup>11</sup> This phenomenon doesn’t pose a toxicity concern for intravascular catheters since excess NO is rapidly consumed by the surrounding oxyhemoglobin in blood. Therefore, an intravascular catheter’s therapeutic window is maximized, accounting for the entire duration of NO release (at least 26 days). Further, NO is not foreign to the urothelium, as

it is naturally produced and released by urothelial and other neighbouring cells;<sup>46</sup> however, to the best of our knowledge, the normal NO flux has not been measured from urothelial cells. Consequently, it is not possible to make a direct conclusion regarding the effects of the burst release on the urothelium. The effects of long-term exposure to high concentrations of SNAP (2.5-5 mM) has been shown to decrease transepithelial resistance; however, following a washout of SNAP the effects were reversed.<sup>46</sup> In future work, It will be necessary and interesting to determine how the levels and duration of NO release affect the urothelial function and integrity.

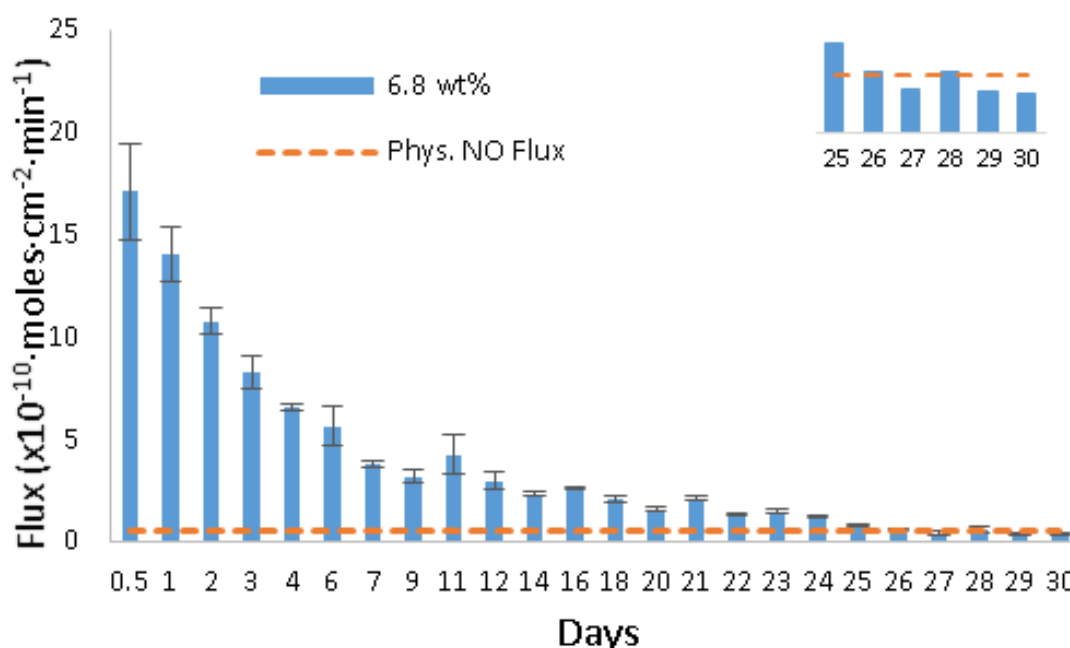


**Figure 3.7** Long-term NO flux for the 6.8wt % loaded SR tubing stored under physiological conditions (37 °C, PBS + EDTA buffer, in dark).

### 3.3.4 Leaching Tests

Many NO donors have been studied within polymers, but leaching remains a significant problem for non-covalently bound molecules.<sup>17</sup> Leaching decreases the effectiveness of NO releasing polymers for localized treatments because the NO donors not retained in the polymer will release NO at undesired locations and times. Seabra *et al.* improved GSNO's lifetime by dispersing it throughout PVA and PVPD blended films. Unfortunately, 90% of the GSNO was released during the first 24 h when the material was exposed to physiological conditions.<sup>47</sup> In the case of RSNOs, potentially leached species include the original RSNO and the corresponding

disulfide, formed within the polymer or in the soaking solution. Shining a broad spectrum halogen light on the soaking solutions can assure complete conversion of any RSNO to RSSR. This allowed for the detection of any RSSR to account for all leached species. In comparing the DTDD content with the initial amount of SNTDM impregnated, approximately 2.5% of the impregnated RSNO leached from the SR tubing during the 30 d NO release measurements (Figure 3.7). Measurements following one day of soaking indicated ~2% had been released. The larger initial release is likely due to the effect of higher water content within the SR polymer phase at the outermost surfaces of the material.<sup>16,42</sup> Leaching during subsequent days was quite minimal, thus requiring the daily soaking solutions to be combined before extraction and concentration in CHCl<sub>3</sub> in order to quantitate the levels of the thiol dimer. The 2.5% leach rate determined for SNTDM from SR over 30 d is much lower than the leaching of SNAP or other RSNO's reported in similar experiments.<sup>17,18</sup> SNTDM's highly lipophilic nature likely accounts for its retention, particularly within a lipophilic polymer like silicone rubber which has a 1.2 +/- 0.3 wt% water uptake in the bulk of the polymer phase.<sup>3</sup>

### 3.3.5 Storage Stability

SNTDM's storage stability was tested under various conditions including as a neat material, in solution, and impregnated within silicone rubber. Tertiary alkyl substitution should render SNTDM more stable than other less substituted RSNOs such as S-nitroso-cysteine or GSNO, NO donors whose biomedical use has been limited by low stability.<sup>28,48</sup> Giles and Kumari *et al.* recently reported on SNTDM's substantial photoactivity.<sup>25,26</sup> Previous research using SNAP has found its NO release profile to essentially not be affected by laboratory light (fluorescent).<sup>17</sup> In contrast, the SNTDM in SR samples show a 7-fold increase in flux upon turning on laboratory lights. Additionally, shining light from a 100 W broad spectrum halogen lamp at close proximity results in a ~60 fold increase of NO flux, relative to a dark room (see Figure 3.8). After removing light sources, the NO flux returns to the original baseline level.

General storage stability in the absence of light is another important property of any potential NO release medical device. By incorporating SNTDM into SR tubing, its lifetime can be

extended relative to the neat and solution phase samples (see Figure 3.9), however, not to the extent to allow the SNTDM-doped SR tubing to be stored in ambient conditions.

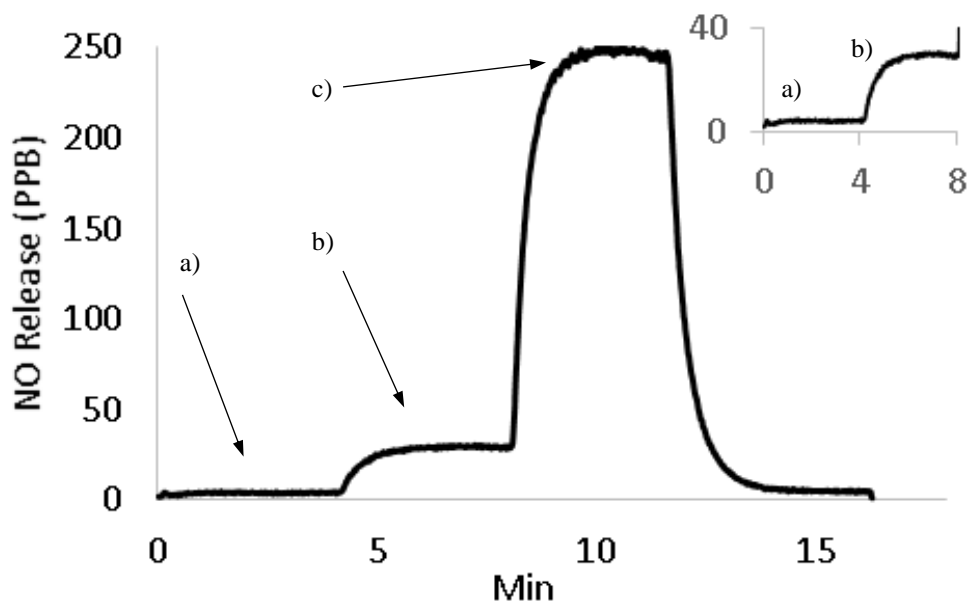


**Figure 3.8** SR tubing impregnated with 1.3 wt% SNTDM (S.A.  $0.42 \text{ cm}^2$ ) at  $22.5 \text{ }^\circ\text{C}$  in the dark, with a) fluorescent light, with b) fluorescent light and a broad spectrum halogen lamp, and again, in the c) dark.

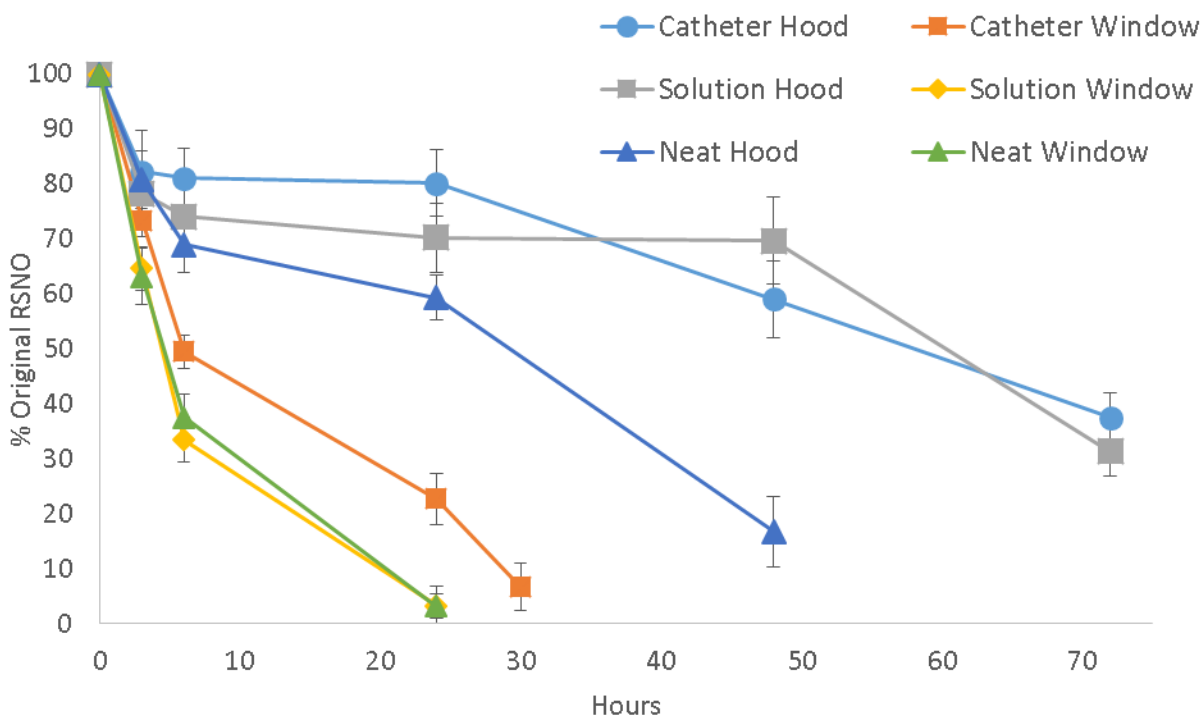


**Figure 3.9** The effects of light sources and phase dependence on SNTDM's NO release



This is a limitation of the presented system, since SNAP has shown significant stability under ambient conditions. Recently, our group reported ~87% of the SNAP impregnated in SR to still be present after 8 months of storage in the dark.<sup>11</sup> While SNAP impregnated SR provides superior storage stability, one must also keep in mind that the higher levels of RSNO may not be beneficial since a larger portion of them will leach from the polymer. For clinical applications, SNTDM impregnated SR devices could be stored in foil packages containing desiccant at reduced temperatures to extend their lifetime.

In contrast with its considerable photoactivity, SNTDM's tertiary substitution provides substantial thermal stability, likely due to the steric hindrance at the site of dimerization. This makes storage in dark environments viable (see Figure 3.10). SNTDM/SR storage in the freezer provided the highest stability with 75% of the initial SNTDM remaining even after 3 months (see Figure 3.11). As expected, SNTDM had a shorter lifetime during refrigerator and cupboard storage. SR's stabilizing effect was more significant regarding photo induced decomposition likely because the disulfide product increased the polymer's opacity and impeded the penetration of incoming light. SNTDM/SR, neat, and  $\text{CHCl}_3$  samples were stored in a freezer for the duration of their lifetimes. Within error, no stabilizing effects were observed by SR, nor were there statistical differences between the neat and solution phases (see Figure 3.11).

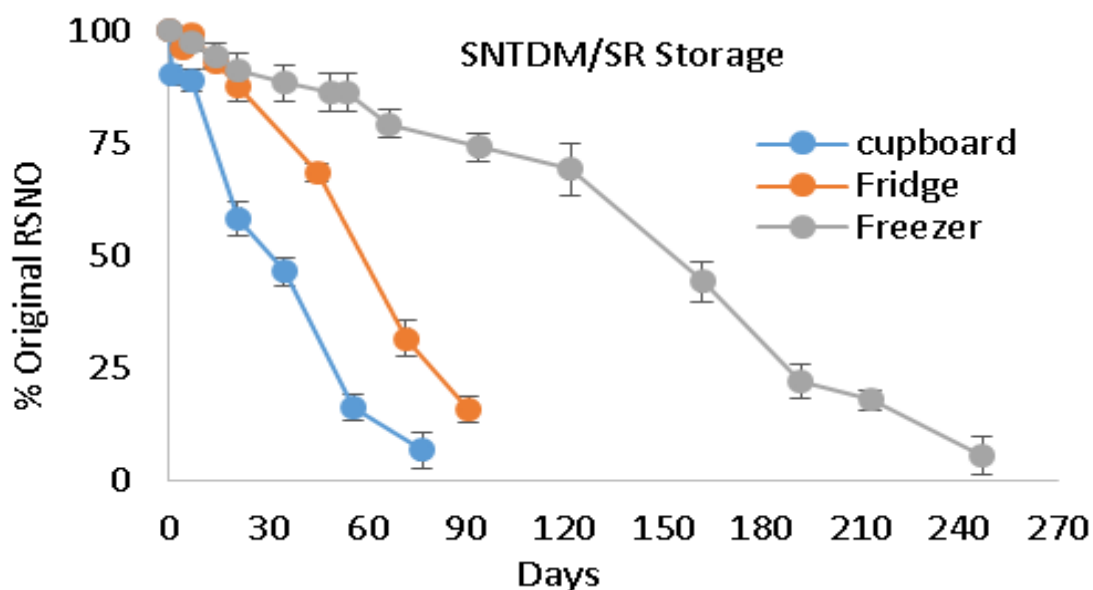
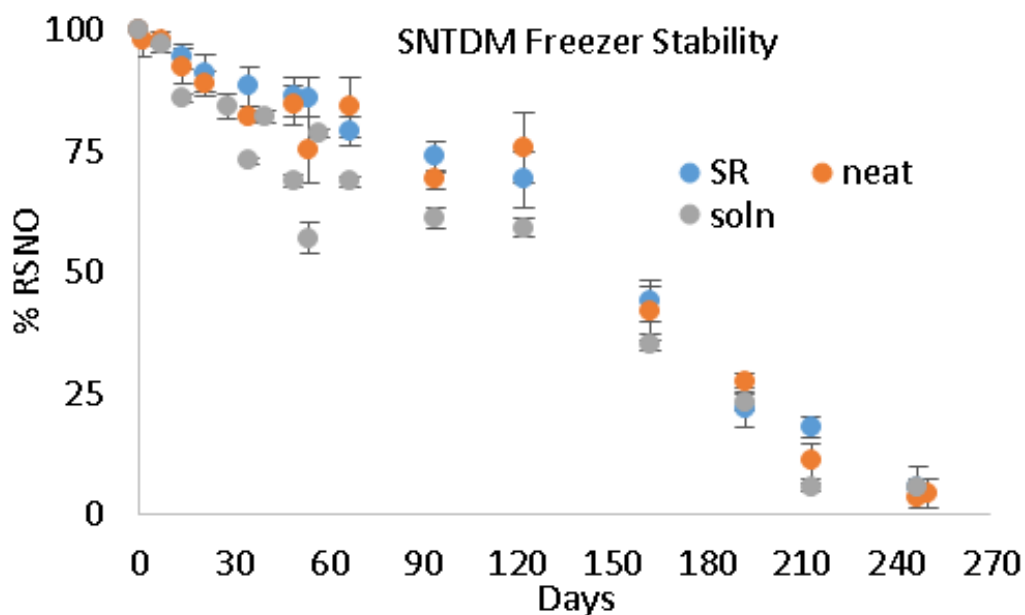


Figure 3.10 SNTDM impregnated SR tubing stored in various environments



**Figure 3.11** Freezer storage for SNTDM in various phases.

### 3.3.5 EtO Sterilization

Given RSNOs' thermal or photo-induced decomposition, biomedical devices incorporating RSNOs are not suitable to sterilization procedures requiring high heat. To evaluate the SNTDM impregnated SR tubing's behavior under applicable conditions, we submitted SR tubing segments impregnated with several different wt% levels of SNTDM to the University of Michigan hospital's sterilization facility to undergo EtO sterilization. Following the sterilization procedure, the NO flux levels from the samples were measured at different time points (see Figure 3.12). The samples were stored in the dark while submerged in PBS containing EDTA between measurements so as to mimic physiological conditions. All tubing segments exhibited NO fluxes above physiological levels for several days, with even the 4 wt% tubings lasting 5 d. The 6.8 wt% tubings lasted ~6 d, while the higher concentrations released NO above physiological flux for 8 d. Although care was taken to minimize light exposure, the samples were not sterilized immediately following their submission, and several days elapsed before the procedure was performed. Consequently, the SR tubing's NO release duration would likely be extended were this not the case.

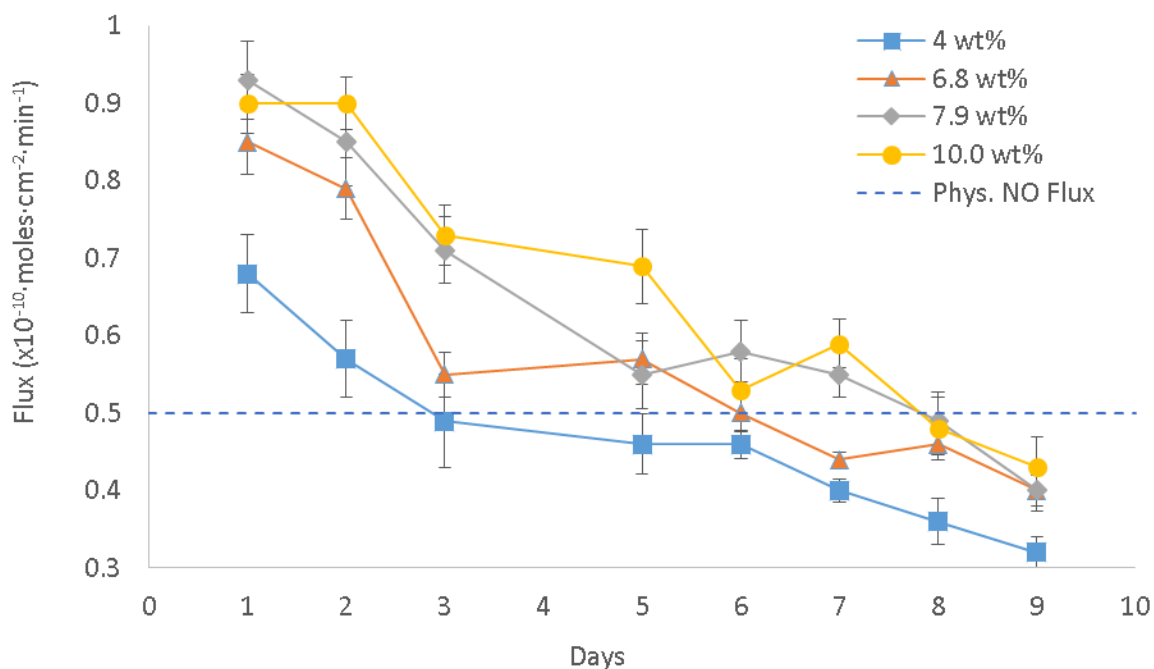


**Figure 3.12** Various wt% SNTDM/SR tubing's NO fluxes following EtO sterilization.

Despite the reduced SNTDM levels following EtO sterilization, recent work within our group has discovered that even lower levels of NO flux (e.g.,  $0.3 \times 10^{-10} \text{ mol cm}^{-2}\text{min}^{-1}$ ) are able to produce substantial antimicrobial effects on silicone rubber surfaces against *Pseudomonas aeruginosa*. Hence, it is anticipated that the EtO sterilized SNTDM impregnated catheters will still have considerable antimicrobial activity despite some loss of active SNTDM during this sterilization process. Other sterilization techniques are also possible and remain to be explored, including methods which do not require elevated temperatures such as gamma and glutaraldehyde sterilizations.

### 3.3.6 Anti-biofilm Activity

Although biomedical devices are essential for medical care, microbial infections remain a serious concern. Bacteria bear attached to implanted medical devices. Biofilm formation often coincides with this colonization and complicates medical procedures by further increasing the risk of infection. Biofilm formation can decrease the effectiveness of antibiotics and hinder opsonophagocytosis, thus leading to chronic infections.<sup>49</sup> For bloodstream catheters, if the

devices emit NO at levels similar to endothelial cells, there is zero risk of any toxicity to tissue cells, since the liberated NO is immediately scavenged by excess oxyhemoglobin in the blood. Therefore, we tested our SNTDM/SR system against *Staphylococcus aureus*, a microbe. Periodically, the SR tubing pieces were vortexed in PBS solutions to remove and homogenize bacteria/biofilms. The solutions were serially diluted before plating them on agar. Colonies were incubated overnight and then counted. After 1 week, the NO releasing tubings had 4 orders of magnitude less *S. aureus* relative to controls (see Figure 3.13). After 14 days, the control bacteria levels had remained constant, within error, while the SNTDM/SR tubing had a further reduction in amount of live bacteria. Even after 3 weeks, the SNTDM doped tubings had 3 orders magnitude less live bacteria on their surface than the controls, indicating the NO had killed or inhibited growth of 99.9% of the bacteria (see Figure 3.13). The catheters' outer surfaces were examined because they are in more direct contact with the bacterial culture when in the bioreactor. Since the NO flux from the catheters' inner and outer surfaces are equivalent, it is expected that the same level of antimicrobial activity will be observed on each surface.

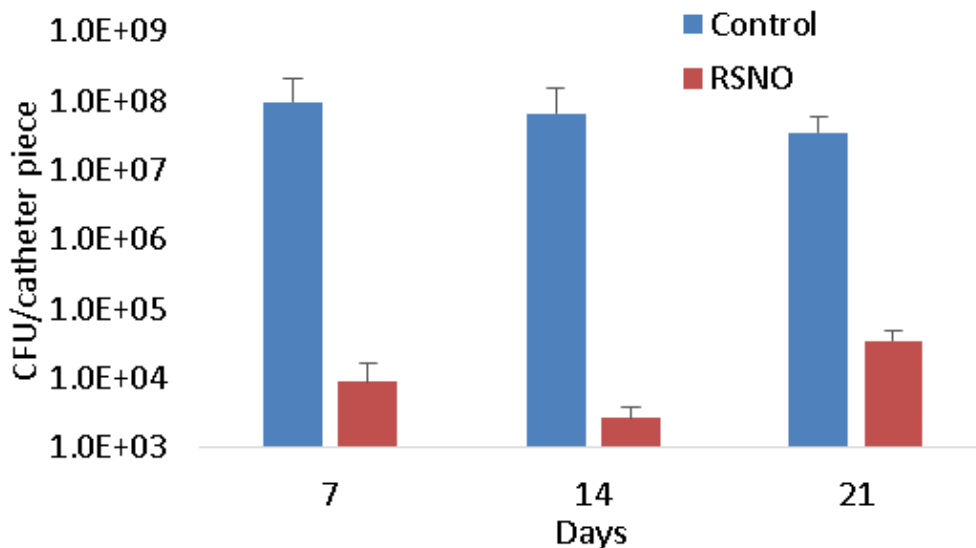


**Figure 3.13** *S. aureus* levels determined from the SR tubing pieces' homogenized solution cell counts. n=3 for each day. (P < 0.01)

When tubing pieces were removed for cell counting and biofilm testing, pieces were also tested via NOA measurements to compare NO flux before and after the CDC experiments

(see Figure 3.14). Before the CDC experiment, a set of tubing pieces had comparable NO fluxes with the oven samples stored at the same temperature. This also held true for the samples measured on days 14 and 21. By the end of the 3<sup>rd</sup> week, the tubings in the CDC were releasing NO below physiological levels (0.33 +/- 0.12 vs. 0.5). Despite this, they still exhibited a 99.9% reduction in live *S. aureus* bacteria on their surfaces, thus indicating their effective window of treatment can potentially extend further than originally expected.

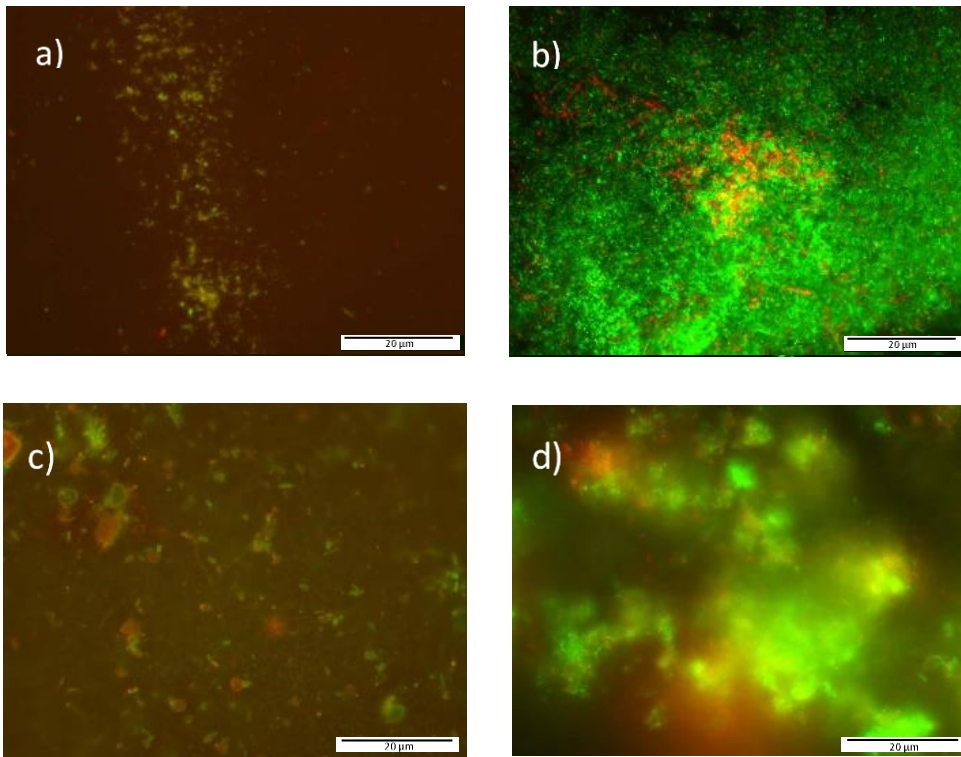


**Fig. 3.13** (a) SNTDM impregnated and (b) control silicone rubber tubing images after 7 days demonstrating NO's effect at reducing *S. aureus* levels. (c) SNTDM and (d) control tubing images from day 21 indicating difference in biofilm formation.

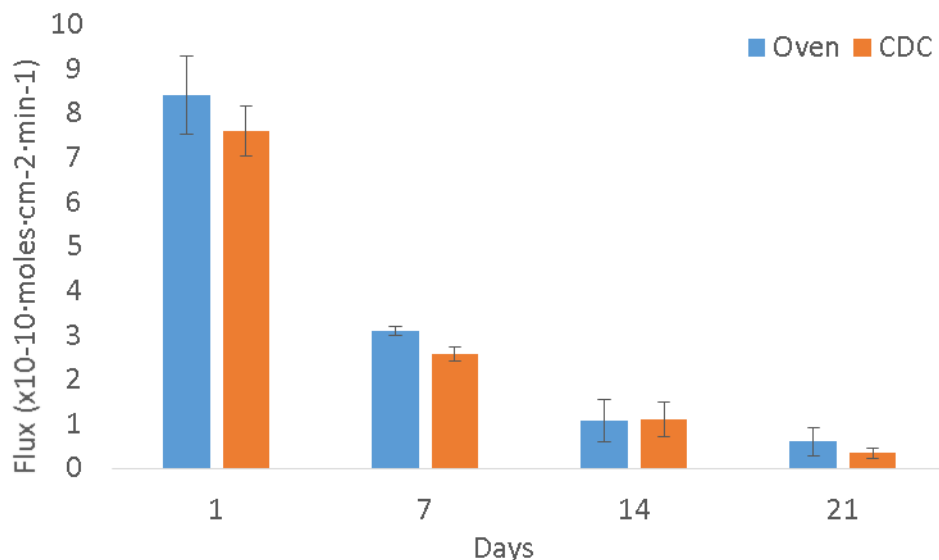


**Figure 3.14** NO Flux levels measured throughout an antimicrobial experiment compared to oven storage.

### 3.4. Conclusions

In summary, *S*-nitroso-*tert*-dodecyl mercaptan has been examined for its use as a long-term NO donor within silicone rubber tubing. A solvent swelling/impregnation method has proven useful for impregnating SNTDM at ranges from 1.3–12.9 wt% within the tubing. When impregnated with 6.8 wt% SNTDM, the tubings exhibit long-term NO release, lasting more than 3 weeks above the normal physiological flux that occurs at the endothelium/blood interface. SNTDM's lipophilicity combined with silicone rubber's hydrophobicity provides a low leaching system in which >97% of the original molecule is retained within the polymer after 3 weeks of soaking. Given SNTDM's tertiary substitution, the impregnated SR tubings exhibit reasonable stability during storage in a freezer, retaining 75% SNTDM after 3 months. Due to SNTDM's thermal stability, 7.9 and 10 wt% impregnated SR tubings are able to release NO for 8 d above physiological flux levels following EtO sterilization. This level could likely be increased following further optimization. During a 3-week incubation in a CDC bioreactor, the impregnated tubings reduced surface levels of *S. aureus* by 4 orders of magnitude during the first 2 weeks and 3 orders after the third week. These results confirm the potential for SNTDM impregnated SR materials to improve the biocompatibility and antimicrobial activity of medical devices such as urinary and

intravascular catheters for at least 3 weeks. Current efforts are focused on exploring the effect of incorporating SNTDM in other biomedical grade polymers, especially with respect to photoactivated NO release applications (e.g., to create a source for inhaled NO gas, etc.). In addition, efforts to improve the shelf life of this new NO release polymer using additives to help stabilize the NO donor are underway. Lastly, a proprietary polyurethane from Braintree Scientific, Inc. (Braintree, MA) was discovered very recently to have substantial stabilizing effects regarding both photolytic and thermal NO release from SNTDM impregnated into this material. Therefore, SNTDM's behavior in alternate biomedical polymer matrices warrants considerable investigation.

### 3.5 References

- 1 A. Colas, J. Curtis, in *Biomaterials Science: An Introduction to Materials in Medicine*, ed. B. D. Ratner, A. S. Hoffman, F. J. Schoen, J. E. Lemons, Elsevier, Inc., San Diego, London, 2<sup>nd</sup> Ed., 2004, Ch. 2.3, 80-86.
- 2 J. Curtis, A. Colas, in *Biomaterials Science: An Introduction to Materials in Medicine*, ed. B. D. Ratner, A. S. Hoffman, F. J. Schoen, J. E. Lemons, Elsevier, Inc., San Diego, London, 2<sup>nd</sup> Ed., 2004, Ch. 7.19, 697-707.
- 3 A. S. Breitbart, V. J. Ablaza, in *Grabb and Smith's Plastic Surgery*, ed. C. H. Thorne, Lippincott Williams & Wilkins, Philadelphia, 6<sup>th</sup> Ed., 2007, Ch. 7, 58-65.
- 4 J. Curtis, P. Klykken, in *A Comparative Assessment of Three Common Catheter Materials*, Dow Corning Corp., USA, 2008.
- 5 S. Ebnesajjad, K. Modjarrad, in *Handbook of Polymer Applications in Medicine and Medical Devices*, ed. S. Ebnesajjad, K. Modjarrad, Elsevier, Inc., Oxford, San Diego, 1<sup>st</sup> Ed., 2014,
- 6 S. H. Bosch W., K. M. Thompson, W. C. Hellinger, *The Neurohospitalist* 2013, **3**, 144-151.
- 7 Centers for Disease Control and Prevention, [http://www.cdc.gov/HAI/ca\\_uti/uti.html](http://www.cdc.gov/HAI/ca_uti/uti.html), (accessed June 2015).
- 8 G. O'Toole, H. B. Kaplan, R. Kolter, *Annu. Rev. Microbiol.*, 2000, **54**, 49-79.

- 9 P. S. Stewart, *Int. H. Med. Microbiol.*, 2002, **292**, 107-113.
- 10 C. von Eiff, B. Jansen, W. Kohnen, K. Becker, *Drugs*, 2005, **65**, 179-214.
- 11 Y. Wo, Z. Li, E. J. Brisbois, A. Colletta, J. Wu, T. C. Major, C. Xi, R. H. Bartlett, A. J. Matzger, M. E. Meyerhoff, *ACS Appl. Mater. Interfaces.*, 2015, **7**, 22218–22227.
- 12 P. Lin, C. Lin, R. Mansour, F. Gu, *Biosens. and Bioelectron.*, 2013, **47**, 451-460.
- 13 J. M. Goddard, J. H. Hotchkiss, *Prog. Poly. Sci.*, 2007, **32**, 698-725.
- 14 Y. Ikada, *Biomaterials*, 1994, **15**, 725-736.
- 15 K. Davenport, F. X. Keeley, *J. Hosp. Infect.*, 2005, **60**, 298–303.
- 16 W. Cai, J. Wu, C. Xi, M. E. Meyerhoff, *Biomaterials*, 2012, **33**, 7933-7944.
- 17 E. J. Brisbois, H. Handa, T. C. Major, R. H. Bartlett, M. E. Meyerhoff, *Biomaterials*, 2013, **34**, 6957-6966.
- 18 A. Colletta, J. Wu, Y. Wo, M. Kappler, H. Chen, C., Xi, M. E. Meyerhoff, *ACS Biomater. Sci. Eng.*, 2015, **1**, 416-424.
- 19 C. Sousa, M. Henriques, R. Oliveira, *Biofouling*, 2011, **27**, 609-620
- 20 G. Regev-Shoshani, M. Ko, C. Miller, Y. Av-Gay, *Antimicrob. Agents. Chemother.*, 2010, **54**, 273-279.
- 21 M. R. Miller, I. L. Megson, *Br. J. Pharmacol.*, 2007, **151**, 305-321.
- 22 D. L. H. Williams, *Acc. Chem. Res.*, 1999, **32**, 869-874.
- 23 H. H. Al-Sa'doni, A. Ferro, *Clin. Sci (Lond)*, 2000, **98**, 507-520.
- 24 B. Roy, A. du M. d'H., M. Fontecave, *J. Org. Chem.*, 1994, **59**, 7019-7026.
- 25 N. M. Giles, S. Kumari, B. P. Gang, C. W. Yuen, E. M. Billaud, G. I. Giles, *Chem. Biol. Drug. Des.*, 2012, **80**, 471-478
- 26 S. Kumari, I. A. Sammut, G. I. Giles, *Eur. J. Pharmacol*, 2014, **737**, 168-176.
- 27 ChemBioDraw Ultra 13, *CambridgeSoft*, Cambridge MA, USA.
- 28 D. A. Riccio, P. N. Coneski, S. P. Nichols, A. D. Broadnax, M. H. Schoenfisch, *ACS Appl. Mater. Interfaces*, 2012, **4**, 796-804.
- 29 M. G. de Oliveira, S. M. Shishido, A. B. Seabra, N. H. Morgan, *J. Phys. Chem. A*, 2002, **106**, 8963-8970.
- 30 J. N. Lee, C. Park, G. M. Whitesides, *Anal. Chem.*, 2003, **75**, 6544-6554.



- 31 E. J. Brisbois, R. P. Davis, A. M. Jones, T. C. Major, R. H. Bartlett, M. E. Meyerhoff, H. Handa, *J. Mater. Chem. B*, 2015, **3**, 139-1645.
- 32 BioSurface Technologies Corporation CDC Biofilm Reactor description and schematic, <http://www.biofilms.biz/wp-content/uploads/2010/12/web-CDC-InfoPricing-2010.pdf>, (accessed October 2015).
- 33 H. Ren, A. Colletta, D. Koley, J. Wu, C. Xi, T. C. Major, R. H. Bartlett, M. E. Meyerhoff, *Bioelectrochemistry*, 2015, **104**, 10-16.
- 34 K. Szacilowski, Z. Stasicka, *Prog. React. Kinet.*, 2001, **26**, 1-58.
- 35 P. Girard, N. Guillot, W. B. Motherwell, R. S. Hay-Motherwell, P. Potier, *Tetrahedron*, 1999, **55**, 3573-3584.
- 36 K. A Broniowska, A. R. Diers, N. Hogg, *Biochim., Biophys. Acta.*, 2013, **1830**, 3173-3181.
- 37 K. Fang, N. V. Ragsdale, R. M. Carey, T. Macdonald, B. Gaston, *Biochem. Biophys. Res. Commun*, 1998, **252**, 535-540.
- 38 L. P. Yap, H. Sancheti, M. D. Ybanez, J. Garcia, E. Cadenas, D. Han, *Methods Enzymol.*, 2010, **473**, 137-147.
- 39 D. Tsikas, *Nitric Oxide*, 2003, **9**, 53-55.
- 40 R. J. Singh, N. Hogg, J. Joseph, B. Kalyanaraman, *FEBS Letters*, 1995, **360**, 47-51.
- 41 R. Bayston, N. Grove, J. Siegel, D. Lawellin, S. Barsham, *J. Neurol., Neurosurg., Psychiatry*, 1989, **52**, 605-609.
- 42 H. Handa, E. J. Brisbois, T. C. Major, L. Refahiyat, K. A. Amoako, G. M. Annich, R. H. Bartlett, M. E. Meyerhoff, *J. Mater. Chem. B*, 2013, **1**, 3578-3587.
- 43 D. N. Soulas, K. G. Papadokostaki, M. Sanopoulou, *J. Appl. Polym. Sci.*, 2013, DOI: 10.1002/APP.38711.
- 44 B. Vazquez-Gonzalez, H. I. Melendez-Ortiz, L. Diaz-Gomez, C. Alvarez-Lorenzo, A. Concheiro, E. Bucio, *Macromol. Mater. Eng.*, 2014, **299**, 1240-1250.
- 45 P. Sriamornsak, J. Nunthanid, K. Cheewatanakornkool, S. Manchun, *AAPS PharmSciTech*, 2010, **11**, 1315-1319.

- 46 L. C. Weaver, C. Polosa, *Autonomic Dysfunction After Spinal Cord Injury (Progress in Brain Research)*, Elsevier Science, place, 1<sup>st</sup> ed., 2005,
- 47 A. B. Seabra, M. G. de Oliveira, *Biomaterials*, 2004, **25**, 3733-3782.
- 48 E. Bechtold, S. B. King, *Antioxid. Redox Signal.*, 2012, **17**, 981-991.
- 49 C. Cucarella, M. A. Tormo, E. Knecht, B. Amorena, I. Lasa, T. J. Foster, J. R. Penades, *Infect. Immun.*, 2002, **70**, 3180-3186.

## **CHAPTER 4.**

### **PHOTOACTIVATED NITRIC OXIDE RELEASE FROM LIPOPHILIC S-NITROSOTHIOLS WITHIN BIOMEDICAL GRADE POLYMERS**

#### **4.1 Introduction**

S-Nitrosothiols (RSNOs) are a class of NO donor that release NO when exposed to light and thus have considerable potential for photoactivation therapies.<sup>5,6,7</sup> NO's antimicrobial and antithrombotic properties, as well as its ability to kill cancer cells, offer utility for many applications such as wound healing patches that prevent infection, or dialysis tubing with decreased thrombus formation. Oplander *et al.* discovered that shining 420-453 nm light on human skin induced NO generation from the inherent S-nitrosoalbumin species. They proposed that this blue light treatment could be therapeutically used to treat hemodynamic disorders resulting from impaired bioavailability of NO.<sup>8</sup> Previously, Schoenfisch *et al.* demonstrated that upon photoactivation, xerogels modified with an S-nitroso-N-acetylpenicillamine (SNAP) siloxy derivative exhibit a 90% reduction in *Pseudomonas aeruginosa* adhesion, as well as kill adhered bacteria relative to the controls.<sup>5</sup>

NO's role in tumors is not well understood and has in fact been shown to take part in both cancer cell progression and death, acting on a survival/anti-apoptotic loop.<sup>2</sup> NO synthesis pathways are often upregulated in cancer cells and thought to facilitate tumor angiogenesis and cell proliferation;<sup>1,4</sup> however, the presence of macrophages can increase the local levels of NO flux, which provides a cytotoxic effect toward cancer cells. At high levels, resulting from an external source such as a photoactivated RSNO, NO plays an increased role in the generation of the ROS, and thus cytotoxicity. Research has suggested that the inherent presence of NO in

tumors promotes their growth and proliferation, however, the additional application of NO induces its cytotoxic effects.<sup>1</sup> In one study, Rapozzi *et al.* exposed mice with tumors to diethylenetriamine NONOate, a diazeniumdiolate NO donor. Exposure to the exogenous source of NO inhibited the cancer cells' anti-apoptotic loop, thus facilitating cell death.<sup>2</sup>

In this chapter, the photoactivated NO release from two of the exogenous RSNOs introduced in Chapter 2, *S*-nitroso-*tert*-dodecylmercaptan (SNTDM) and *S*-nitrosotriphenylmethanethiol (SNTPMT), as well as *S*-nitroso-*N*-acetylpenicillamine (SNAP), is examined to identify their behavior in biomedical grade polymers, and determine their potential for photoinduced NO releasing medical devices. SNTDM's and SNTPMT's low leaching and stability make them viable candidates for such devices, and SNTDM's photosensitivity provides a highly effective and efficient contrast between dark and photoactivated NO release levels.

## 4.2 Experimental

### 4.2.1 Materials

*N*-Acetyl-DL-penicillamine (NAP), glutathione, sodium chloride, magnesium sulfate, sodium phosphate dibasic, potassium phosphate monobasic, ethylenediaminetetraacetic acid (EDTA), tetrahydrofuran (THF), sulfuric acid, diethyl ether (Et<sub>2</sub>O), *N,N*-dimethylacetamide (DMAc), hexane, chloroform (CHCl<sub>3</sub>), silica gel, molecular sieves, methanol (MeOH), sodium nitrite (NaNO<sub>2</sub>), *t*-butylnitrite (*t*-BuNO<sub>2</sub>), dodecanethiol (DDT), *tert*-dodecylmercaptan (TDM), *tert*-butanethiol (TBT), *d*<sub>6</sub>-chloroform (CDCl<sub>3</sub>), dimethylsulfoxide (DMSO), graphite powder (GP), and triphenylmethanethiol (TPMT) were purchased from Sigma-Aldrich (St. Louis, MO). Hydrochloric acid and sulfuric acid were purchased from Fisher Scientific (Pittsburgh, PA). Tecoflex SG-80A (TF), Pellethane 2363-80AE (PELL), and Carbothane PC 3585A were obtained from Lubrizol Advanced Materials Inc. (Cleveland, OH). Dow Corning RTV 3140 Silicone Rubber (SR) was purchased from Ellsworth Adhesives (Germantown, WI). CarboSil 20 90A (CS) was obtained from the Polymer Technology Group (Berkeley, CA). LEDs were purchased from LuxeonStar (Brantford, Ontario, Canada), Elast-eon TM E2As (E2As) was purchased from AorTech International, PLC (Scoresby, Victoria, Australia). All aqueous solutions were prepared with 18.2 MΩ deionized water using a Milli-Q filter (Millipore Corp., Billerica, MA). Phosphate buffered

saline (PBS), pH 7.4, containing 138 mM NaCl, 2.7 mM KCl, 10 mM sodium phosphate, and 100  $\mu$ M EDTA was used for all *in vitro* experiments.

#### 4.2.2 Nitrosation

TDM and TPMT were nitrosated using excess *t*-BuNO<sub>2</sub> in Et<sub>2</sub>O, DMSO, THF, or CHCl<sub>3</sub> as described in Chapter 2, while SNAP's synthesis used acidified inorganic nitrite in a methanol solution. All nitrosations were performed in the dark at room temperature (RT).

#### 4.2.3 Preparation of RSNO Doped Films

A known mass of RSNO was dissolved in a THF/polymer solution. The solution was stirred for a few minutes to ensure homogeneity of the film-casting solution composition. The solutions were then cast into Teflon rings on a Teflon plate and dried overnight under a low stream of N<sub>2</sub>. Following solvent evaporation, discs were punched out of the films using a d=0.7 cm hole punch, weighed, and if desired for the experiment, dip-coated in a pure 200 mg polymer/4 mL THF solution before being dried under vacuum.<sup>9</sup>

#### 4.2.4 NO Release Measurements

Nitric oxide was measured using a Sievers chemiluminescence Nitric Oxide Analyzer (NOA) 280 (Boulder, CO). Samples were placed in the sample vessel either neat, dissolved in DMSO, or when in films, immersed in PBS (pH 7.4) containing 100  $\mu$ M EDTA. Nitrogen was bubbled into the solution and any liberated NO was purged and swept from the headspace into the chemiluminescence detection chamber of the NOA. The sample vessels varied depending on the experiment, with either clear or amber cells were used to provide control over light exposure. If applicable, a DMSO/CuSO<sub>4</sub>/cysteine solution could be injected to catalyze NO release in addition to the photo-irradiation process. To ensure film samples remain submerged in the chamber buffer during experiments, they were impaled on needles and suspended in solution to measure NO release rates with the NOA.<sup>9,10</sup> All fluxes reported have units of 10<sup>-10</sup> mol-cm<sup>-2</sup>-min<sup>-1</sup>.

#### 4.2.5 Photoactivated NO Release

The RSNOs or RSNOs within polymer films were exposed to a light source (100 W halogen floodlight (GE model 17986)) at variable distances for photolysis experiments, overhead fluorescent ambient light, or on a westward facing windowsill.

#### **4.2.6 Determining the RSNO Levels in Polymer Films**

For initial experiments, the amount of RSNO was determined by stimulating NO release from a piece of polymer with a known mass using heat, light, and a Cu(I)/cysteine solution, and integrating the NO release curve. After obtaining the molar absorptivity of compounds, the amount of RSNO in a polymer could also be determined by extracting the RSNO content into solution (usually  $\text{CHCl}_3$ ), or as with the case of soluble polymers, dissolving a known mass (usually in THF or DMAc).<sup>10</sup>

#### **4.2.7 Graphite Powder Topcoat**

A specific mass (X) of graphite powder was vortexed with a polymer/THF solution containing 200 mg-X polymer and 4 mL of THF.

### **4.3 Results and Discussion**

#### **4.3.1 Polymer Incorporation and Steady-state NO Release**

While the photoinduced NO release from RSNOs is at times a hindrance regarding device storage or the duration of treatments, it makes the molecules well suited for photo-controlled treatments. The NO release behavior of RSNOs are, at times, altered when they are incorporated into a polymer, with some RSNOs being stabilized in terms of their photo and/or thermal decomposition. Any stabilizing effects are often evident soon after polymer incorporation and generally represent themselves with some of the following behaviors: a) decreased rates of NO release; b) more stable NO flux; and c) reduction in the initial burst NO release. As this chapter's research will demonstrate, different RSNOs respond uniquely to different polymers and stimuli.

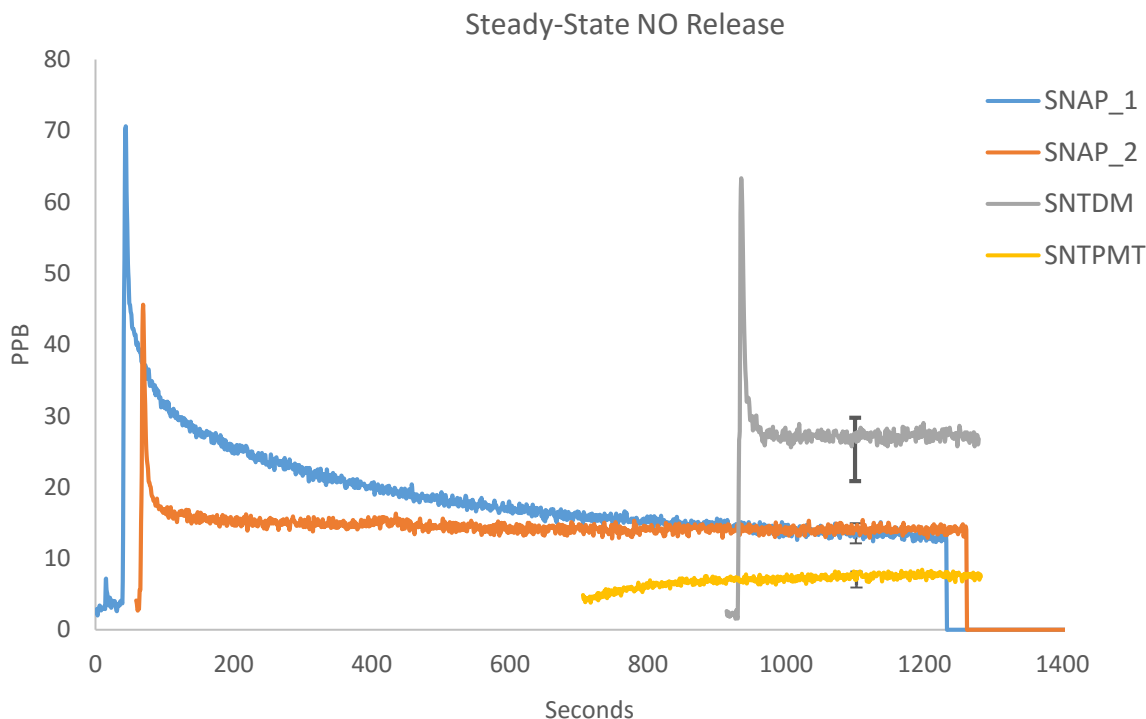


**Figure 4.1.** Equal amounts of SNTDM, SNTPMT, and SNAP's (0.5 $\mu$ mol) steady NO flux. Average releases and standard error of the mean are indicated as point values at X=1100 sec. n=3

SNTDM, SNTPMT, and SNAP's neat phase NO release at RT in the dark was measured and is shown in Figure 4.1. Dissolving the RSNOs in Et<sub>2</sub>O (SNTDM/SNTPMT) or THF (SNAP) before charging them into an NOA cell and then evaporating the solvent via a stream of N<sub>2</sub> allowed the use of precise amounts of solids otherwise not feasible to dispense with accuracy. Decomposition during the process does not occur at a detectable level, as indicated in Chapter 2. Each sample was measured < 2 h following purification. A clear trend is apparent between the solid RSNOs, with SNTDM having the greatest thermal release at room temperature from the solid state and SNTPMT the least. Although less so with tertiary species, obtaining a fairly steady flux can be difficult. The phenomenon is inconsistent, with a steady-state NO release obtained sometimes more readily than others. For example, Figure 4.1 shows two samples of equal amounts of SNAP crystals that reach the same steady-state after different time periods. One sample required 15 min, while the other only took 1 min. It appears that the phenomenon does not depend on the RSNO's phase because SNTDM, a liquid, also exhibits this behavior although

less frequently. It also occurs when in polymers, but less so with stable RSNOs such as SNTDM, SNTPMT, or SNAP. Flux is reported as moles  $\times 10^{-10}\text{cm}^{-2}\text{min}^{-1}$ .

#### **4.3.2 Silicone Rubber Films Doped with SNTDM, SNTPMT, and SNAP**

NO releases from the RSNO/polymer systems were tested in the absence of light, with ambient room light, and with exposure to a 120-watt halogen bulb at 8". The NO releases between neat and the samples incorporated into the polymers are an indication of any potential stability effects provided by the polymeric matrix (see Figures 4.2a-c). SR did not grant SNTDM nor SNTPMT any stabilizing effects in regard to their photoactivity. In fact, SNTPMT may be somewhat destabilized by SR, particularly with respect to photoactivated NO release, although further experiments are needed to reduce error and draw a sound conclusion. Under ambient light, the average NO flux from SNTPMT/SR was 20% higher than the neat phase. It was 25% greater in response to a halogen bulb. In contrast, relative to the neat phase, the SNAP doped SR films showed approximately a 13% reduction in NO flux during exposure to ambient light or a halogen bulb. Typically, RSNOs are considerably less sensitive to ambient light than to broad spectrum lightbulbs or sunlight. When incorporated in SR, SNTDM, SNTPMT, and SNAP's NO releases are unique to each species (see Figures 4.2a-c). SNAP shows a small increase upon exposure to ambient light ( $6.1 \pm 0.3$  and  $6.3 \pm 0.4$  flux units, respectively), and a more significant difference when exposed to broad spectrum light ( $6.1 \pm 0.3$  to  $13.9 \pm 0.4$  flux). Despite SR's potential destabilizing effects on SNTPMT, NO release from the SNTPMT/SR films was actually more stable than SNAP in the dark and with the halogen lamp. For example, when exposed to a halogen bulb, SNTPMT films released  $11.6 \pm 1.0$  flux units of NO whereas for SNAP, the flux was  $13.9 \pm 0.5$ . This is a significant finding considering SNAP is accepted as one of the most stable RSNOs. Again, additional samples will need to be evaluated to more precisely discern their differences.

As observed in Chapters 2 and 3, SNTDM exhibits an uncharacteristically strong response to light, both ambient and from a halogen bulb (Figure 4.2a). The NO fluxes between each species in SR are shown in Table 4.1, normalized to the values observed in the dark. SNDDT is also shown to emphasize the rarity of SNTDM's behavior. Despite being a structural isomer, with primary



alkyl substitution, SNDDT's sensitivity to light is markedly less. Exposure to a halogen bulb more than tripled its NO flux; nevertheless, this pales in comparison to SNTDM's change, a 56-fold increase.

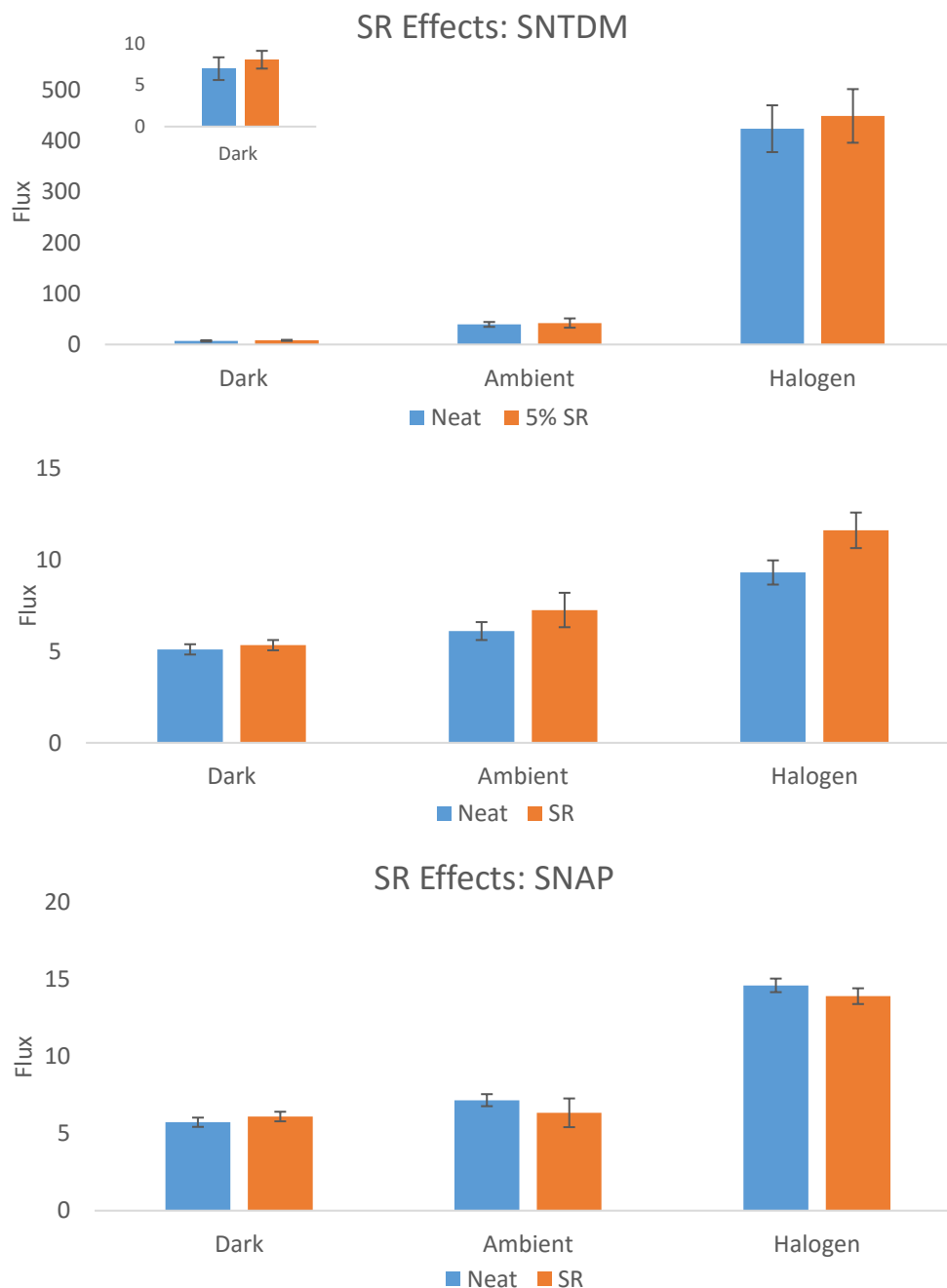


**Figure 4.2** SR rubber films were doped with 5 wt% of the following RSNOs (a) SNTDM, (b) SNTPMT, and (c) SNAP, and the NO release upon exposure to ambient and broad spectrum light compared to that from the neat phase (n=3). Flux values are in units of 10<sup>-10</sup> mol·cm<sup>-2</sup>·min<sup>-1</sup>.

**Table 4.1** The normalized flux values depict SNTDM’s extreme response to both ambient and broad spectrum light.

	Dark	Ambient	Halogen
SNTDM	1	5.3	56
SNDDT	1	1.6	3.4
SNTPMT	1	1.4	2.2
SNAP	1	1.1	2.3

### 4.3.3 Photoinduced NO Release from Silicone Rubber, CarboSil, E2As, and Tecoflex SG80A Doped with SNTDM, SNTPMT, and SNAP

A polymer’s stabilizing effect in regard to thermolytic NO release does not necessarily correspond with photolytic stability (and vice versa). For the polymer films tested, it seems that SNTDM has the greatest photosensitivity in the various matrices where it is the most thermally (dark) stable (see Figure 4.3). For example, SNTDM/SR films have a low NO release in the dark (6

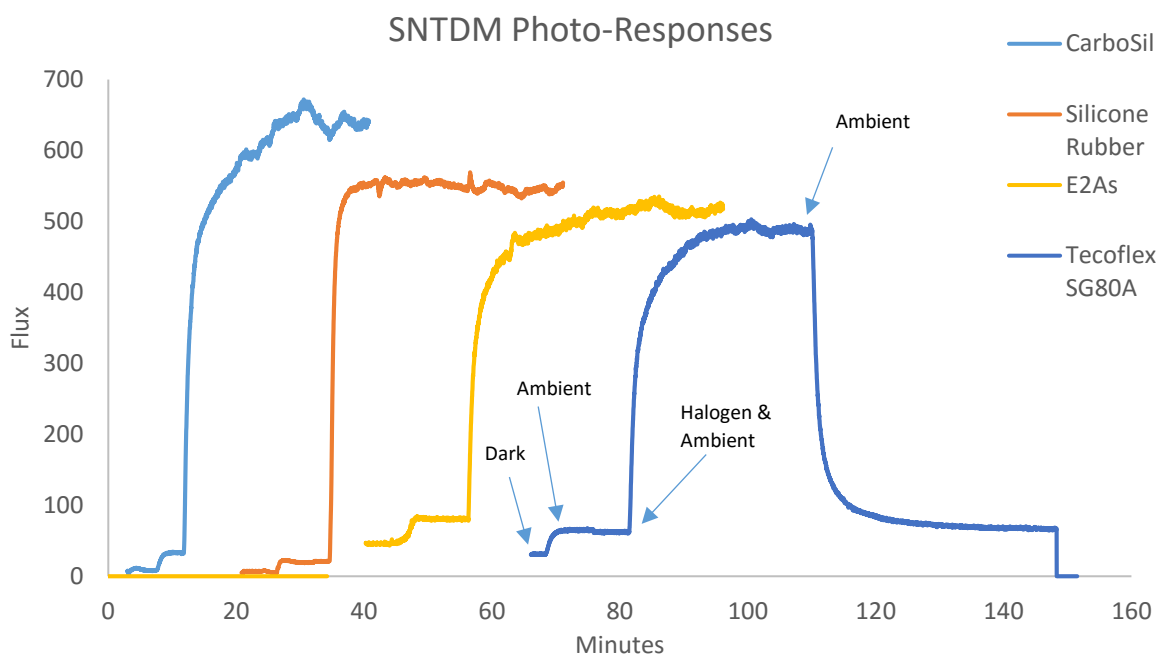


**Figure 4.3** SNTDM/SR shows NO release profiles that are unique to specific polymers. From left to right within polymer: the sample was exposed to no light, ambient light, and ambient+halogen light, sequentially. The halogen lamp was turned off in the final sample to demonstrate the rapid decrease in NO flux.

flux) and a flux of ~540 upon exposure to a halogen light bulb. When in Tecoflex films, SNTDM releases NO at 30 flux in the dark and 485 flux when exposed to a halogen bulb. Similarly, SNTDM has a NO flux of 8 from CS without light and 603 with a halogen light bulb. In E2As, SNTDM's very high NO flux of 43 in the dark contrasted with a lower one (517) with a halogen bulb. This trend was not observed with SNAP or SNTPMT. Different RSNO/polymer combinations require different times to plateau (if they do). In Figure 4.3, it can be observed that even under identical conditions, SNTDM's time required to reach maximum flux is very different, depending on the polymer. In SR, SNTDM's NO release maximizes almost immediately. This contrasts with SNTDM in Tecoflex which required ~18 minutes. The effects are even more dramatic with SNTPMT (see Figure 4.4); for example, in CS, SNTPMT, reaches maximum NO release in under 1 min for ambient light and less than 2 min for broad spectrum light. In Tecoflex, it requires 20 min under ambient conditions and 80 min using a halogen bulb (see Figure 4.4). Some RSNOs do not return to their lower level flux for a considerable period of time following light exposure. During this thesis research, it has been consistently observed that films doped with SNTDM return to their lower rate of NO release after terminating exposure light as quickly, if not more so, than all other RSNOs (data not shown).

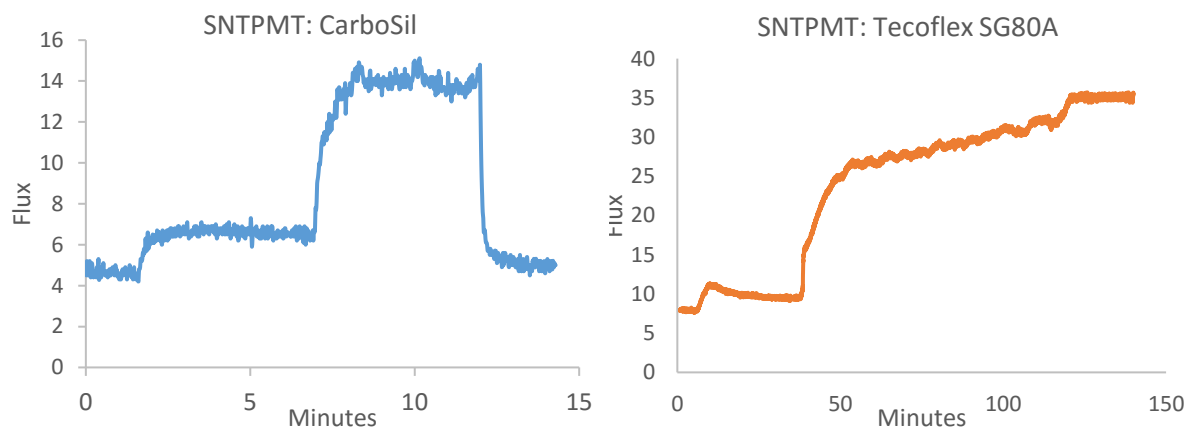


**Figure 4.4** SNTPMT reaches maximum flux rapidly while doped in CS, but requires considerably longer in TF.

SNTDM's rapid rates of achieving maximum NO flux values and being able to quickly return to baseline fluxes in the absence of light, enhances the use life of the SNTDM-doped films as the levels of NO released during times of gradual increase or decrease is not wasted (i.e., would not be at target values during these periods).

Each RSNO's flux from the four polymers is shown in Figure 4.5. Given that SNTDM's NO flux is an order of magnitude greater than SNAP or SMTDM's, a logarithmic scale is used for the y-axis. SNTDM releases NO at a higher flux than the other RSNOs in all the polymers tested and with all the light exposures. SNTPMT is less sensitive to a halogen bulb than SNAP when in SR,

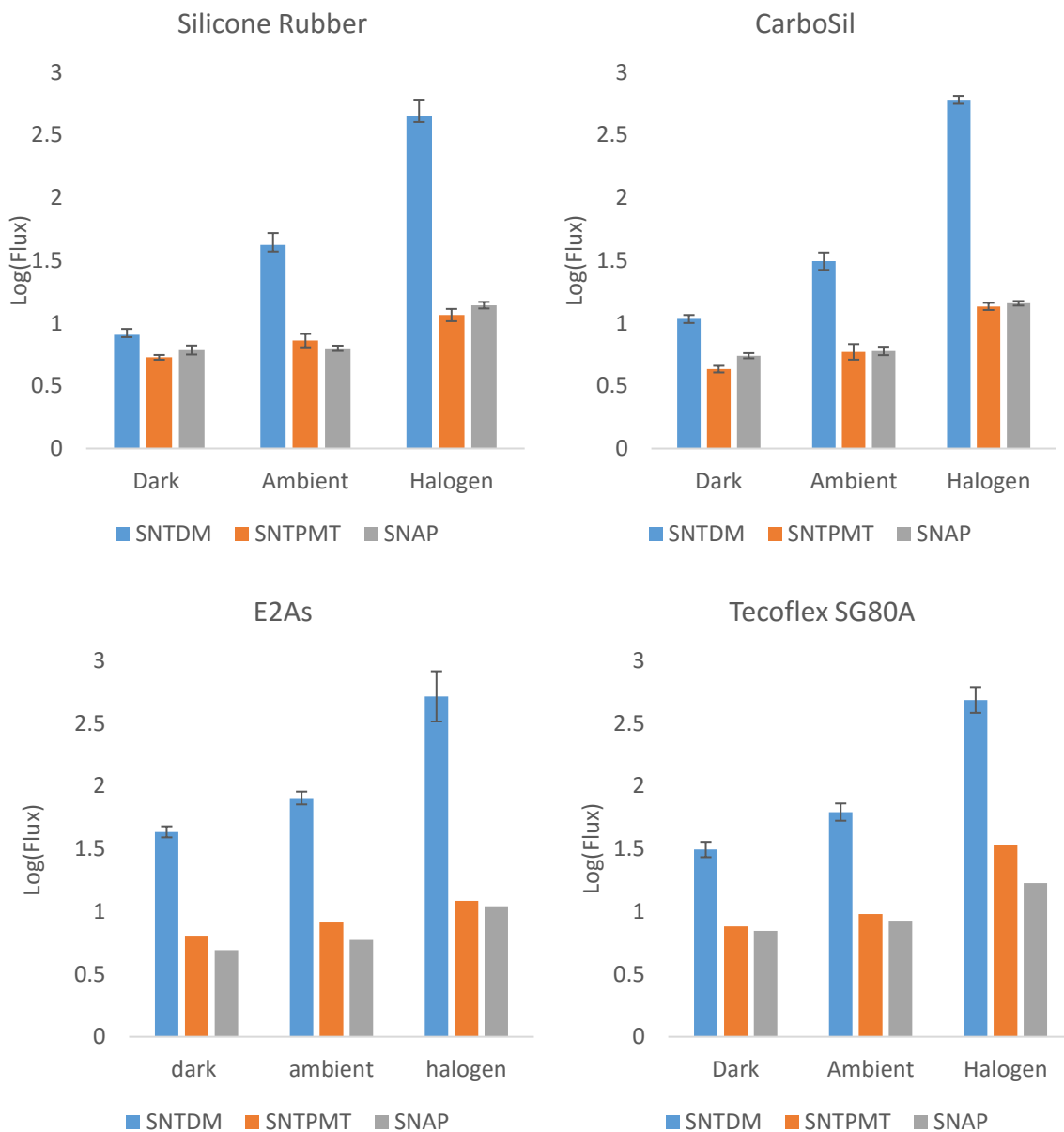


**Figure 4.5** 5 wt% SNTDM, SNTPMT, and SNAP were incorporated into SR, CS, E2As, and TF and their NO flux determined in the dark, with ambient light, and exposed to a halogen bulb. n=3 for all measurements of the RSNOs in SR and CS. For E2As and TF: n=3 for SNTDM, n=1 for SNTPMT, and n=1 for SNAP.

and comparable in CS. Preliminary studies suggest SNAP is more stable in E2As and TF; however, additional trials will need to be performed to confirm this observation.

#### 4.3.4 Controlling NO Release: Distance to Light Source

The NO flux rate during photolytic conditions is directly affected by the distance to the light source. This can also allow control over the amount of NO delivered to patients. Figure 4.6 shows the NO release from SNTDM doped SR films in response to a halogen bulb at 4, 8, 12, and 16 inches distance from the films. The release increases ~5x between 4 and 16 inches.

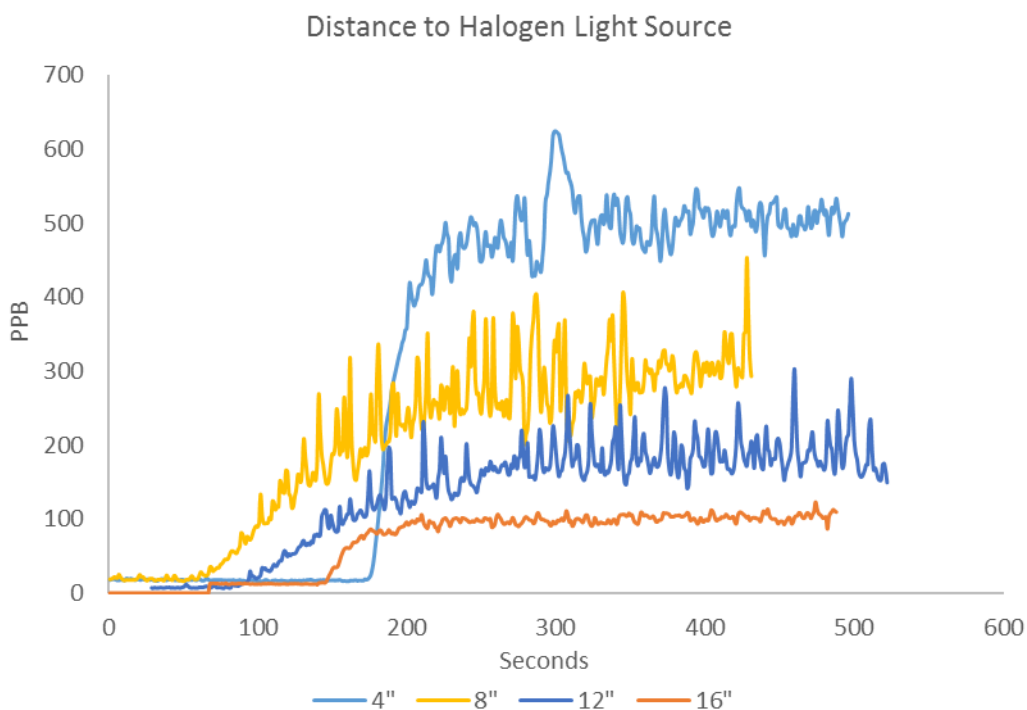


**Figure 4.6** SNTDM/SR's proximity to a light source affects its rate of NO release. As the film is moved from 4 inches to 16 inches away the rate of NO noticeably decreases.

#### 4.3.5 Controlling NO Release: Graphite Powder Topcoat

SNTDM's photosensitivity is excellent for inducing NO release; however, it is so extreme that it may be excessive for certain applications and undesirably shorten a device's lifetime. Recently, research has begun exploring the use of graphite powder (GP) topcoats to increase the polymers' opacity and control SNTDM's photoactivated NO release (see Figure 4.7). At this point, the NO threshold levels required for antimicrobial activity are not known, but effective fluxes have been reported. In Chapter 3, SNTDM killed 99.9% *S. aureus* successfully with  $\geq 0.5$  flux NO. When SNTDM is incorporated into various polymers its photoactivated NO fluxes often exceed this value.

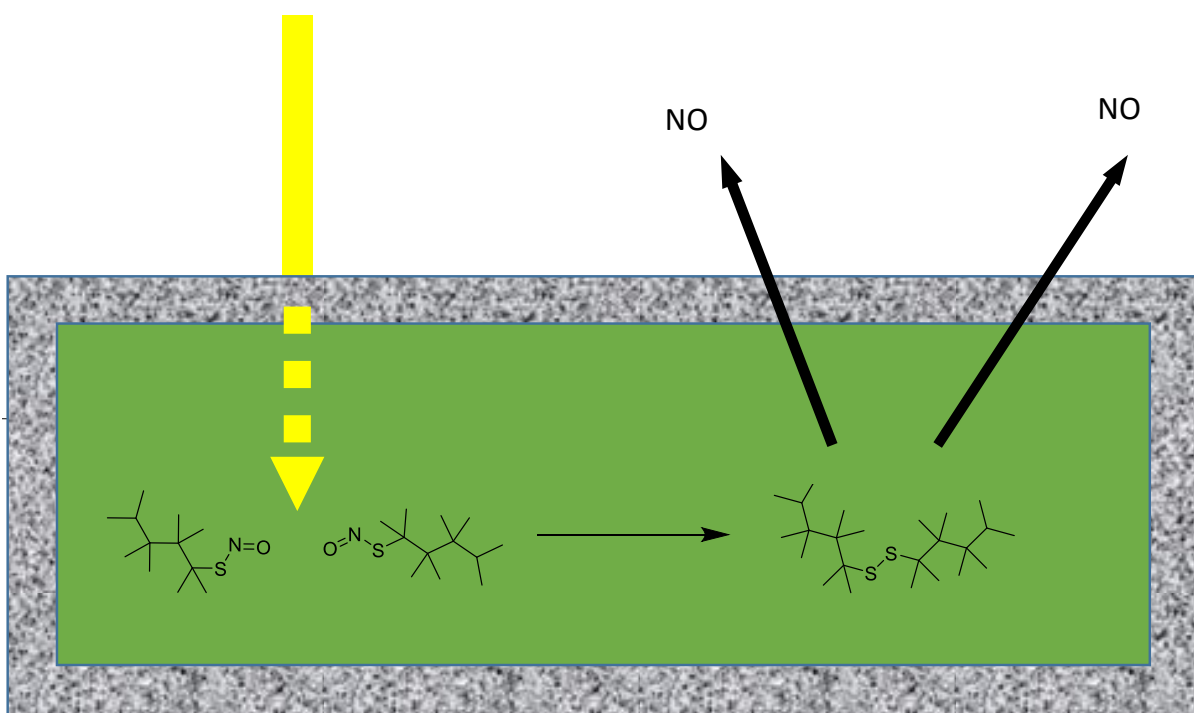


**Figure 4.7** SR films containing SNTDM are dipcoated into a GP/THF slurry and allowed to dry. The GP layer diffracts/blocks some light, thus extending the lifetime of the device.

After applying a 25 wt% GP topcoat, the flux was reduced by half (see Figure 4.8). Interestingly, although the photoactivated flux change from light decreased by 50%, the NO after release without light (thermal) increased by 100%. The process could potentially have affected the polymer's water uptake and increased the rate thermal decomposition.

SNTDM's photoinduced high NO release levels come at the expense of stability during storage or routine procedures before treatments. Consequently, SNTDM can prematurely decompose and reduce the efficacy of any devices. SNTDM/SR/GP samples containing 10 and 25 wt% topcoats were compared with control samples (no GP topcoats) exposed to ambient light (shelf storage) or direct sunlight. The GP topcoats substantially increased the lifetime of the SNTDM/SR films that were exposed to sunlight (See Figure 4.9). Whereas the SNTDM/SR controls had fully decomposed by 3 d, the 10 and 25 wt% SNTDM/SR/GP films lasted 5 and 7 d, respectively. This is likely due to the devices' increased opacity which reduces light transmission, and slows the photolysis of SNTDM. The films were also stored on a shelf that was exposed to ambient light. The stabilizing effects were again evident, but their effects were less pronounced. Also, the 10 and 25 wt% GP/SNTDM/SR films performed very similarly. The difference in opacity may play less a role because being further from the window decreases the photolysis decomposition mechanism's contribution (which the GP helps with). The intensity of an RSNO/polymer's NO release usually is inversely proportional to its duration. After an effective antimicrobial threshold is determined, decreasing the NO flux to this level (with increased graphite powder) will provide the maximum duration of NO release.

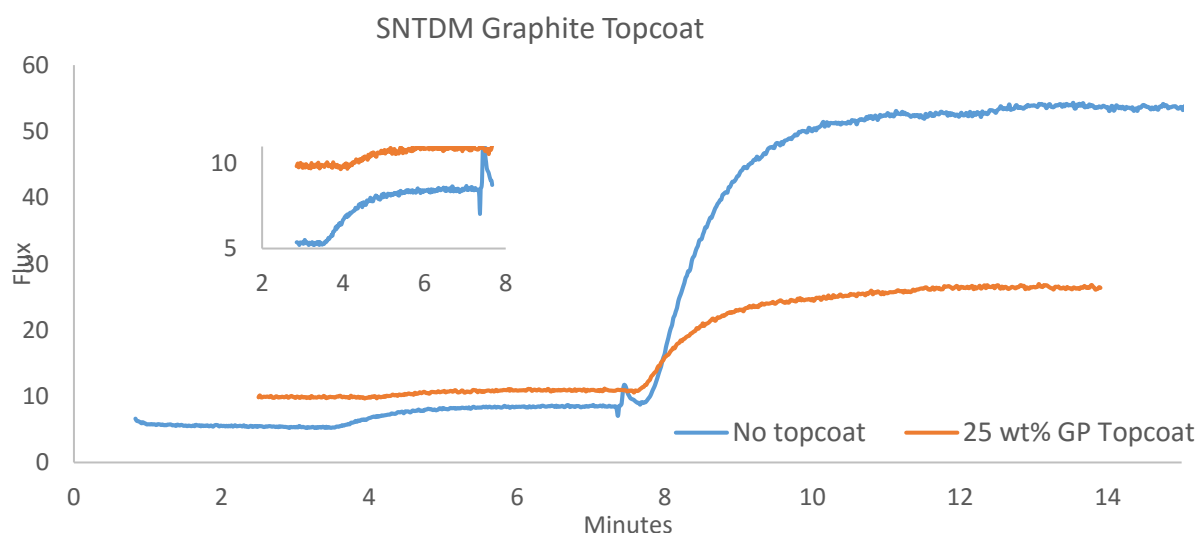


**Figure 4.8** The comparative photoresponses of SNTDM/SR with and without a GP topcoat to no light, ambient light, and ambient+halogen. Inset is the dark→ambient light transition.

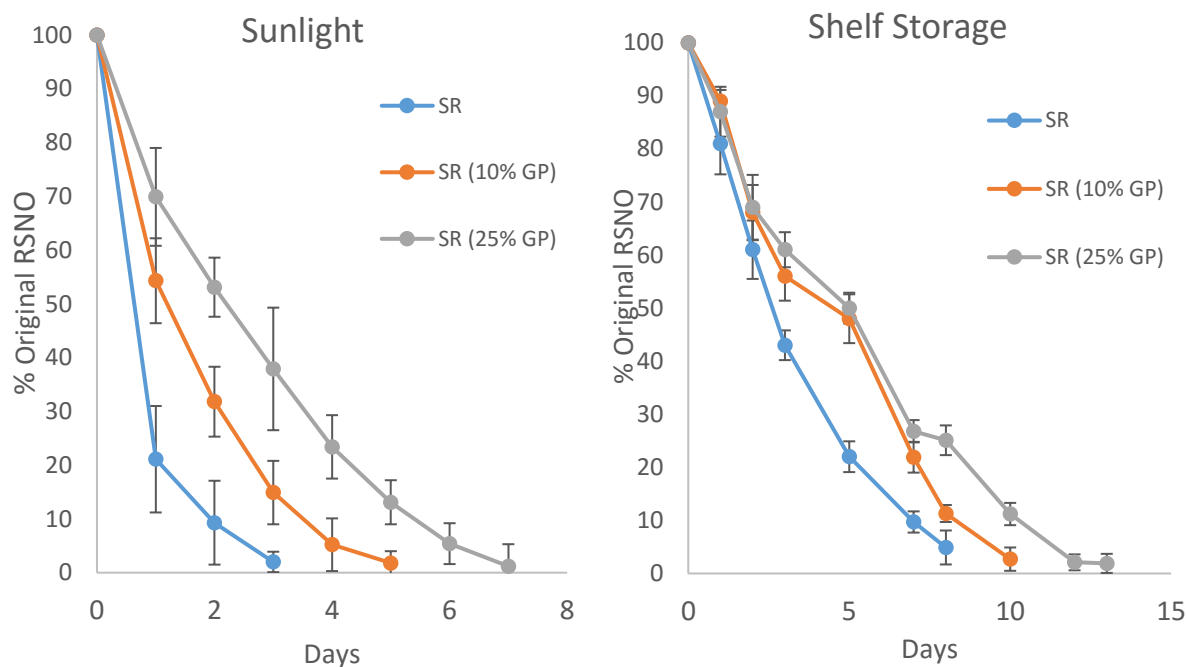


**Figure 4.9** The SNTDM/SR system’s stability, with and without GP topcoats when exposed to sunlight and ambient light.

#### 4.4 Conclusions

SNTDM’s properties are promising for photoactivated NO release applications. Its minimal leaching facilitates localized treatments by conserving levels of the NO donor, and prevents the RSNO from entering healthy cells that would otherwise be damaged. SR, E2As, and CS are the most promising polymers that have been tested thus far, as SNTDM is fairly stable without external light exposure in these polymers, yet it releases very large amounts of NO upon activation with a halogen bulb. SNAP and SNTPMT also exhibit photoinduced NO release, but at substantially lower levels, by more than an order of magnitude in some cases. Although less suitable for photoactivated NO release devices, these studies further elucidated SNTPMT’s considerable photolytic stability. SNTPMT is even more stable than SNAP when incorporated into SR and exposed to a halogen light source.

SNTDM adopts a steady-state NO release more quickly and consistently than many other RSNOs, including SNAP. The phenomenon is observed for both the increased NO release upon photactivation and decreased levels following the removal of a light source. This in combination



with the significant difference between dark and photoactivated NO releases allows more NO to be conserved for longer and/or more intense treatments. Additionally, varying the distance between the SNTDM/polymer and the light source provides a straightforward means to control the NO release.

Because SNTDM's photosensitivity is so extreme, a means to adjust the NO release by altering the polymer's opacity was developed. Applying a SR topcoat containing graphite powder to SNTDM/SR films resulted in a decreased photoactivated release. The concentration of graphite powder can be altered to produce unique NO release profiles. The GP topcoat reduces undesirable decomposition during exposure to ambient light.

#### 4.5 References

- 1 K. J. Reeves, M. W. R. Reed and N. J. Brown, *J. Photochem. Photobiol. B Biol.*, 2009, **95**, 141–147.
- 2 V. Rapozzi, E. Della Pietra, S. Zorzet, M. Zacchigna, B. Bonavida and L. E. Xodo, *Nitric Oxide*, 2013, **30**, 26–35.
- 3 L. B. Josefsen and R. W. Boyle, *Met. Based. Drugs*, 2008, **2008**, 276109.
- 4 V. Rapozzi, E. Della Pietra and B. Bonavida, *Redox Biol.*, 2015, **6**, 311–7.
- 5 D. A. Riccio, P. N. Coneski, S. P. Nichols, A. D. Broadnax and M. H. Schoenfisch, *ACS Appl. Mater. Interfaces*, 2012, **4**, 796–804.
- 6 N. M. Giles, S. Kumari, B. P. Gang, C. W. W. Yuen, E. M. F. Billaud and G. I. Giles, *Chem. Biol. Drug Des.*, 2012, **80**, 471–478.
- 7 S. Kumari, I. A. Sammut and G. I. Giles, *Eur. J. Pharmacol.*, 2014, **737**, 168–176.
- 8 C. Opländer, A. Deck, C. M. Volkmar, M. Kirsch, J. Liebmann, M. Born, F. van Abeelen, E. E. van Faassen, K.-D. Kröncke, J. Windolf and C. V. Suschek, *Free Radic. Biol. Med.*, 2013, **65**, 1363–1377.

- 9 E. J. Brisbois, H. Handa, T. C. Major, R. H. Bartlett and M. E. Meyerhoff, *Biomaterials*, 2013, **34**, 6957–66.
- 10 A. R. Ketchum, M. P. Kappler, J. Wu, C. Xi and M. E. Meyerhoff, *J. Mater. Chem. B*, 2016.
- 11 G. E. Gierke, M. Nielsen and M. C. Frost, *Sci. Technol. Adv. Mater*, 2011, **12**, 55007–5.
- 12 M. N. and M. C. F. Genevieve E Gierke, *Sci. Technol. Adv. Mater.*, 2011, **12**, 055007.
- 13 P. Dungal, J. Hartinger, S. Chaudary, P. Slezak, A. Hofmann, T. Hausner, M. Strassl, E. Wintner, H. Redl and R. Mittermayr, *Lasers Surg. Med.*, 2014, **46**, 773–80.

## CHAPTER 5.

### CONCLUSIONS AND FUTURE DIRECTIONS

#### 5.1 Conclusions

Biomedical devices can increase the risk of infection and thrombosis, both of which are serious health concerns.<sup>1-3</sup> The research reported in this dissertation prepared and studied a number of different lipophilic *S*-nitrosothiols (RSNOs) for use as controllable sources of nitric oxide (NO) to potentially improve the biocompatibility of polymeric medical devices. The RSNOs' leaching and stability were evaluated in biomedical grade polymers. Additionally, photoactivation, antimicrobial, and antiplatelet studies were performed. The studies further demonstrated the RSNOs' value as NO-donors.

In Chapter 2, numerous lipophilic RSNOs were prepared and evaluated as potential NO donor candidates. Several of the RSNOs could easily be ruled out because of their inherent instability, which caused preparation and isolation to be detrimental to the amount of available NO. *S*-Nitroso-*tert*-dodecylmercaptan (SNTDM) and *S*-nitrosotriphenylmethanethiol (SNTPMT) leached minimally from silicone rubber (SR), CarboSil (CS), and Elasteon-E2As, a trait which combined with their significant stability made them very promising NO release donors. Although *S*-nitroso-*tert*-butylthiol (SNTBT) was fairly stable, its significant leaching provided no advantage over *S*-nitroso-*N*-acetylpenicillamine (SNAP), SNTDM, or SNTPMT, thus making it less attractive for further studies.

SNTDM and SNTPMT, when incorporated into SR, E2As, and CS, and exposed to physiological conditions, released NO over an extended time period. SNTDM lasted approximately a month at or above physiological flux in each of the polymers, while SNTPMT's stability provided a 41 d NO

flux when in SR or CS. This duration is unprecedented and promises to prolong the intravascular or urinary device's duration of use by reducing thrombosis or biofilm formation.<sup>1,2,6,7</sup> E2As, SR, and CS polymers impregnated with SNTDM or SNTPMT were exposed to platelet rich plasma (PRP) and demonstrated a significant reduction in platelet adhesion at specific wt%, relative to the controls.

Chapter 3 was based on work recently published in the Journal of Material's Chemistry B (2016, 4, 422-430) involving the development and preparation of SNTDM/silicone rubber catheters via a solvent swelling impregnation method.<sup>6</sup> Leaching, storage stability, and their long-term NO release factors were evaluated and the results indicated that this RSNO system was indeed a very promising candidate for improving the biocompatibility of SR catheters. This was further demonstrated by observing a marked reduction in *Staphylococcus aureus* levels and biofilm formation during *in vitro* studies in a CDC bioreactor.

Within Chapter 4, experiments examined SNTDM's and SNTPMT's photoinduced NO release from SR, CS, Tecoflex SG 80A (TF), and E2As and compared them to SNAP. SNTDM was very sensitive to not only broad spectrum light bulbs and direct sunlight, but also demonstrated a considerable response to ambient light (in lab fluorescent lighting). SNTPMT and SNAP, in turn, are both stable RSNOs, even when stored under sunlight, broad spectrum bulbs, and laboratory light. SNTDM, SNAP, and SNTPMT in different polymer films provided a wide spectrum of NO release rates.

In addition to the polymers' effects on SNTDM's photoactivation, varying the distance to the light source proved a simple yet effective way of controlling the NO release. Lastly, a means to alter SR's opacity using graphite powder was developed and proven to affect the extent of photoactivation.

Overall, this thesis has provided the first extensive studies regarding the preparation and NO release behavior of a series of lipophilic RSNOs. Particularly noteworthy, SNTDM and SNTPMT have properties that may enable them to be useful in developing new NO release polymer-based biomedical devices. They complement one another, as SNTPMT's stability can provide a longer duration of NO release at lower levels, while SNTDM releases more intense NO levels for a shorter duration. Although both exhibit significant platelet reduction relative to the

control polymers, SNTDM's higher NO flux is likely responsible for its even greater antiplatelet effects. Again, this comes as a trade-off, as SNTDPM's stability better lends itself to device storage. Both demonstrated several advantages compared to SNAP, which is currently one of the most promising RSNOs. They leached dramatically less than SNAP from SR, CS, and E2As. SNTDPM films released physiological levels of NO for longer duration than SNAP. SNTDM's NO release provided superior antiplatelet properties compared to SNAP in each of the tested polymers. As such, this dissertation work has made significant contributions to the rapidly growing field of NO releasing biomaterials.

## 5.2 Future Directions

SNTDM and SNTDPM are novel for potential use in biomedical devices, and although much future work lies ahead before they are ready for clinical studies, their properties lend themselves to improving the biocompatibility of biomedical devices.

As RSNO loading concentrations often vary inversely with the flux, duration of NO release, and the leaching, optimal conditions will need to be determined.<sup>6</sup> To provide more precise measurements and account for any RSSR, an HPLC method needs to be developed. Any levels of RSNO and RSSR that still leach from polymers will need to be tested to confirm their safety for medical use. Wound healing patch applications may tolerate higher levels of leached species than intravascular catheters. If necessary, leaching can likely be reduced via polymer topcoats, which has been demonstrated previously to help with similar systems.<sup>7,8</sup>

At this point, the reason for SNTDM's photosensitivity has not been determined. The current understanding of RSNOs' stability predicts that SNTDM would be more stable than the primary RSNO, SNDDT, in regard to both light and heat activated decomposition.<sup>1,6</sup> Other than the tertiary alkyl substitution, SNTDM's structure only differs from SNDDT's by the methyl groups substituted along its backbone, which is consequently shorter (6 vs. 12 carbons). The RSNOs' alkyl lengths do not directly affect their photosensitivities to the extent observed with SNTDM (as demonstrated in Chapter 2). Consequently, the methyl groups are the predominate structural difference. This variable could be removed by first synthesizing the tertiary thiol via the reactions

shown in Figure 5.1. Reacting 2-undecanone with a methyl Grignard Reagent would yield a tertiary alcohol that in turn could be converted to a bromide-leaving group using phosphorous tribromide ( $\text{PBr}_3$ ). The bromide-leaving group facilitates an  $\text{S}_{\text{N}}1$  substitution with a  $\text{SH}^-$ , thus forming the thiol precursor to SNDDT's tertiary analog, S-nitroso-2-methylundecanethiol (SNMUT). SNMUT and SNDDT will provide a more direct comparison and indicate whether the photosensitivity is attributable to the methyl substituents.

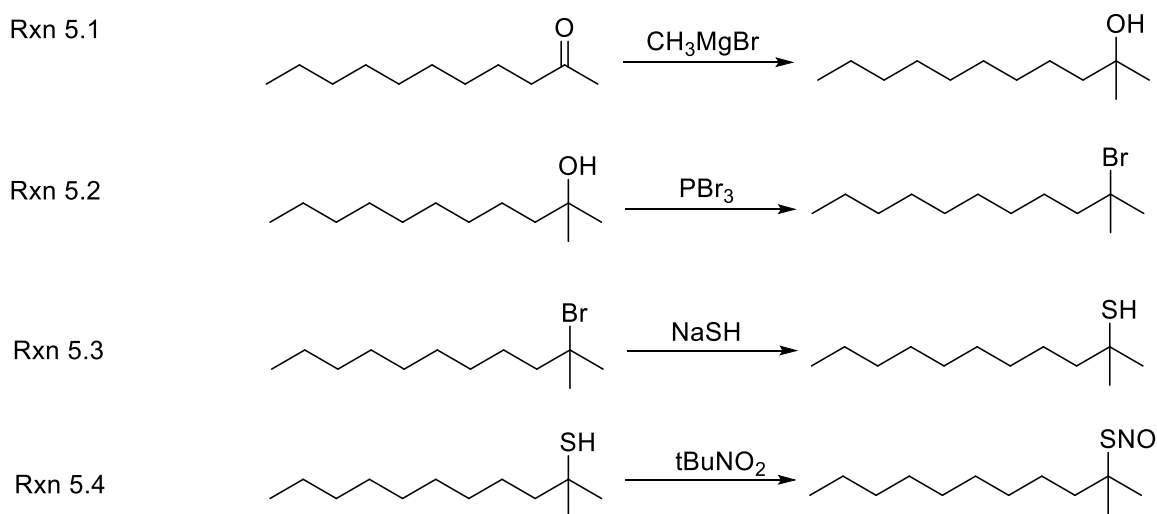


**Figure 5.1** Proposed synthesis of S-nitroso-2-methyl-2-undecanethiol.

SNTDM's and SNDDT's UV-Vis absorbance spectra (see Figure 5.2) only differ minimally in the ranges commonly used for RSNO measurements 330-350 nm ( $\pi \rightarrow \pi^*$ ) and 550-650 nm ( $n_{\text{N}} \rightarrow \pi^*$ ),<sup>10</sup> thus not providing insight into their distinct photosensitivities. The extinction coefficients at SNTDM's and SNDDT's  $\lambda_{\text{max}}$  (~341nm) are 596 and 522  $\text{M}^{-1}\text{cm}^{-1}$ , respectively. The most distinct difference is the  $n \rightarrow \sigma^*$  transition. The shoulder of SNDDT's  $n \rightarrow \sigma^*$  transition is very apparent, thus indicating it occurs at a longer wavelength. This difference also cannot explain SNTDM's greater photosensitivity.

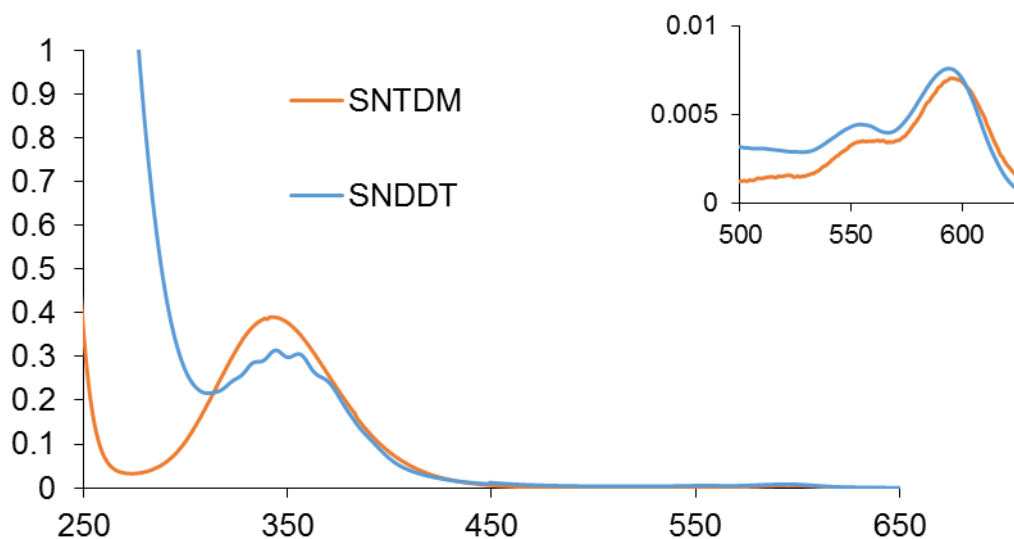


**Figure 5.2** Comparative UV-Vis absorption spectra of 0.7 mM SNTDM and SNDDT.

RSNOs are more stable when the C-S-N-O bonds are in the anti-conformation.<sup>9</sup> DFT calculations have shown that primary RSNOs' red color and tertiary RSNOs' green color are due to the fact that primary RSNOs exist in the syn conformation while tertiary RSNOs are predominately anti.<sup>9</sup> SNTDM has exhibited a unique phenomenon in that its green color appears to have a slight red shade. This contrasts with SNAP and SNTDPM which are purely green. This suggests that the syn conformer may play a larger role in SNTDM's behavior. An <sup>15</sup>N NMR experiment would be able to compare the relevant amounts of each conformer.<sup>9</sup>

Regarding the NO release from an RSNO, many mechanisms have been proposed and found to coexist or be circumstantially dependent.<sup>9-11</sup> Scientists commonly assume that both thermal and photoinduced NO release occur via homolytic mechanisms;<sup>9</sup> however, Singh *et al.*, using ESR and a radical trapping agent, determined that only GSNO's photoactivated NO release generates the thiyl radical present in the homolytic NO release.<sup>11</sup> SNTDM's tertiary substitution may offer thermal stability by sterically limiting dimerization, however, other structural factors may discourage the more stable anti-conformation, and consequently facilitate a photoactivated mechanism. See Figure 5.3 for mechanisms that have previously been proposed.<sup>9-11</sup> In Reactions 5.5 and 5.6, the RSNOs' tertiary alkyl substitution may hinder dimerization; however, in Reaction 5.7 the homolytic release of NO would not be impeded by the RSNOs' substitution.

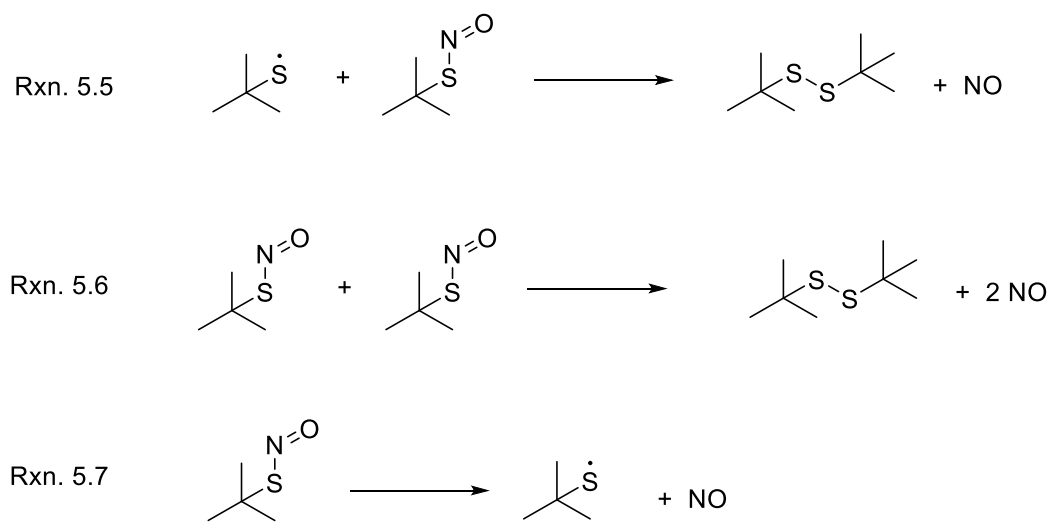


**Figure 5.3** Three commonly proposed reaction mechanisms for NO release from RSNOs.

Much of the limitation hindering NO's use for applications involves its difficulty with controllable delivery. While RSNOs are significantly more stable and easier to use, their thermal and photolytic NO release has hindered progress.<sup>1,6</sup> At this point, attaining a means for NO release only at desired times is one of the ultimate goals for the advancement of RSNOs.<sup>6</sup> SNTPMT's stability may result in suitable levels of NO release to extend a medical device's use; however, ongoing extended stability studies may indicate that an undesirable amount of decomposition still occurs during device storage.

An additional RSNO, *S*-nitroso-tris(2,2'',6,6''-tetramethyl-*m*-terphenyl-5'-yl)methylthiol, may ameliorate this problem and is thus worth investigating (see Figure 5.4). This RSNO has previously been synthesized and has demonstrated increased stability (relative to SNTPMT) which is attributable to its "bowl-shaped" steric protecting group;<sup>12,13</sup> however, its behavior in polymers has never been evaluated. Given its stability and extremely lipophilic character, it may be a very promising candidate for improving biomedical devices' biocompatibilities. Researchers reported low yields following its nitrosation in biphasic conditions (57%)<sup>12</sup> which would limit its utility. However, the methods developed in Chapter 2 will likely award greater yields.



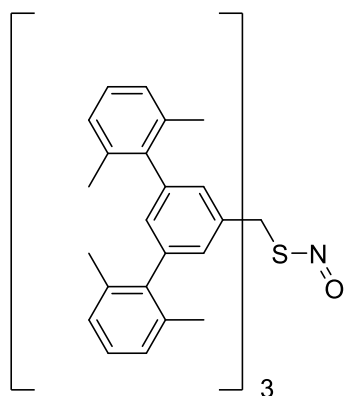


**Figure 5.4** Structure of *S*-nitroso-tris(2,2'',6,6''-tetramethyl-*m*-terphenyl-5'-yl)methylthiol. Its lipophilicity and stability make it a promising RSNO worth investigating.

Additionally, a new RSNO/SR system is being developed and studied that utilizes SNTDM's and SNTPMT's complementary NO release behavior. SNTDM can provide intermittent and intense fluxes of NO, while SNTPMT offers a lower level sustained "maintenance" NO flux. This system could be used in wound healing patches following surgery or injury. The patches could be exposed to light periodically to reduce bacteria as well as promote blood flow, angiogenesis, and healing.<sup>4,5</sup>

Photodynamic therapy (PDT) is a fairly new medical technique that is currently used in ophthalmology, antiviral treatments, oncology, and dermatology.<sup>14</sup> PDT uses three components: a photosensitizer, oxygen, and light.<sup>15</sup> A typical PDT treatment involves administration of the photosensitizer, activation by light, and the generation of free radicals. The radicals are transferred to oxygen and form reactive oxygen species (ROS). The ROS are responsible for the cytotoxicity associated with PDT. Photofrin was the first photosensitizer to gain approval for PDT and is registered for use in treating a wide range of cancers. Despite its effectiveness, patients suffer from substantial photosensitivity following PDT.<sup>16</sup> Typically, photosensitizers are administered intravenously and thus are taken up by all cells. Eventually, the concentration in cancer cells is usually greater; however, optimal selectivity has never been achieved and thus normal cells are damaged as well.<sup>16</sup>

SNTDM's photoactivated NO release may provide a promising alternative to traditional PDT. For accessible tumors, polymeric patches containing SNTDM could provide a localized NO release with minimal damage to healthy tissue (unlike with systemic photosensitizers). Frost *et al.* proposed that fiber optic catheters containing an RSNO can be used to reach otherwise inaccessible treatment locations.<sup>17</sup> SNTDM is well suited for such an application. Recently, scientists have begun using light emitting diodes (LEDs) of different wavelengths to produce different NO release profiles. Gierke *et al.* demonstrated that 470 nm LED effectively releases NO from a SNAP-cyclam derivative.<sup>17</sup> Dungal *et al.* used the same LEDs to induce NO release from nitrosyl hemoglobin in order to induce angiogenesis.<sup>18</sup>

Given its promising photosensitivity, SNTDM in SR polymer was exposed to blue (470 nm) and green (530 nm) LEDs and compared to a 100 W halogen bulb (see Fig. 5.5). This resulted in three distinct NO release profiles. The green LED caused a low NO release (20 ppb) that plateaued quickly and maintained a steady release over the duration of the experiment. The blue LED caused the most intense NO release and did not plateau. The halogen light induced an NO release that was essentially a compromise between the green and blue light values. These three unique profiles could provide different treatment options. For example, procedures requiring a shorter and more intense NO release would use a blue light to activate SNTDM. These experiments comparing the effects of blue LED, green LED, and halogen bulbs are merely

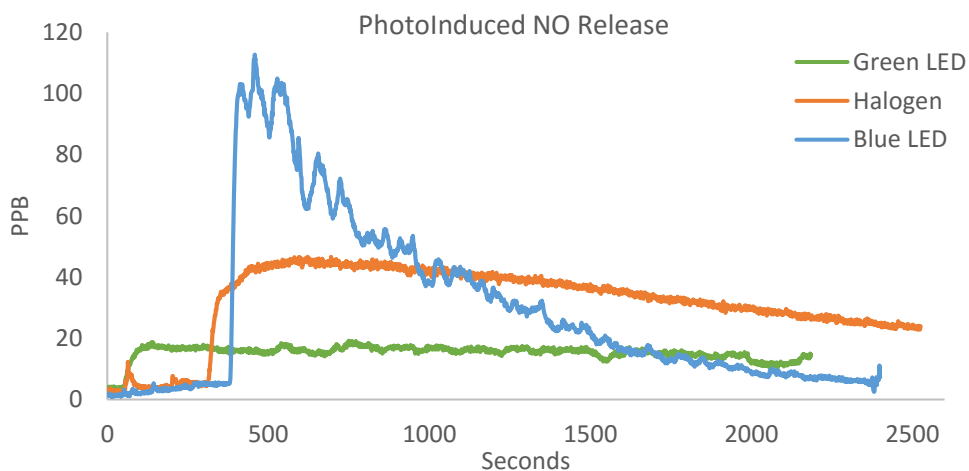


**Figure 5.5** Exposing SNTDM to a green or blue LED, or halogen bulb results in three drastically different NO release profiles.

preliminary. To fully understand SNTDM's behavior and develop a correlation between light source and NO release profile, the lights' intensities will need to be adjusted to comparable levels. A pulse width modulator could be used for this purpose.<sup>19</sup>

### 5.3 References

- 1 E. J. Brisbois, R. P. Davis, A. M. Jones, T. C. Major, R. H. Bartlett, M. E. Meyerhoff and H. Handa, *J. Mater. Chem. B*, 2015, **3**, 1639–1645.
- 2 A. Colletta, J. Wu, Y. Wo, M. Kappler, H. Chen, C. Xi and M. E. Meyerhoff, *ACS Biomater. Sci. Eng.*, 2015, **1**, 416–424.
- 3 Y. Onuki, U. Bhardwaj, F. Papadimitrakopoulos and D. J. Burgess, *J. diabetes Sci. Technol.*, 2008, **2**, 1003–1015.
- 4 M. Neidrauer, U. K. Ercan, A. Bhattacharyya, J. Samuels, J. Sedlak, R. Trikha, K. A. Barbee, M. S. Weingarten and S. G. Joshi, *J. Med. Microbiol.*, 2014, **63**, 203–9.
- 5 C. Tison, <http://lunainc.com/wp-content/uploads/2014/04/NO-White-Paper-August-2013.pdf>, accessed 7-29-2016.
- 6 A. R. Ketchum, M. P. Kappler, J. Wu, C. Xi and M. E. Meyerhoff, *J. Mater. Chem. B*, 2016.
- 7 Y. Wo, Z. Li, E. J. Brisbois, A. Colletta, J. Wu, T. C. Major, C. Xi, R. H. Bartlett, A. J. Matzger and M. E. Meyerhoff, 2015.

- 8 J. M. Joslin, S. M. Lantvit and M. M. Reynolds, *ACS Appl. Mater. Interfaces*, 2013, **5**, 9285–94.
- 9 P. R. McCarren; *Computational Investigations of Organometallic and S-Nitrosothiol Reaction Mechanisms*, 2009, pp 102-133 UCLA, Los Angeles.
- 10 D. L. Williams; *Nitrosation Reactions and the Chemistry of Nitric Oxide*, Elsevier, Amsterdam, 2004.
- 11 R. J. Singh, *J. Biol. Chem.*, 1996, 271, 18596-18603.
- 12 K. Goto, *Tetrahedron Letters*, 2000, 41, 8479-8483.
- 13 T. C. Harrop, *J. Am. Chem. Soc.*, 2008, 130, 15602-15610.
- 14 K. J. Reeves, M. W. R. Reed and N. J. Brown, *J. Photochem. Photobiol. B Biol.*, 2009, **95**, 141–147.
- 15 V. Rapozzi, E. Della Pietra, S. Zorzet, M. Zacchigna, B. Bonavida and L. E. Xodo, *Nitric Oxide*, 2013, **30**, 26–35.
- 16 L. B. Josefsen and R. W. Boyle, *Met. Based. Drugs*, 2008, **2008**, 276109.
- 17 G. E. Gierke, M. Nielsen, M. C. Frost, *Sci. Technol. Adv. Mater*, 2011, **12**, art. #55007–5.
- 18 P. Dungal, J. Hartinger, S. Chaudary, P. Slezak, A. Hofmann, T. Hausner, M. Strassl, E. Wintner, H. Redl and R. Mittermayr, *Lasers Surg. Med.*, 2014, **46**, 773–80.
- 19 K. Szolusha, *LT J. Analog Innov.*, 2012, 34-35.

## APPENDIX A

# Synthesis, Spectroscopy, and Stability of the Nitric Oxide Donor *S*-Nitroso-*N*-acetylpenicillamine: An Undergraduate Laboratory Experiment

Alex R. Ketchum<sup>1</sup>, Alexander K. Wolf<sup>1</sup>, Mark E. Meyerhoff<sup>1\*</sup>

<sup>1</sup>Department of Chemistry, University of Michigan, Ann Arbor, 48109, USA

\*Corresponding author

---

**Abstract** In the following experiment, organic chemistry students will gain hands-on experience with ultraviolet-visible spectroscopy and <sup>1</sup>HNMR spectrometry after synthesizing *S*-nitroso-*N*-acetyl-*D*-penicillamine (SNAP). SNAP is a popular small nitric oxide (NO) donor that has shown considerable promise for biomedical applications. Our group has consistently demonstrated that polymers such as silicone rubber or polyurethanes containing SNAP can release NO and use its antithrombotic and antimicrobial properties to prevent clot and bacteria biofilm formation. Following the straightforward acid catalyzed synthesis, students will characterize the product with <sup>1</sup>HNMR. Studying SNAP's HNMR spectrum provides students with an opportunity to experience and learn many important concepts including chemical shifts, integration, topicity, multiplicity, and coupling constants. Students will also calculate SNAP's molar absorptivity using UV-Vis spectroscopy and use it to monitor the compound's stability in various environments. The experiment is presented in a manner most appropriate for an undergraduate second semester organic laboratory course; however, it can be readily tailored to first semester students by

omitting the  $^1\text{H}$ NMR portion. The stability tests are suitable for various environments and durations, allowing the experiment to be used for single or multiple class periods if desired.

## A.1 Introduction

$^1\text{H}$ NMR spectrometry is a synthetic chemist's most powerful and common tool for characterizing and studying a molecule's structure and behavior. Additionally, UV-Vis spectroscopy is ubiquitous throughout many fields within the scientific community, ranging from organic, inorganic, analytical, materials science, and biochemistry. It can be used to identify molecules, observe reactions, and quantify molecular species [1-3]. Students with experience using these methods/instrumentation are likely to be better prepared and more competitive for entering graduate school or starting an industrial position. In this undergraduate experiment, students will synthesize an *S*-nitrosothiol (RSNO), *S*-nitroso-*N*-acetylpenicillamine (SNAP), and use these spectroscopic and analytical techniques to characterize and test its stability in various environments (Figure A.1).

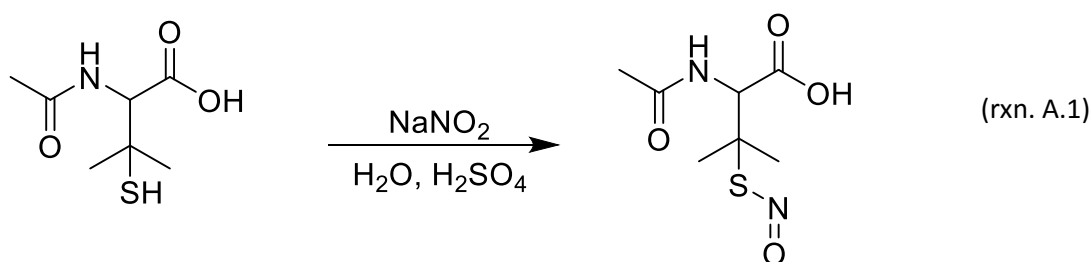


**Figure A.1.** Synthesis of *S*-nitroso-*N*-acetylpenicillamine via the nitrosation of *N*-acetylpenicillamine using acidified nitrite.

RSNOs are a class of molecules containing a nitrosonium group bound to the sulfur on a thiol molecule. There are three known endogenous RSNOs, *S*-nitrosocysteine, *S*-nitrosogluthathione, and *S*-nitrosoalbumin, each of which functions as a nitric oxide (NO) donor [4]. In the 1980's, scientists identified NO as the "endothelium derived relaxing factor," due to the fact that it is released by the endothelium and promotes smooth muscle relaxation (controlling blood pressure). After this discovery, NO has been found to also have important

antithrombotic and immunological roles, and serve as a signaling molecule for many biological functions [4-6]. Considerable research time and funding has been committed to thoroughly understanding and utilizing its properties for medical applications [4,5]. NO is unique in that it is a gaseous radical-bearing molecule, which is the reason for much of its reactivity. NO is rapidly oxidized to nitrogen dioxide upon exposure to oxygen. Endogenously, it reacts with oxyhemoglobin to form methemoglobin. These reactions are responsible for NO's brief half-life of only a few seconds in blood. Consequently, scientists looking to use NO for medical applications currently study NO donors, such as SNAP, with the goal of creating stable and controllable NO release sources [4-8].

Although SNAP is to date one of the most stable RSNOs, it still is susceptible to decomposition during preparation and storage under some conditions. RSNOs release NO via thermal or photolytic activation—stimuli which are difficult to avoid (Reaction 1). Consequently, considerable research has focused on determining the stability of SNAP and other RSNOs in various environments so as to determine their suitability for biomedical applications [9,10].



In today's world, health or medical applications are often at the forefront of scientific research. Areas such as medicinal chemistry, pharmaceutical science, and materials science are highly interdisciplinary as they frequently involve synthetic, analytical, and spectroscopic techniques [1,3,11-13]. Following the synthesis of this biologically-relevant molecule, students will perform analytical tests similar to those that are commonly used with SNAP or other NO donors during professional research [9,10]. Students will nitrosate the thiol precursor, *N*-acetyl-D-penicillamine (NAP), in an aqueous/methanolic solution using acidified nitrite [6,9,10,14]. Reaction vessels should be covered in aluminum foil to minimize decomposition from exposure to light. Primary RSNOs are red in color; however, tertiary RSNOs such as SNAP are typically green. Consequently, students can visualize the nitrosation via the appearance of the green color (Fig. A.1). In turn, as NO is released, SNAP decomposes into its corresponding disulfide, and loses its color, reverting to an off white solid (the disulfide of NAP) (Fig. A.2). After the reaction to

prepare SNAP has reached completion, students can separate the SNAP crystals via vacuum filtration and confirm SNAP's identity via  $^1\text{H}$ NMR spectroscopy using  $\text{d}_6\text{-DMSO}$  as the solvent. SNAP can be detected and the nitrosation conversion quantified using UV-Vis spectroscopy. RSNOs' strong  $n \rightarrow \pi^*$  absorptions between 320-360 nm allow straightforward and accurate measurements. SNAP's molar absorptivity coefficient has been reported as  $\epsilon_{340} = 1075 \text{ M}^{-1}\text{cm}^{-1}$  in water; however, this experiment provides an opportunity for students to learn about the Beer-Lambert Law (Eq. A.2) by determining the molar absorptivity coefficient and using it to measure SNAP's stability [9,10,14]. The Beer-Lambert Law is fundamental to UV-Vis spectroscopy, thus making it a critical skill for students to master in their studies and eventually apply in almost any scientific research field.

$$\text{Absorbance} = \epsilon \cdot l \cdot C \quad (\text{eq. A.1})$$

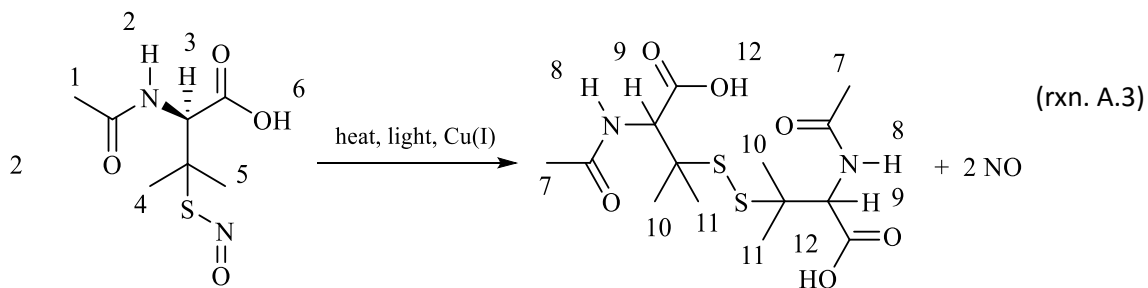


**Figure A.2.** SNAP decomposes to form the corresponding disulfide (RSSR) and NO. Positions are numbered as references for Figures 3, 4, 5, and Table 1.

## A.2 Experimental

### A.2.1. Materials and Methods:

*N*-Acetylpenicillamine, deuterated dimethyl sulfoxide, sodium nitrite, ethylenediaminetetraacetic acid (EDTA), potassium chloride, sodium phosphate dibasic, potassium phosphate monobasic, and methanol were purchased from Sigma-Aldrich (St. Louis,



MO). Concentrated hydrochloric and sulfuric acids were products of Fisher Scientific (Pittsburgh, PA). Aluminum foil was purchased from Meijer (Ann Arbor, MI). Calculations were performed using Microsoft Excel (version 10). UV-Vis measurements were obtained using a Lambda 35 UV-Vis spectrophotometer (Perkin-Elmer, MA).  $^1\text{H}$ NMR spectroscopy was performed using a Varian 400 MHz spectrometer and the data processed using MestReNova. pH 7.4 phosphate buffered saline (PBS), containing 10 mM sodium phosphate, 138 mM NaCl, 2.7 mM KCl, and 100  $\mu\text{M}$  EDTA was prepared using DI water. Depending on the experience level of the students, the PBS buffer and acidic stock solutions can be prepared in advance by staff. All reagents used are relatively inexpensive, further facilitating the adaptation of this experiment for an undergraduate class.

### **A.2.2. SNAP Synthesis:**

SNAP was synthesized using a modified version of previously reported methods [9,10,13,14]. 18 mL of 1:1 v/v MeOH/1M  $\text{HCl}_{(\text{aq})}$  solution containing 1 mL of conc.  $\text{H}_2\text{SO}_4$  was prepared and poured into a 50 mL RB flask containing 1.0 g NAP (5.2 mmoles) and a stir-bar. Following dissolution, which required vigorous stirring, the flask was covered with aluminum foil and charged with 0.71 g  $\text{NaNO}_2$  dissolved in 10 mL DI water over the course of 5 min. The aluminum foil can be briefly peeled back to observe the green color change corresponding with the appearance of SNAP. After 45 min of stirring, the solution was chilled on ice and the SNAP precipitate was isolated via filtration. SNAP crystals were spread over a Buchner funnel's filter paper to maximize surface coverage. Crystals were rinsed with ice cold water to remove salt byproducts and then subsequently with acetone previously chilled in an ice bath [9,10]. Finally, the SNAP crystals were briefly rinsed with ice cold diethyl ether to remove acetone and facilitate drying. The SNAP crystals were scraped into a beaker and spread out to maximize surface area before drying under a low stream of  $\text{N}_2$ . Crystals were weighed to determine yield, taking care to minimize light exposure.

### **A.2.3. Proton Magnetic Resonance ( $^1\text{H}$ NMR) Spectroscopy:**

Spectra were obtained in d6-DMSO and shifts identified were referenced to DMSO's resonance at 2.5 ppb. Peaks were picked, coupling constants measured, and the integration determined.

#### **A.2.4. Molar Absorptivity:**

The molar absorptivity was determined for SNAP following synthesis. Solutions of 0.80, 0.50, and 0.25 mM of SNAP in PBS buffer were prepared for UV-Vis measurements. Students should be sparing when making samples to conserve SNAP for subsequent spectroscopic measurements. After testing each sample, a calibration curve was determined using Microsoft Excel using the absorbance values at 340 nm wavelength. The 0.80 mM SNAP solution was used for further stability studies.

#### **A.2.5. Stability Studies**

The 0.80 mM SNAP<sub>(PBS)</sub> samples were prepared in 20 mL vials using PBS buffer with EDTA present and exposed to varying degrees of heat and light. Exposure conditions can vary and be tailored to the number of students, and access to available light sources, e.g. windows, fluorescent lights, etc. Samples were placed on a window sill and in a hood, cupboard, and refrigerator [10] to provide a variety of thermal and light exposures. Samples were also covered in a dark 37 °C oven to simulate physiological conditions. Each sample's RSNO concentration was tested via UV-Vis spectroscopy at regular intervals. The vials were immediately returned to their appropriate storage conditions following measurements. Absorbances at 340 nm were recorded and used to calculate remaining SNAP levels, which were in turn plotted over time to exhibit the varying effects of the stimuli [10]. The time intervals are flexible and can be modified to allow for variation in class duration and frequencies.

### **A.3. Results and Discussion**

### A.3.1. SNAP Synthesis

Although nitrosation is commonly a quantitative reaction, the workup causes some product to be lost in the process due to SNAP's partial solubility in both water and acetone. We obtained  $36 \pm 5\%$  yields for  $n=3$  preparations. Assuming the procedure is accurately followed, and the molar absorptivities are calculated soon following the synthesis (to minimize sample decomposition), students should obtain molar extinction coefficients close to the reported value,  $\epsilon_{340}=1075 \text{ M}^{-1}\text{cm}^{-1}$  [9]. If instrumentation is limited, SNAP samples can be stored in a cupboard or refrigerator to prolong lifetimes. Since the reaction is quite reproducible, some students can determine the molar absorptivity prior to performing  $^1\text{H}$ NMR spectroscopy if necessary. As long as samples are stored in the dark at or below room temperature, negligible decomposition will occur during the processes [10].

### A.3.2. $^1\text{H}$ NMR Spectrometry

SNAP's  $^1\text{H}$ NMR spectrum was taken following synthesis and is displayed in Figure A.3a. The peaks are numbered as shown in Figure A.2, with the corresponding proton shifts detailed in Table 1. At this point minimal disulfide is present, allowing easy and accurate characterization. SNAP's synthesis is easily integrated within undergraduate curriculum as the reaction is reliably quantitative, and consequently has minimal residual starting material that would otherwise convolute the spectra [9,10,14]. There is minimal overlap of shifts and the integration aligns well between SNAP's protons. The N-H and adjacent C-H protons at positions 2 and 3, respectively, are distinct, and this serves as an opportunity for students to determine the coupling constants. These protons also work superbly for comparing SNAP:RSSR concentrations during decomposition, as they too are distinct (Fig. A.4). Due to inherent chirality, the protons at positions 4 and 5 in SNAP and 10 and 11 in the corresponding disulfide are diastereotopic. The resulting upfield resonances are useful traits for teaching students about topicity (See Figure A.5b).

An intermediate spectrum was obtained following partial SNAP decomposition so as to demonstrate the SNAP:RSSR proton resonances relative to each other. The amide and

neighboring C-H proton shifts can be integrated to compare concentrations. RSNOs' 2:1 stoichiometric decomposition must be taken into account when comparing the relative composition of each species. Protons at positions 3 and 9 serve as integration comparisons due to their aprotic nature. In Figure A.4b,  $0.54/(0.54+1.00/2) = 52\%$  of SNAP remains. If time is available, students can take spectra during and/or following decomposition to compare SNAP and the dimer's coupling constants: 9.4 and 8.8 Hz, respectively. Finally, Figures A.3c, A.4c, and A.5 display the dimer following decomposition.

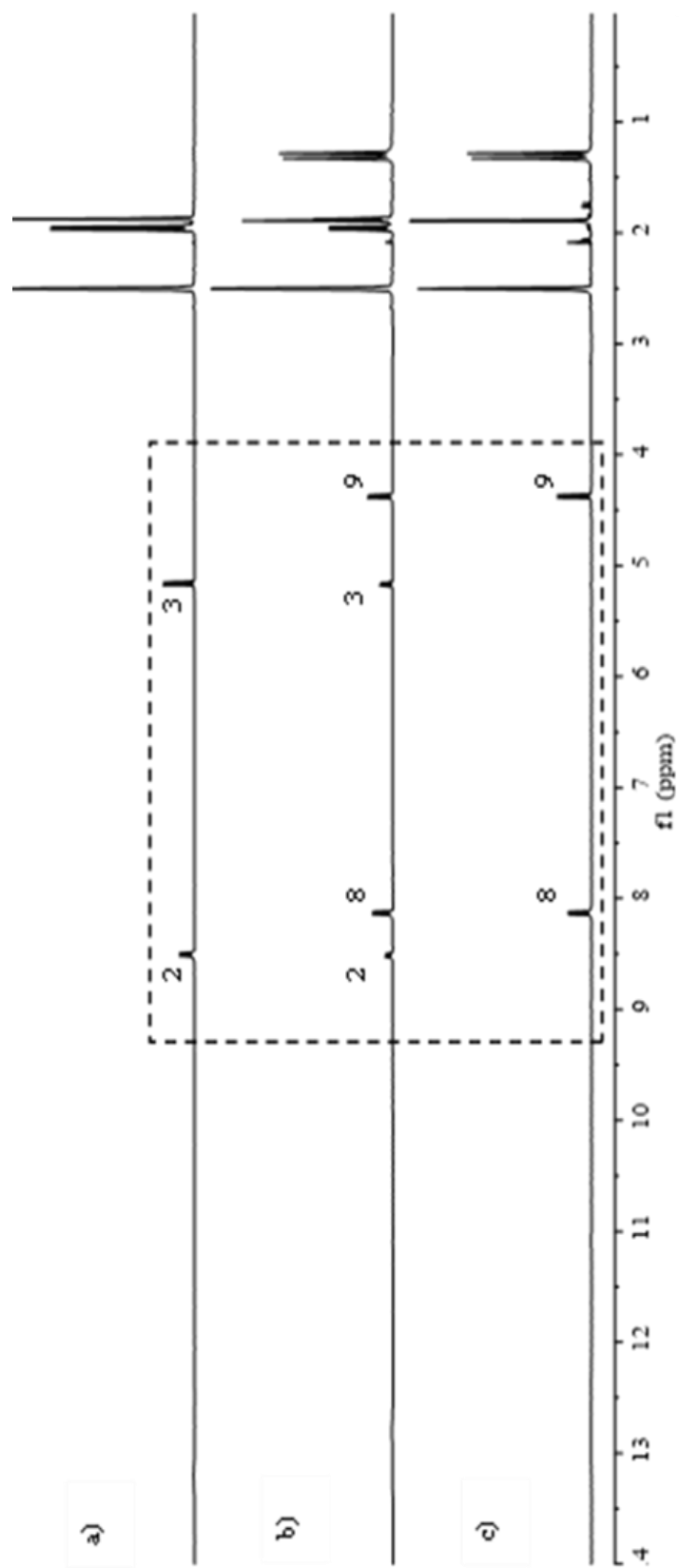


**Figure A. 3.** <sup>1</sup>H NMR spectra corresponding to a) pure SNAP, b) partially decomposed SNAP, and the c) disulfide decomposition product. Samples were dissolved and tested in d<sub>6</sub>-DMSO on a 400 MHz Varian NMR spectrometer.

**Table A.1.** Proton shifts, splitting, and coupling constants for SNAP (1-6), and the RSSR (7-12)

$^1\text{H}$	ppm	Multiplicity	J (Hz)
1	1.84	Singlet	
2	8.47	Doublet	9.4
3	5.13	Doublet	9.4
4/5	1.91/1.93	Singlets	
6	13.18	Broad	
7	1.85	Singlet	
8	8.09	Doublet	8.8
9	4.34	Doublet	8.8
10/11	1.25/1.29	Singlets	
12	12.73	Broad	

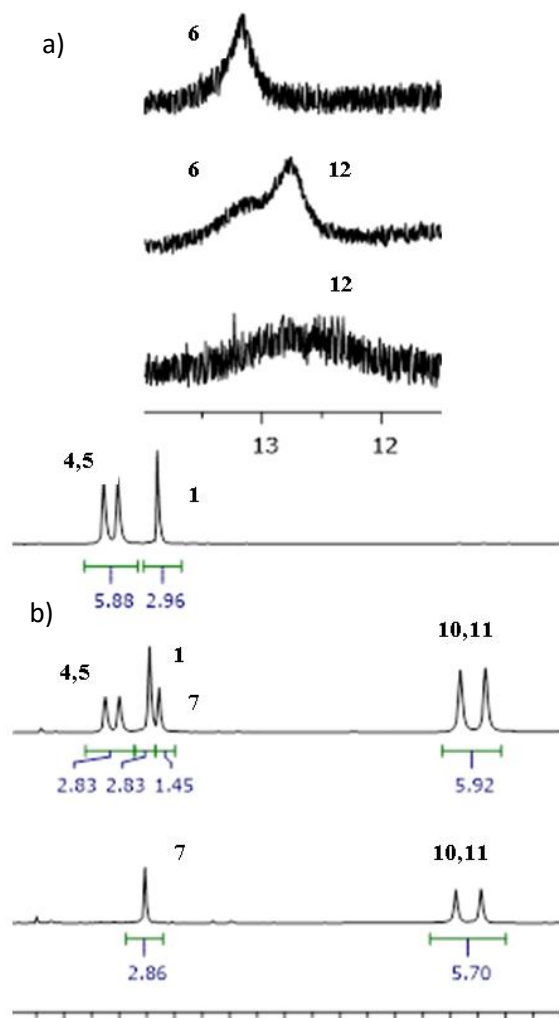


**Figure A.5.** Expanded region showing SNAP and the disulfide's a) carboxylic acid b) methyl protons.

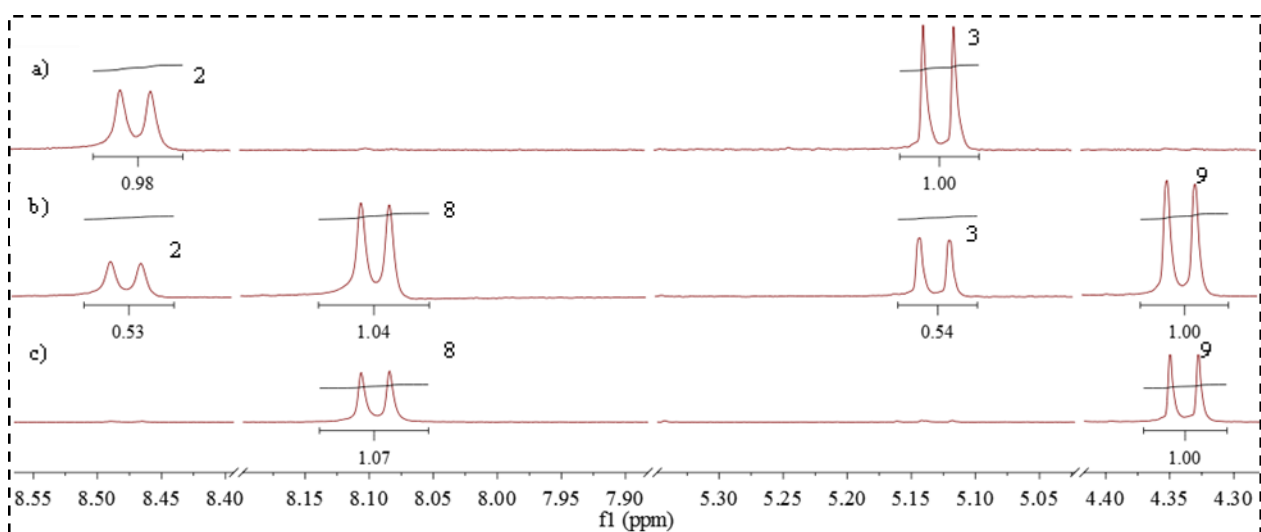


**Figure A.4.** Close-up of the pair of doublets corresponding to SNAP's N-H and C-H at positions 2 and 3, respectively, as well as the corresponding disulfide protons at positions 8 and 9. Integration is referenced to the C-H at position 3 and 9 of SNAP and the disulfide, respectively. Spectra correspond with a) pure SNAP, b) partially decomposed SNAP, and c) disulfide product.

### A.3.3. UV-Vis Spectroscopy

RSNOs absorb light in the visible range; however, this absorption is considerably weaker than typically observed for organic molecules in the ultraviolet region. Nonetheless, we determined SNAP's molar absorptivities to be  $\epsilon_{340}=1079 \text{ M}^{-1}\text{cm}^{-1}$  and  $\epsilon_{591}=17.3 \text{ M}^{-1}\text{cm}^{-1}$ . This agrees well with the recently reported value,  $\epsilon_{340}=1075 \text{ M}^{-1}\text{cm}^{-1}$ . The corresponding spectra and calibration curves are shown in Fig. A.6.

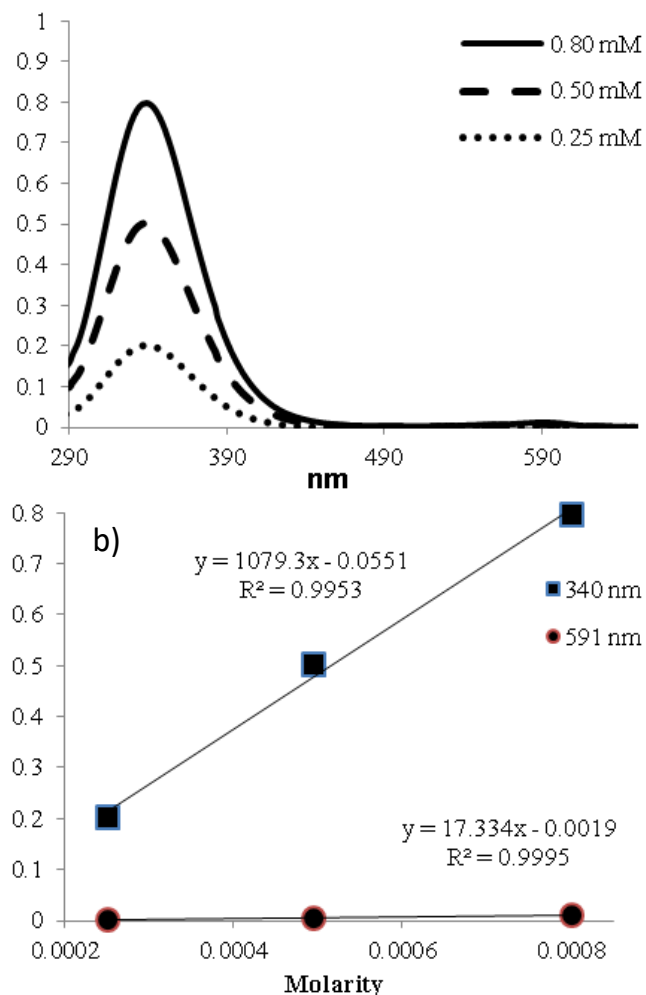


**Figure 6.** a) UV-Vis spectrum of SNAP at 3 different concentrations. The absorbance at 340 nm was subsequently used to determine the molar absorptivity as shown in the calibration curve (b).

### 3.4. Stability

We tested the SNAP solutions for 4 days in a range of different conditions (Figs. A.7 and A.8); however, this variety is not required for a successful experiment. The most useful conditions for drawing comparisons would be those separately displaying the effects of temperature and light; *i.e.* a combination of available dark environments: covered vial in a cupboard/refrigerator/37 °C oven, and separately: windowsill/hood/cupboard, to observe the effects of light. It is worth noting that the observed stabilities are circumstantially dependent, and the students' SNAP concentrations may differ from ours due to factors such as room temperature, distance from windows, and cloud cover. The significance lies in the results relative to one another. Photolytic decomposition can be observed in as little as 30 min, with 12, 6, and 2% SNAP lost for window, hood, and cupboard samples, respectively. The rapid photolytic decomposition allows the experiment to be concluded within a single class period, if desired. The effects of light on NO release become increasingly apparent during subsequent measurements. After 2 h, 5% of SNAP had decomposed for samples at room temperature that were not exposed to the light (cupboard), compared to 9% with the hood samples. SNAP solutions exposed to direct sunlight had lost 21% by the 2 h timepoint. The samples with direct light exposure had

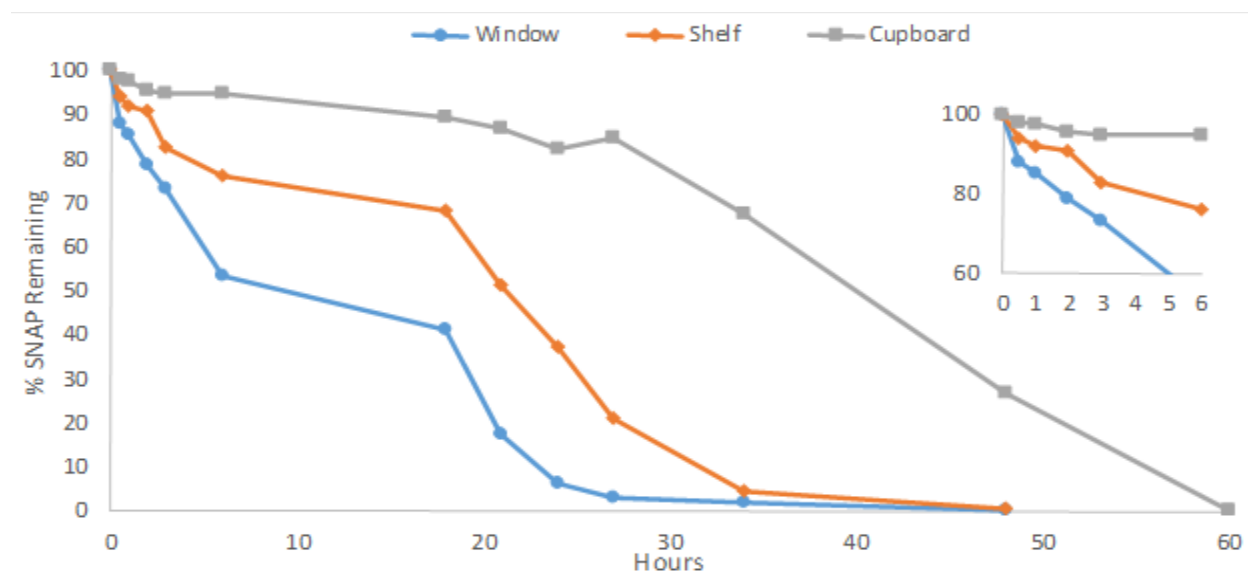


**Fig.A.7** 0.8 mM SNAP<sub>(aq)</sub> solutions exposed to varying degrees of light while stored in 3 different locations. The inset shows the initial 6 h expanded.



fully decomposed to the disulfide after 2.5 days. Students should readily be able to conclude that light exposure stimulates NO release.

SNAP is more stable with regard to the tested temperature range (Fig. A.8). Approximately 6% of the SNAP had decomposed from the 37 °C samples after 30 min, while 2 and 0% had been lost from the cupboard and refrigerator, respectively. After 2 h, 83, 95, and 97% SNAP remained in the oven, cupboard, refrigerator respectively. The distinct SNAP concentrations facilitate the students' abilities to draw a conclusion regarding the effects of temperature on NO release. The oven, cupboard, and refrigerator samples had released all their NO after approximately 1, 2.5, and 3.5 days. Additional data points, as well as optionally monitoring the decomposition with  $^1\text{H}$ NMR, allows the stability study to be extended for subsequent class periods if so desired.

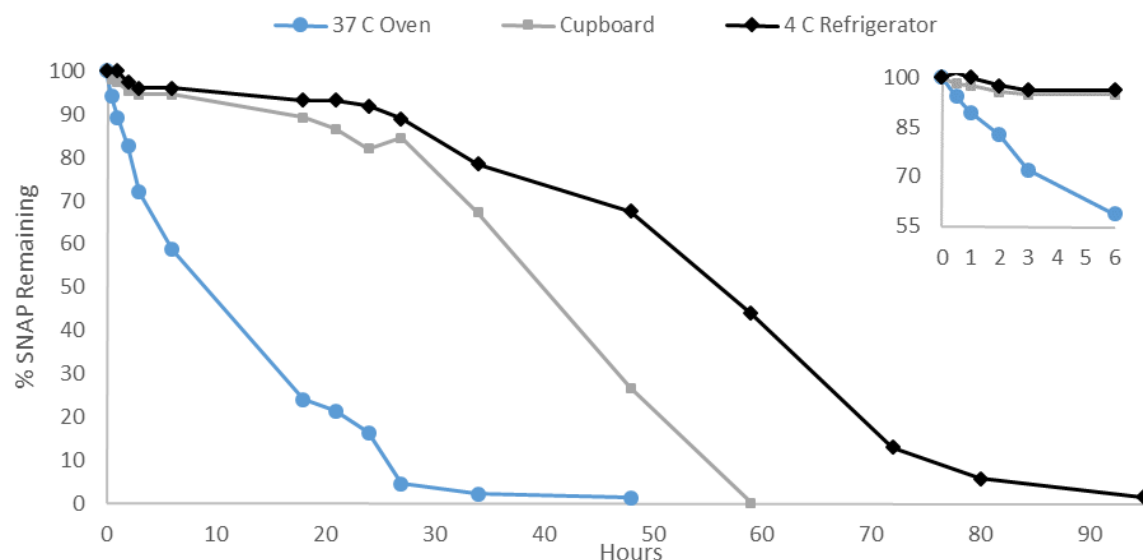


Fig.A.8 0.8 mM SNAP<sub>(aq)</sub> solutions exposed to varying degrees of heat while stored in 4 different locations. The inset is the initial 6 h

#### A.4. Conclusions

The experiment described herein provides an opportunity for undergraduate chemistry students to develop and strengthen several crucial skills that are applicable in many scientific fields [1-3,9-11]. Students will gain valuable experience using a UV-Vis spectrometer and learn about the Beer-Lambert Law by determining SNAP's molar absorptivity. In d<sub>6</sub>-DMSO, SNAP's structure is inherently useful for gaining experience with  $^1\text{H}$ NMR spectrometry. In addition to measuring SNAP's proton resonances and integrations, students can investigate spectroscopic topics including multiplicity and coupling constants. Testing the molecule's stability places

students within a model that closely simulates industrial chemistry research, as they witness firsthand the relevance of stability for potential products. [9,10]. Indeed, SNAP and other RSNOs are being examined as NO donors to develop a new generation of thromboresistant and antimicrobial intravascular and urinary catheters, etc. [9,10].

RSNOs are rarely included, and thus critically underutilized, in undergraduate organic lectures and laboratories despite their popularity and significance in current biomedical research. This experiment is applicable in a wide range of laboratory settings, allowing variation for the number of students, experience levels, desired experimental duration, and available instrumentation. Due to SNAP's useful properties, it provides a simple addition to any curriculum to expand upon thiol or disulfide chemistry, while allowing students to practice using two of the most important scientific instruments in chemistry [1-3].

## **ACKNOWLEDGEMENT**

We thank the NIH (grants EB000783 and HL128337) for supporting research in our laboratory relating to use of SNAP to develop new biomedical devices.

## **REFERENCES**

- [1] A. Rahman, M. I. Choudhary, *Structure-Activity Relationship Studies in Drug Development by NMR Spectroscopy*, Sharjah, United Arab Emirates: Bentham Science Publishers, 2011, vol. 1.
- [2] J. W. Robinson, E. S. Frame, G. M. Frame II, *Undergraduate Instrumental Analysis*, Boca Raton, USA: CRC Press, 2014, 7 Ed.
- [3] A. L. Skinner, J. S. Laurence, "High-field Solution NMR Spectroscopy as a Tool for Assessing Protein Interactions with Small Molecule Ligands", *J. Pharm. Sci.*, 2008, 97, pp. 4670-4695.
- [4] H. H. Al-Sa-doni, A. Ferro, "S-nitrosothiols as Nitric Oxide-Donors: Chemistry, Biology and Possible Future Therapeutic Applications", *Curr. Med. Chem.*, 2004, 11, 2679-2690.

- [5] N. Tuteja, M. Chandra, R. Tuteja, M. K. Misra, "Nitric Oxide as a Unique Bioactive Signaling Messenger in Physiology and Pathophysiology", *J. Biomed. Biotechnol.*, 2004, 4, 227-237.
- [6] I. Chipinda, R. H. Simoyi, "Formation and Stability of a Nitric Oxide Donor: *S*-Nitroso-*N*-acetylpenicillamine", *J. Phys. Chem. B.*, 2006, 110, 5052-5061.
- [7] A. J. Gow, B. P. Luchsinger, J. R. Pawloski, D. J. Singel, J. S. Stamler, "The oxyhemoglobin reaction of nitric oxide", *Proc. Natl. Acad. Sci.*, 1999, 96, 9027-9032.
- [8] U. Schedin, C. G. Frostell, L. E. Gustafsson, "Formation of nitrogen dioxide from nitric oxide and their measurement in clinically relevant circumstances", *Br. J. of Anaeseth.*, 1999, 82, 182-192.
- [9] A. Colletta, J. Wu, Y. Wo, M. Kappler, H. Chen, C. Xi, "*S*-Nitroso-*N*-acetylpenicillamine (SNAP) Impregnated Silicone Foley Catheters: A Potential Biomaterial Device to Prevent Catheter Associated Urinary Tract infections, *ACS Biomater. Sci. Eng.*, 2015, 1, 416-424.
- [10] E. J. Brisbois, H. Handa, T. C. Major, R. H. Bartlett, M. E. Meyerhoff, "Long-Term Nitric Oxide Release and Elevated Temperature Stability with *S*-nitroso-*N*-acetylpenicillamine (SNAP)-Doped Elast-eon E2As Polymer", *Biomaterials*, 2013, 34, 6954-6966.
- [11] A. F. Repko, *Interdisciplinary Research: Process and Theory*, Thousand Oaks, USA: SAGE, 2008.
- [12] <http://benefunder.org/causes/501/debbie-crans>; accessed Aug 10, 2015.
- [13] L. S. Choi, H. Bayley, "*S*-Nitrosothiol Chemistry at the Single-Molecule Level", *Angewandte Chemie – Internat. Ed.*, 2012, 51, 7972-7976.